Eidgenössische Technische Hochschule Zürich
Swiss Federal Institute of Technology Zurich

Entrepreneurial Risks

MASTER THESIS - MSC PHYSICS:

Constrained Random Walk Models

A discussion of constrained random walks and their applications to the euro/Swiss franc exchange rate

written by:
SANDRO LERA
(SLERA@ETHZ.CH)

supervisor and examiner:
PROF. DIDIER SORNETTE
(DSORNETTE@ETHZ.CH)

START DATE: 29.09.2014

END DATE: 10.02.2015

ETH ZÜRICH

ACKNOWLEDGEMENTS:

First and foremost, I would like to thank Prof. Didier Sornette for enabling me this interesting project and for his continuous support and mentoring throughout my thesis. Writing my master thesis with Prof. Sornette and his team has meant much more to me than just researching a specific topic. The interdisciplinary approaches to problem solving taught at the Chair of Entrepreneurial Risk have given me the opportunity to extend my knowledge in fields far beyond physics. The weekly meetings with the entire research team have given me a good impression of the daily work as a researcher at the Chair of Entrepreneurial Risk and have motivated me to continue my studies in this field.

I also want to thank Dr. Philipp Rindler for his help with problems in stochastic calculus and its applications in finance. Last but not least, I thank Dr. Vladimir Filimonov who has helped me access various data sets and computing facilities.

ABSTRACT:

We study the performance of the euro/Swiss franc exchange rate in the extraordinary period from September 6, 2011 and January 15, 2015 when the Swiss National Bank enforced a minimum exchange rate of 1.20 Swiss francs per euro. Within the general framework built on geometric Brownian motions (GBM), the first-order effect of such a steric constraint would enter a priori in the form of a repulsive entropic force associated with the paths crossing the barrier that are forbidden. It turns out that this naive theory is proved empirically to be completely mistaken. The clue is to realise that the random walk nature of financial prices results from the continuous anticipations of traders about future opportunities, whose aggregate actions translate into an approximate efficient market with almost no arbitrage opportunities. With the Swiss National Bank stated commitment to enforce the barrier, traders's anticipation of this action leads to a volatility of the exchange rate that depends on the distance to the barrier. This effect described by Krugman's model [P.R. Krugman. *Target zones and exchange rate dynamics*. The Quarterly Journal of Economics, 106(3):669-682, 1991] is supported by non-parametric measurements of the conditional drift and volatility from the data. Despite the obvious differences between "brainless" physical Brownian motions and complex financial Brownian motions resulting from the aggregated investments of anticipating agents, we show that the two systems can be described with the same mathematics after all. Using a recently proposed extended analogy in terms of a colloidal Brownian particle embedded in a fluid of molecules associated with the underlying order book, we derive that, close to the restricting boundary, the dynamics of both systems is described by a stochastic differential equation with a very small constant drift and a linear diffusion coefficient.

The thesis comes with three appendices: (i) a thorough derivation of important random walk properties, (ii) a method for the perturbative calculation of cumulants of solutions to stochastic differential equations using Feynman path integrals and diagrams, (iii) a functional renormalization group calculation of the interaction between a D-dimensional fluctuating surface and a hard wall.

Contents

1 Currencies, target zones and efficient markets

In this section we present a qualitative overview on the fundamental concepts that the thesis is based on. We start by explaining the efficient market hypothesis and its mathematical implementation in terms of random walks. We then go on to describe how foreign-exchange markets determine exchange rates and what role central banks play in this market. Finally, we explain the target zone that was implemented by the Swiss National Bank in September 2011.

The reader is provided with references for more detailed reviews throughout the text. A basic understanding of physics, mathematics, finance and economics is assumed.

1.1 The efficient market hypothesis

Surely, you have already seen pictures or movies of the busy stock exchanges that exist all over the world. You have seen traders attentively studying rapidly fluctuating prices that flatter over dozens of screens in real-time. You have seen them reacting hectically to certain events by giving orders to buy or to sell.
If you have a background in natural sciences you are used to studying empirical data sets taken from experiments and then deducing theoretical models on the basis of these observations. On the other hand, if you are given a model, you know that with certainty (within the realms of a certain precision) the model is going to hold at all places and times. Therefore, given some initial values, we can, in some sense, predict the future. So it is only natural that you ask yourself how the traders on financial markets do this. What models are they applying? How can they, by studying past prices, infer what the future prices will be? The *efficient market hypothesis* (EMH) provides a simple answer to this question: they can't!
This answer might be surprising to you and it possibly raises more questions than it has actually answered. So let us review step by step what the efficient market hypothesis says and where it is coming from.

Let us start by giving the definition of an ideal efficient market. A market is called *efficient* if [102]:

(i) the participants quickly and comprehensively obtain all information relevant to trading.

(ii) it is *liquid*. This means that an investor can easily buy or sell a financial product at any time. The more liquid a market is, the more secure it is to invest. The investor knows that he can always cash-in his assets. This easy exchange between money and financial product raises the attractiveness of the market. On a liquid market, the myriad transactions efficiently balance the decision of a single investor (or a small group of investors) so that individual purchases or sales are possible at any time without destabilizing the asset prices.

(iii) there is low *market friction*. Market friction is a collective expression for all kinds of trading costs. These include trader provisions, transaction costs, taxes etc. The sum of these costs is negligible compared with the transaction volume if the market friction is low.

Recall that the price of an asset, for instance a stock, that is traded on a financial market is nothing but the point at which supply and demand meet. If demand for the asset is increased, the price rises and for the supply it works the other way around. Now assume that we are trading such an asset

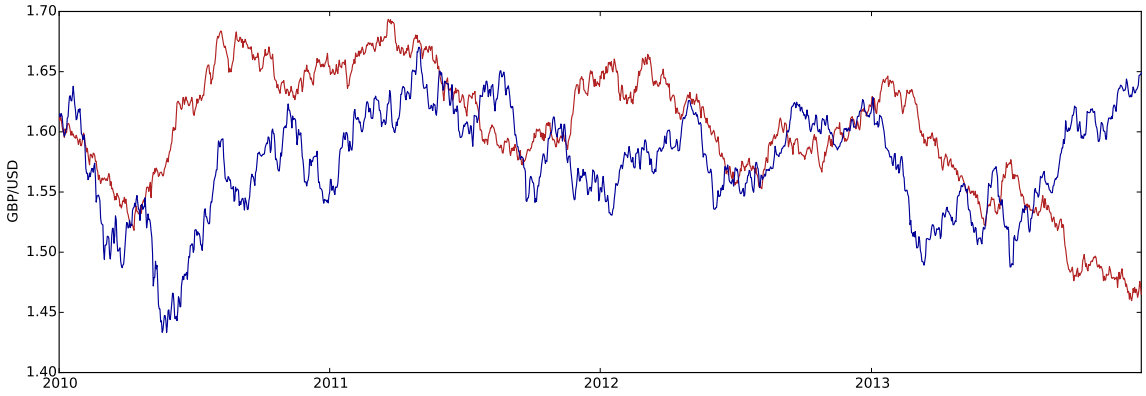

Figure 1.1: The blue line shows the daily GBP/USD exchange rate from January 2010 to December 2013. The red line shows an artificially created random walk with the same starting point and the same average step length as the exchange rate. It seems hard to tell them apart. The efficient market hypothesis makes this observation concrete by stating that the development of asset prices on financial markets is indeed of stochastic nature.

on a perfectly efficient market. What can we say about its price? By assumption, we know that the participants have all the possible information that can be used to value the asset, all trades can be executed and market friction is negligible. Therefore, supply and demand must balance exactly at the fair underlying value of the asset. Assume this was not so. Assume that the value of the asset would be undervalued, say. According to the first property of efficient markets the information "asset is undervalued" is accessible to traders. Knowing that the asset is worth more than they have to pay for traders immediately start to bid on this asset. Consequently, the price is increased. This process continues until the asset price reaches its fair value. Through this process market equilibrium is immediately readjusted to its fair value. This is of course a highly dynamical process. All information that becomes available to traders through news and other information channels is immediately incorporated into the market price. Therefore, at any point in time the price of the asset reflects its fair value.
In essence, this is exactly the statement of the efficient market hypothesis: financial markets are complex, highly efficient systems in which all possible information is aggregated, immediately digested and reflected in fair asset prices.

Mathematically, we consider the price X of an asset as a function of time t. The EMH states that we cannot predict future price developments with certainty. Hence, $X(t)$ denotes a *random walk*. We assume that the fundamental properties of random walks are known. See for instance [14, 24] for an introduction.
But $X(t)$ is not just any random walk. Since the EMH states furthermore that all the available information is fully incorporated in the present price, past prices do not have any influence on the statistical properties of future prices at all. In the language of mathematics this just means that the random walk is a *Markov Process*. As an example we show the exchange rate of British pounds (GBP) to US dollars (USD) in figure 1.1. In the same figure we have plotted an artificially generated random walk. Indeed, the two paths show a striking resemblance and it seems difficult to tell them apart.

The analogy between asset prices and random walks is not a new one but dates back to Bachelier's famous paper *Théorie de la Spéculation* [4] published in 1900. In his paper, Bachelier suggested that prices (of the Paris stock market) follow a random walk. Furthermore, he introduced and solved the

diffusion equation five years before Einstein's famous publication on Brownian motion [21]. Bachelier's ideas fell into oblivion for more than sixty years. In the 1960s, his work was rediscovered and largely enhanced in the following decades by Mandelbrot, Samuelson, Fama and others. See [96] and references therein for more details on the recent history of the EMH.

While the EMH sounds very plausible in theory, we must remind ourselves that all this reasoning relies on the assumption of efficient markets. Clearly, reality can only be an approximation of a truly efficient market. Fama's work (see [96] and references therein) has contributed largely to showing that, in good approximation, real markets can be modeled as efficient. In fact, Fama [22] distinguishes between three different forms of market efficiency:

(i) *Weak Form Efficiency:* The weakest form of the EMH states that market prices reflect all historical price information. This means that future returns cannot be predicted with only the analysis of past prices, no matter how smart the applied method. All information that could be extracted has already been incorporated in the latest price.

(ii) *Semi-Strong Form Efficiency:* The semi-strong version of efficient markets assumes that market prices also reflect all publicly available information (e.g. geopolitical developments, new scientific discoveries etc.). Even if a trader has all this information available, he or she can still not make money on the financial markets without being exposed to a certain risk. We also say that the market cannot be *arbitraged* or that there is *no free lunch*.

(iii) *Strong Form Efficiency:* In its strongest form, the EMH claims that market prices reflect *all* information on an asset. Neither publicly available nor private information (insider information etc.) can be used to arbitrage the market.

Fama was awarded for his work with a Nobel price in 2013. Nevertheless, the EMH goes not without criticism. It is for a good reason that in 2013, the same year that Fama received the Nobel price for showing that the EMH holds, Shiller was awarded with the same Nobel price for showing that the EMH does not hold in real markets (see [96] and references therein). For a natural scientist this might sound contradictory: How can two economists be awarded with the same prize, one for showing that a theory holds and the other one for showing that it does not? It turns out that there is an important and omnipresent difference between natural sciences and economics. While in natural sciences we are used to thinking stationary and of systems being in equilibrium in economics everything is conditional. This is not different for the efficient market hypothesis: If prices are next to impossible to predict in the short run, this does not mean that they are unpredictable in the long run. Stock prices are excessively volatile in the short run, and at a horizon of a few years the overall market is quite predictable. On average, the market tends to move downward following periods when prices are high and upward when prices are low [96]. See also [54] for further discussions of the EMH and its limits. What is important for us is that, in good approximation, we may assume that the market considered in this thesis is efficient. We will see in the next section why this is the case.

1.2 The foreign-exchange market

There are many types of asset classes that market participants can choose to invest in. Among the most prominent there are equities, fixed income, commodities, real estate and currencies. In this thesis we will be mainly concerned with currencies.

In every country prices are expressed in units of currency. The value of a currency itself, however,

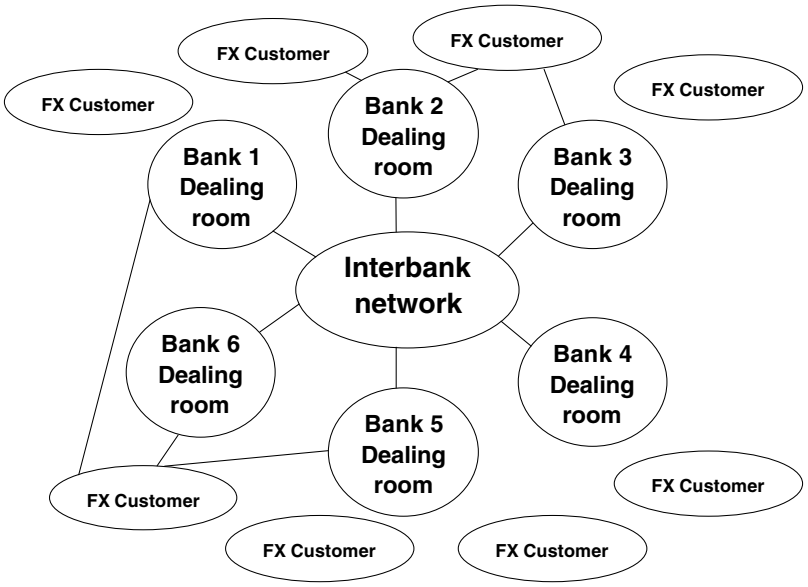

Figure 1.2: Schematic structure of the foreign-exchange market (FX), borrowed from [67]. The market-making banks form the interbank-network through which deals are "cleared". There are no brokerage fees. The banks which interact with other banks on the one side and with customers on the other make only profit through the bid-ask spread.

can only be judged against an external reference. This reference, the exchange rate, thus becomes the fundamental price in any economy. Most often, the references against which a currency's value is measured are other currencies. Determining the relative values of different currencies is the role of the *foreign-exchange market* (FX) [48].
The FX is very different from for instance a stock market in the sense that it has no (physical) location. We are talking about a *decentralized market*. It is relatively clear how the price of an asset traded at a centralized market is established. As an example, think about the price of a Nestlé stock traded at the Swiss Exchange (SIX). Since demand (ask price) of all buyers and supply (bid price) of all sellers are aggregated at one and the same localized market, the SIX [1], one can readily read of the price of a Nestlé stock as the position where supply and demand meet. For the FX, however, no such centralized market exists. Figure 1.2 sketches the basic structure of the large, unregularized FX. In the center we have the *market-making banks* (each working from its own *dealing room*) which span the *interbank-network*. The exchange rate of a currency pair that the costumers see is determined through this network. This can be understood best in terms of a simple example [67]:

A customer contacts a bank of his choice and buys a six-month forward of 10 million US-dollars vs. yen. To avoid running overnight risk, which is risky and regulatorily expansive, the bank will need to unwind its short dollar/long yen position before the end of the day, if possible at a profit. The method by which it does this are two-fold: it can either hope that another customer will contact them and ask to buy yen/sell dollars on their quoted prices, or it can go to other banks asking for prices to sell yen/buy dollars. The likelihood of the right customer coming to that specific bank at the right time by chance is slim but in the countless thousands (probably millions) of trades done each day, there will be customers around the world taking the positions that our bank desires to square its book. These interbank deals, which make up about 59% or the entire trading volume on the FX, therefore represent the *clearing system* for exposure to "find" another customer. This mechanism is extremely efficient and essentially leads to the situation that customers around the world see the same prices at

[1] Nowadays, "localized" is of course understood in a more abstract sense as trades are executed via internet. The physical location of the SIX is less important.

every time.

We have mentioned in section 1.1 that the efficient market hypothesis is only an approximation of reality. It turns out that the FX has all the ingredients for an efficient market if ever there was one [67]: The FX is by far the largest market in the world, with unparalleled liquidity. The market is open 24 hours a day except for the weekends. Information flows almost instantaneously through the market, and there are no insider trading laws and no common taxation regime to distort market prices. There is no brokerage commission on wholesale trading, and the only form of payment to banks for market-making is the difference between their quoted buying and selling prices, so-called *bid-ask* spreads. The number of participants in the market is huge - measured in hundreds of millions if direct and indirect players are included. For instance, the volume of FX dealing in April 2001 was 1.2 trillion USD per day. This daily trading volume is to be contrasted for instance with a daily trading volume of the New York stock exchange (NYSE) of 50 billion USD.

Customers as referred to in the above example and depicted in figure 1.2 are a varied collection of organizations. They include financial institutions like smaller banks and insurance companies, active investment trading houses like hedge funds, industrial and commercial companies, investment managers and many more. Some of these customers (the *dealers*), among them of course the (smaller) banks, then trade the exchange rates further with their clients (called *retail customers*) earning a fee by charging a wider bid/ask spread.

This basic and traditional understanding of the FX price mechanism is all we need to know in the realms of this thesis. More detailed, classical introductions can be found for instance in [67, 79]. However, trading technology in the FX has undergone a radical change since the early 1990s, when electronic broking systems have been introduced [13]. See [20, 76] for a more recent review of the FX focusing on the structural changes due to the advent of high-frequency trading.

In the above examples of participants in the FX we have not yet mentioned one player that is of particular importance: the central bank. Central banks may trade currencies for the purpose of affecting exchange rates. A government's deliberate attempt to alter the exchange rate between two currencies by buying one and selling the other is called an *intervention* [48]. There is a continuum of flexibility, along which it is possible to place the value of one currency to another. Specifically, nine distinct forms can be observed in real currency markets [30]. Starting with the most flexible one and going to more and more fixed exchange rates, we discuss here only the five systems which are most relevant in this thesis. See [30] for a detailed explanation of all nine forms.

(i) *Free float:* The central bank does not intervene in the foreign exchange market, but rather allows private supply and demand to clear on their own. The United States is the closest to a pure example of a free float.

(ii) *Managed float:* Also known as a "dirty float" it is defined as a readiness to intervene in the FX, without defending any predetermined exchange rate. Most intervention is intended to lean against the wind - buying the currency when it is rising and selling when it is falling. As of 2013, examples in this category are Romania and Afghanistan [37].

(iii) *Target zone or band:* The authorities pledge to intervene when the exchange rate hits pre-announced margins on either side of a central parity. As we will discuss below, Switzerland has been a prominent example of this type.

(iv) *Basket peg:* The exchange rate is fixed in terms of a weighted basked of currencies instead of any one major currency, an approach that makes sense for countries with trade patterns that are highly geographically diversified, as many in Asia.

(v) *Currency board:* A currency board is a monetary institution that only issues currency that is fully backed by foreign assets. Often, this exchange rate is fixed not just by policy, but by law. This form of currency control was widespread in the British colonies. The purpose was to provide the colonies with a stable currency without the associated difficulty of issuing sterling notes and coins that were costly to replace if lost or destroyed.

Which of the above is the optimal exchange rate regime depends on the circumstances of the particular country and time. Floating is often desirable in large economies. Fixity may be desirable for very small open economies. Small political units that have tight economic links with their neighbors are too small to float. If the boundaries of a geographic area are drawn sufficiently large that the trade links and income links among its constituent parts are strong compared to the trade links and income links with its neighbors, then it is of the optimal size to constitute an independent currency area. More rigid exchange rates are also useful for countries with history of hyperinflation which has rendered confidence scarce and independent monetary policy no longer usable [30].

1.3 The Swiss franc target zone

Future prices move randomly due to the efficient market hypothesis. In hindsight, however, prices reflect more than just a random process. Since prices are assumed to always reflect the exact value of an asset at every time they tell us a story about the development of this asset. This is particularly true for exchange rates because they express the relative economic health and prosperity of two currency unions.

In this thesis we will be mainly concerned with the analysis of euro to Swiss franc (EUR/CHF) exchange rate. Let us thus review the history of the EUR/CHF exchange rate in order to have not just a quantitative, but also a qualitative understanding of the data sets that will be analyzed with several mathematical tools in the following sections.

The Swiss franc has a long reputation as being a *safe haven currency*, meaning a relatively stable currency in a politically and economically well-developed, secure state. While this can be mainly attributed to Switzerland's reputation as a safe country in general, investors also perceive the Swiss franc as a stable currency since Switzerland has always had a large percentage of its currency backed with gold reserves. During most of the twentieth century, and long after the breakdown of Bretton Woods [98], the Swiss franc remained legally linked to gold. For one thing, public opinion in Switzerland generally held gold in high esteem as a symbol of monetary stability. More importantly, however, a reduction in the gold stock required a fundamental reform of the legal framework of the Swiss monetary system. The process leading up to suitable legislative reforms was lengthy and complex. In 1999, the Swiss National Bank (SNB) finally decided that gold reserves of 2'500 tons (per capita, this was more than five times the amount of gold than the second-ranked Netherlands) were no longer required for monetary purposes and started to sell more than 1'000 tons over the course of five years. By international comparison, the SNB has continued to hold a very significant stock of gold [35].

As mentioned in section 1.1, economics, unlike physics, is not stationary. When looking at the development of the EUR/CHF exchange rate over the last 15 years (figure 1.3) several regimes can be seen and related to different economic and geopolitical developments. When the euro was introduced in 1999, its value was set to 1.58 Swiss francs. Until March 2000, in regime I, a plateau is observed which implies more or less steady conditions in both economies. This is followed by a depreciation

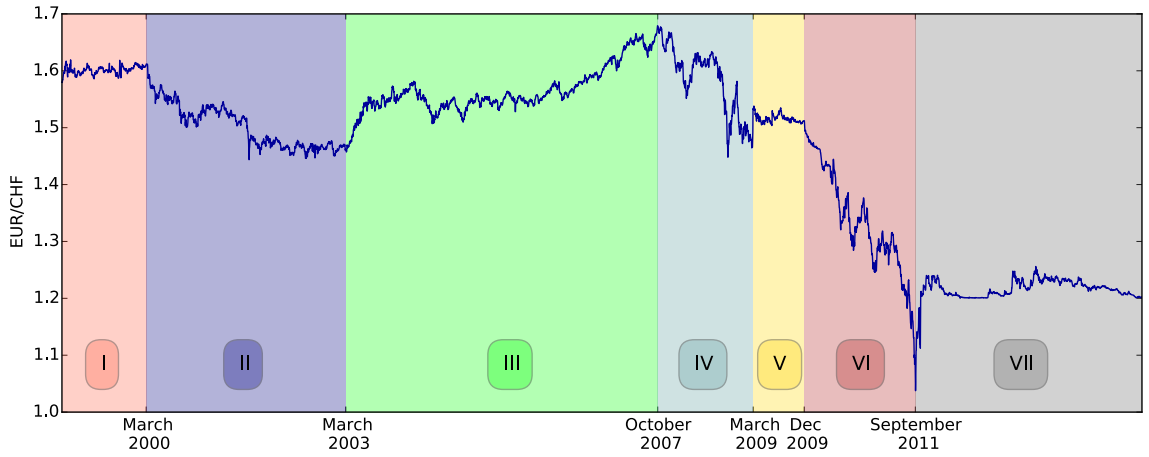

Figure 1.3: Development of the EUR/CHF exchange rate ever since the inception of the euro in 1999. The shaded regions I-VII denote different economic and geopolitical regimes. Starting from a relatively neutral development (I) the Swiss franc gains in value in regime II due to a lack of credibility of the euro zone. In regime III, the tide has turned and the belief in the newly established currency union is high. The Swiss franc appreciates again during the 2008 global financial crisis (IV), stagnates (V), appreciates even more during the European sovereign debt crisis (VI) and is finally halted by the 1 EUR $\geqslant$ 1.20 CHF target zone established by the SNB in September 2011 (VII).

of the euro against the Swiss franc (and several other major currencies) during roughly three years, until March 2003 (regime II). There have been many debates about the economic reasons behind the steady weakening of the euro and indeed many arguments can be found (see for instance [62] for a detailed discussion). Broadly speaking, the weakening can be attributed to an initial lack of credibility of the euro zone. On the one hand, there was a lagging implementation of structural reforms in many of the euro countries which are necessary for the flexibility of the euro market to fully unfold. On the other hand, the identification with the "Euroland", an economically and politically homogeneous union, had not yet fully succeeded. These tendencies are finally turned in the subsequent regime. Regime III shows the period of the "European dream", guided by the belief that the creation of the euro zone leads to prosperity and that the euro would replace or at least be a significant competitor to the US dollar for international commerce. This development peaked in October 2007 at around 1.67 Swiss francs per euro just before entering regime IV, the 2008 global financial crisis. After a short plateau between March and September 2009 (regime V), we can see the deep impact of the European debt crisis in regime VI. The debt crisis lead to investors losing faith in the European currency union and seeking investments in more stable currencies, among them the Swiss franc. This implied a continuous increase in demand and thereby a significant increase in value for the Swiss franc. Although being a country with a highly appreciated currency seems like a good thing, the Swiss economy suffered from the developments in regime VI. Switzerland is largely depending on its exports, of which most of them go to countries in the euro zone. When the value of the Swiss franc rises relative to the euro a potential customer in the euro zone will all of a sudden have to pay more euros for the same Swiss good. This, in turn, leads to a reduced demand of Swiss export goods and hence to a weakened Swiss economy. In September 2011, when the EUR/CHF parity was approaching an incredibly low exchange rate of one euro per Swiss franc, passive monetary policies (e.g. interest rates) were no longer effective and the SNB decided to intervene actively in the market which brings us to regime VII. On the 6th of September 2011, the SNB stated in a press release [92]: "The current massive overvaluation of the Swiss franc poses an acute threat to the Swiss economy

and carries the risk of deflationary development. The Swiss National Bank is therefore aiming for a substantial and sustained weakening of the Swiss franc. With immediate effect, it will no longer tolerate a EUR/CHF exchange rate below the minimum rate of CHF 1.20. The SNB will enforce this minimum rate with the utmost determination and is prepared to buy foreign currency in unlimited quantities." Hence, what we see in region VII is the result of an extremely interesting and uncommon establishment of a target zone. The Swiss franc is freely floating against the euro until it comes close to 1.20. At this point the SNB itself becomes an FX customer and demands large amounts of euro. This leads to an increased supply of Swiss franc and an increased demand for euro on the FX and therefore lowers the relative value of the Swiss franc.

During the several years that the SNB has been defending the exchange rate the euro has indeed never been valued less than 1.20 Swiss francs, with one small exception [93]: On the 5th of April 2012, a few of the transactions were concluded at a rate below the minimum exchange rate set by the SNB. What happened was that within just a few seconds the EUR/CHF exchange rate fell from 1.2020 to 1.2000. Despite SNB offers placed in the trading systems, a few isolated transactions occurred below 1.20 Swiss francs per euro. However, at no time did the best available euro exchange rate in the market fall below the minimum exchange rate of CHF 1.20. Thus, for a short time, what is known as *segment market* could be observed, in which transactions below the best price were concluded. This situation was remedied within very few seconds, however, by means of arbitrage. How could transactions take place below CHF 1.20 per euro despite the fact that the SNB was at all times present in the market? As explained in section 1.2, the FX is a decentralized market. Rather than foreign exchange being traded on a bourse, forex transactions are made directly between market participants. Each bank has its own individual group of counterparties, and, in particular, banks with lower ratings only have a small number of counterparties. The exchange rate below 1.20 Swiss francs per euro were concluded by banks that do not have an agreement relating to limits with the SNB, in other words, by banks that cannot or do not wish to trade with the SNB. The SNB was prepared at all times to buy unlimited quantities of euros. All market participants were at all times aware of this SNB purchase offer, including the banks without an agreement relating to limits. Consequently, banks which sold euros for less than 1.20 Swiss francs did not receive the best market price and had - relatively speaking - to accept losses. Since there is no compulsion to make business transactions at the best prices, such anomalies cannot always be excluded. However, they can only be maintained for a very short period. The following operational organization of the SNB allows the implementation of the minimum exchange rate: Since the introduction of the minimum exchange rate, the SNB has monitored the foreign exchange market from market opening in Asia on Sunday evening to market closing in New York on Friday evening without any interruption. The same applies to holidays. The interbank market, which is the market of relevance for the SNB, includes its counterparties. The SNB accepts well over 100 banks with more than 700 trading desks as counterparties. Thanks to this network of contacts, the global foreign exchange market is almost completely covered. On the part of the SNB, the trading limits amount to some hundreds of billions of euros a day. These limits can be flexibly adjusted by the SNB, should this be necessary. Via electronic trading systems, the banks have access at all times to the offers. The SNB's strategy for implementing the minimum exchange rate has proved effective. On the relevant interbank market, CHF 1.20 per euro qualifies as the lowest exchange rate. Consequently, the minimum exchange rate applied at all times.
A similar case was observed on the 25th of December 2014 where some banks offered euros for less than 1.20 Swiss francs, and hence traded below the highest bid [61].

It is important to note that the classification in figure 1.3 into regimes is not a final, official or unique in any way. It is merely an attempt of the author to provide a rough overview over the different economic and geopolitical circumstances that stood behind the development of the exchange rate during different times. The main message that we want to make here is the importance of conditional thinking in economic analysis. An economic theory is rarely true for all market or for all times.

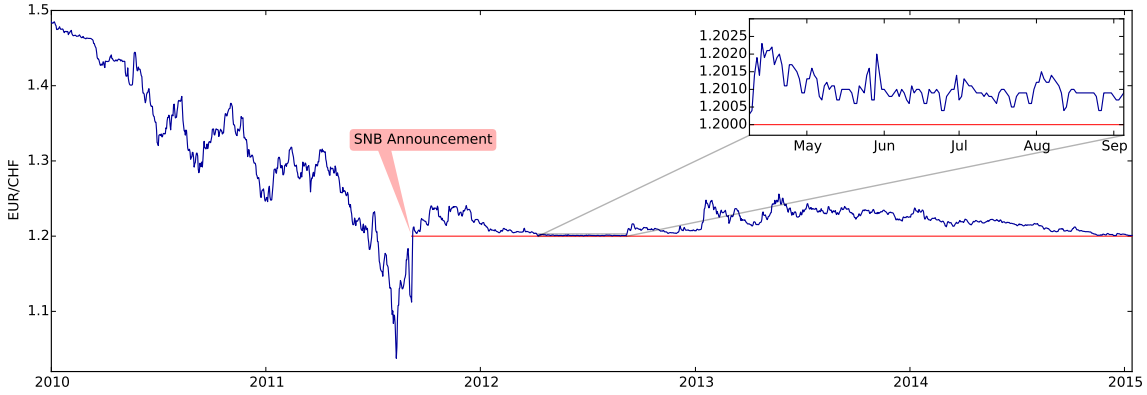

Figure 1.4: Development of the EUR/CHF exchange rate after the announcement of the Swiss franc target zone on the 6th of September 2011. The red line denotes the fixed barrier at EUR/CHF = 1.20. Particular attention should be paid to the time interval between the 8th of April and the 5th of September 2012 (magnified) which comes closest to what we can call stationary conditions. In the second half of 2012 and during 2013 the exchange rate is slightly more departed but remains looming large over the barrier. The dynamics looks clearly different from a free float. In the second half of 2014 the euro slowly but steadily depreciates due to the *Swiss Gold Initiative* and even more importantly due to fiscal and political changes in the euro zone.

Thus, when testing an economic theory it should not be applied blindly to any given data set. One should rather examine the *time series* [2] first by eye and make sure that the data represents relatively steady conditions. The exact definition and appropriateness of "steady conditions" depends on the individual problem at hand.

In this thesis we are interested in the dynamics taking place in regime VII which itself can be subdivided into several regimes. In figure 1.4 the more recent development of the exchange rate is depicted. The red line denotes the fixed EUR/CHF = 1.20 barrier after the SNB announcement on the 6th of September 2011. We can see that right after the announcement the situations seems to relax a bit. This can be either due to the active repulsion by the SNB, due to a a cooling of the market in reaction to the announcement or a decreased demand of Swiss francs triggered by exogenous events. However, we also see that this was just a temporary movement. The trend reverses yet again and the exchange rate approaches the barrier more and more. Particular attention should be paid to the period between April and September 2012 (magnified in figure 1.4). During several months the exchange rate remains remarkably close to the barrier and the dynamics appear particularly steady. This is why in the following, whenever we propose a certain model, we will test the theory with data from this region first. We shall also refer to the regime between the 8th of April and the 5th of September 2012 as *the stationary region*. The pressure on the Swiss franc finally relaxed in September 2012 after European Central Bank's president Mario Draghi's famous speech [19] in which he announced that the European Central Bank would do whatever if takes to preserve the euro. The stationary region is followed by a period in which the exchange rate is slightly more departed from the barrier. But nevertheless it remains looming large over the barrier and does not show the typical behavior of a free float. During this period the SNB has repeatedly stated that they had not actively intervened in the FX market ever since September 2012.

A rough indicator for the activity of the SNB on the FX can be obtained by looking at its balance

[2] A time series is just a sequence of data points where each data point has a timestamp. Data sets of financial assets are typically of this form.

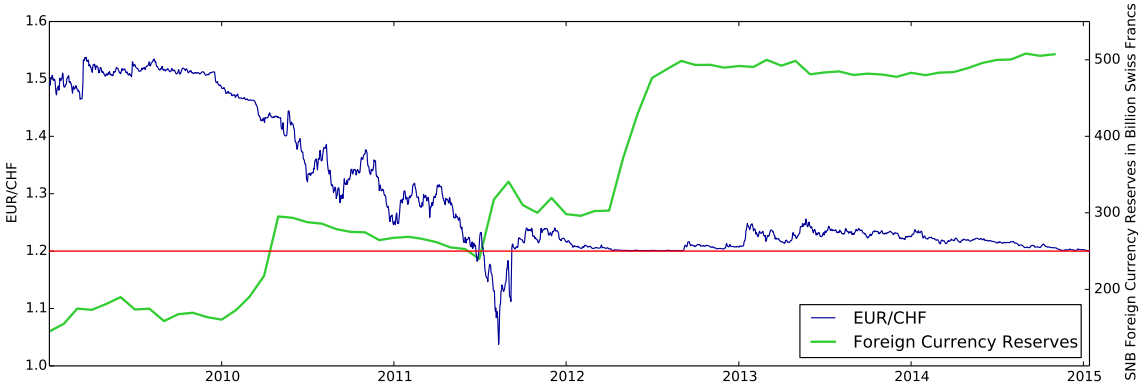

Figure 1.5: The blue line denotes the EUR/CHF exchange rates. The green line represents monthly data of the SNB's foreign currency reserves downloaded from [77]. Increasing reserves serve as a proxy for the active intervention on the FX by the SNB. We can see that the SNB has already intervened heavily during the crises in 2010 but without announcing this to the public. As we will discuss later, an unannounced intervention is much more "expensive" than an announced one. As anticipated, we see a significant increase of reserves in the stationary region and a relatively constant development thereafter, hinting that indeed the SNB had not been active after September 2012. In the last quarter of 2014 the euro had been slowly but steadily depreciating. It came so close to 1.20 Swiss francs that the SNB was forced to intervene yet again in December 2014 and January 2015 resulting in even more foreign currency reserves. This is not visible here because until the time of writing the balance sheet had not been updated on the SNB homepage.

sheet. Figure 1.5 depicts the foreign currency reserves as a function of time where we associate increasing foreign currency reserves with the intervention of the SNB on the FX. We can see that the SNB has already intervened heavily during the crises in 2010 but without announcing this to the public. As we will discuss later, an unannounced intervention is much more "expensive" than an announced one. As anticipated, we see a significant increase of reserves in the stationary region and a relatively constant development thereafter, hinting that indeed the SNB has not been active after September 2012.

In the last quarter of 2014, in light of the *Swiss Gold Initiative* [94] as well as several geopolitical and fiscal changes in the euro zone [60], the euro has been slowly but steadily depreciating. It came so close to 1.20 Swiss francs that the SNB was forced to intervene yet again in December 2014 and January 2015 resulting in even more foreign currency reserves. (This is not visible in figure 1.5 because until the time of writing the balance sheet had not been updated on the SNB homepage).

Completely unexpected for many market participants and during times of consistent pressure on the Swiss franc, the SNB stated on the 15th of January 2015 [95]: "The Swiss National Bank is discontinuing the minimum exchange rate of CHF 1.20 per euro. [...] The minimum exchange rate was introduced during a period of exceptional overvaluation of the Swiss franc and an extremely high level of uncertainty on the financial markets. This exceptional and temporary measure protected the Swiss economy from serious harm. While the Swiss franc is still high, the overvaluation has decreased as a whole since the introduction of the minimum exchange rate. The economy was able to take advantage of this phase to adjust to the new situation. Recently, divergences between the monetary policies of the major currency areas have increased significantly - a trend that is likely to become even more pronounced. The euro has depreciated considerably against the US dollar and this, in turn, has caused the Swiss franc to weaken against the US dollar. In these circumstances,

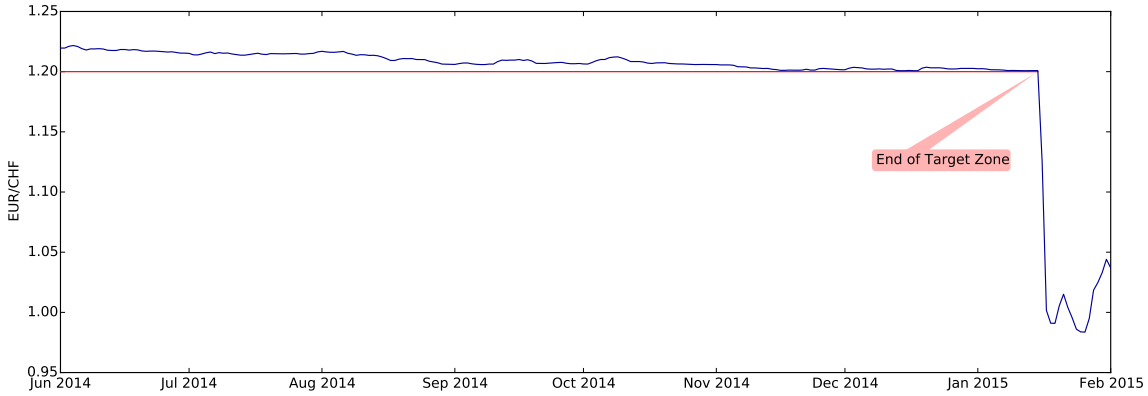

Figure 1.6: On the 15th of January 2015 the SNB abandoned its prevailing target zone policy and let the EUR/CHF exchange rate float freely. The consequence was a 30% decline in just one day.

the SNB concluded that enforcing and maintaining the minimum exchange rate for the Swiss franc against the euro is no longer justified. [...] The SNB will continue to take account of the exchange rate situation in formulating its monetary policy in future. If necessary, it will therefore remain active in the foreign exchange market to influence monetary conditions." (Compare this last statement to the definition of a "dirty float" in section 1.2.)

The consequences were immediate and severe: In just one day (and even more when looking at intra day price fluctuations) the exchange rate dropped by 30 percent (figure 1.6) and the Swiss Market Index (SMI) declined by more than 14 percent. This unexpected decision of the SNB and its tremendous impact on the Swiss economy presents a research topic in and of itself and was documented by a myriad of media reports and interviews all over the world (see for instance [5, 17, 47] and many more). A detailed discussion is beyond the scope of this thesis and we will focus rather on the EUR/CHF exchange rate during September 2011 and early January 2015.

It is the aim of this thesis to examine the dynamics that arise from imposing a lower barrier to the EUR/CHF exchange rate. We start in the next section by comparing this situation to a physical particle that is restricted by a wall. In section 3 we take a more empirical approach and fit the data to a general Itô process. Section 4 backs our findings from a theoretical point of view and establishes a link to other research that has been done in this field. Finally, in section 5, we point out an analogy between physical hindered Brownian motion in a fluid and the movement of market prices seen as the result of a constantly changing order book. Section 6 summarizes.

2 Physical models for foreign-exchange markets

In the previous section we have given a qualitative introduction to the dynamics of the EUR/CHF exchange rate. In this section we aim to quantify the special dynamics of this exchange rate by setting up a mathematical model. Throughout this process we abstract from the problem at hand and rely on purely physical analogies. We start by describing an effective repulsive potential that arises when a Brownian particle is subject to a confined configuration space. We proceed by deriving a stochastic differential equation which is supposed to capture all the essential characteristics of the exchange rate dynamics in the SNB target zone. We then verify the model numerically by estimating the second and third cumulant of the time series. Finally, we propose yet another approach to the problem which is based on renormalization group theory.

2.1 Brownian motion in a potential

Instead of seeing the process depicted in figure 1.4 as the stochastic movement of the EUR/CHF exchange rate we can also rely on a physical analogy: The movement of a one-dimensional Brownian particle subject to a wall at height 1.20. We can then use a well-established law from statistical physics, the emergence of an *effective entropic potential*.

Consider a one-dimensional Brownian particle that can move freely along the entire line of real numbers. What happens if we impose an impenetrable barrier at $x = 0$ such that the particle is restricted to move only in the upper half line $x > 0$ and is repelled whenever it touches the barrier at $x = 0$? Statistically speaking, this amounts to a reduction in entropy since the barrier has bisected the configuration space of the particle. We are now going to show that this change in entropy gives rise to an entropic repulsive potential that drops like the reciprocal of its distance to the barrier.

Denote by Z_N the partition function of a random walker taking N steps in presence of a (reflecting) barrier. In Appendix I we show that the partition function scales in leading order like

$$Z_N \sim N^{-1/2}. \tag{2.1}$$

Following Fisher [27], we can now find the repulsive potential by considering the *reduced free energy per step*

$$f_N \sim -\log\left(\frac{Z_{N+1}}{Z_N}\right) = \frac{1}{2}\log\left(1+\frac{1}{N}\right) \sim \frac{1}{N}. \tag{2.2}$$

Now we use (and show in Appendix I) that the (average) distance x of the random walk from the barrier scales like the square root of N. Hence, statistically speaking, we then arrive at

$$f_N \sim \frac{1}{x^2}. \tag{2.3}$$

So indeed, we have a long-range repulsive $1/x$ potential as was claimed above.

When we simulate a random walk in presence of a barrier (figure 2.1) we can see that the random walk is clearly affected by the barrier when close to it. The more steps taken, the more regions are explored since the average distance to the wall scales like $\sqrt{N}$ (see Appendix I). The behavior of the walk from figure 2.1 is clearly different from what we observe in figure 1.4. This implies that the "particle" in figure 1.4 is not only subject to a repulsive long-range potential but there must also be force $G = G(x,t)$ which pushes the particle towards the barrier. It is a priori not clear what the form

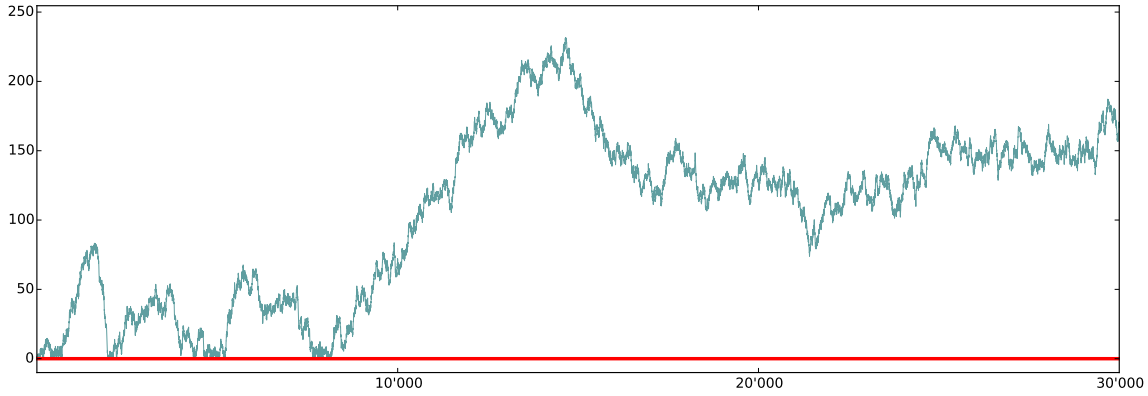

Figure 2.1: Simulation of an unbiased random walk starting at $x = 1$ with $N = 30'000$ steps and a repulsive barrier at $x = 0$ (red line). The average distance from the barrier scales like $\sqrt{N}$.

of G should be. As was already pointed out in section 1.1, in economics everything is dynamic and not stationary like many problems in physics are. This is why we have denoted the force G with an explicit t dependence which makes it extremely difficult to come up with a reasonable form for G. The best we can do is assume that at least during certain time periods G is approximately stationary. Considering the region between April and September 2012 in figure 1.4 it seems plausible to assume that during this time the economic pressure was approximately constant. Therefore, we hypothesize that, in first approximation, the EUR/CHF exchange rate $X(t)$ from figure 1.4 can be modeled as a Brownian particle moving in a potential

$$V(X) = \frac{c}{X - 1.20} + F \times (X - 1.20), \qquad X > 1.20 \tag{2.4}$$

where $c > 0$ and $F > 0$ are some constants (figure 2.3). We expect that if this description holds, then in particular for the data between April and September 2012. It is therefore this region that we examine first.

2.2 Exchange rate dynamics in a target zone

Quite generally, we can make the ansatz that the EUR/CHF exchange rate X (or analogously, a Brownian particle at position X) follows an Itô process

$$\dot{X} = f(X, t) + g(X, t)\eta(t) \tag{2.5}$$

where f, g are two arbitrary, Itô-integrable functions. The function $t \mapsto \eta(t)$ denotes uncorrelated white noise with

$$\mathbb{E}\left[\eta(t)\right] = 0 \tag{2.6}$$

and

$$\mathbb{E}\left[\eta(t)\eta(t')\right] = 2\delta(t - t'). \tag{2.7}$$

where δ stands for the Dirac-delta distribution. Here and in the following, we denote (theoretical) expectation values by $\mathbb{E}$ and (empirical) means by $\langle\cdot\rangle$. Mathematicians prefer to denote an Itô process rather by

$$dX = f(X, t) + g(X, t)dW(t) \tag{2.8}$$

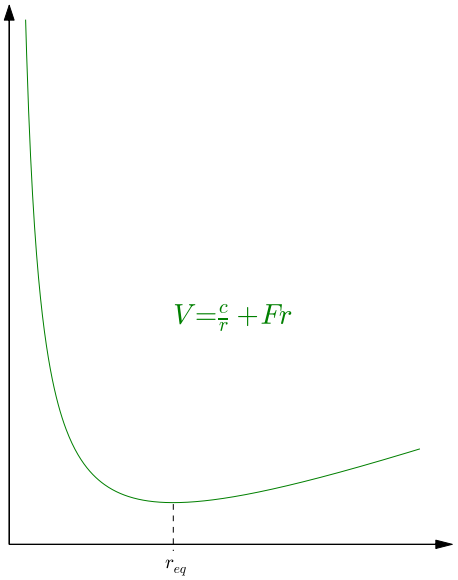

Figure 2.2: Graph of potential (2.4) with $c = F = 1$ and $r \equiv X - 1.20$. The EUR/CHF exchange rate after September 2011, when the SNB started to defend a minimum exchange rate of 1.20 Swiss francs per euro, are expected to be in a potential of this form at least in first approximation of stationarity. The decaying, repulsive part comes from the $1/r$ (long-range) entropic potential due to the barrier. The attractive part represents the economic distress which strengthens the Swiss franc relative to the euro. The minimum r_{eq} represents the stable equilibrium. Clearly, the potential is asymmetric around r_{eq}.

with $dW_t = \eta(t)dt$ the Brownian motion, also called Wiener process. We assume that the reader is familiar with the basics of stochastic differential equations. See [58] for a crash course and [63] for a solid introduction with applications. Stochastic differential equations are part of a mathematical branch called *stochastic calculus*. In-depth mathematical introductions to the topic are given in [39, 66]. Introductions with specific emphasis on applications in finance are found in [38, 81, 82]. For applications in natural sciences [33] may be consulted.

It should be pointed out that throughout this thesis all the stochastic integrals and differential equations are interpreted in the Itô-, and not in the Stratonovich-sense. The Stratonovich calculus best represents situations where rapidly fluctuating quantities with small but finite correlation times are parametrized as white noise. The Itô calculus is used when discrete uncorrelated fluctuations are approximated as continuous white noise. Hence, continuous physical systems are normally described by the Stratonovich calculus, whereas financial markets are best modeled by the Itô calculus [90,102]. Another way to see that finance requires Itô's interpretation is that it respects causality. Think of an investor buying an asset of price X at time t. The price increment dX can only depend on information up to time t and the invested amount is fixed during the infinitesimal time step dt. Only after it has changed by an amount dX at a later time $t + dt$ the investment can be readjusted.

Let us introduce the variable $r \equiv X - 1.20 > 0$ and denote the equilibrium position of potential (2.4) by r_{eq}. Furthermore, we denote by $x = r - r_{\text{eq}}$ the deviation of the EUR/CHF exchange rate from this equilibrium. A first idea to model the exchange rate in the potential V as a stochastic differential equation (2.5) is in terms of an Ornstein-Uhlenbeck process [97] where the curvature

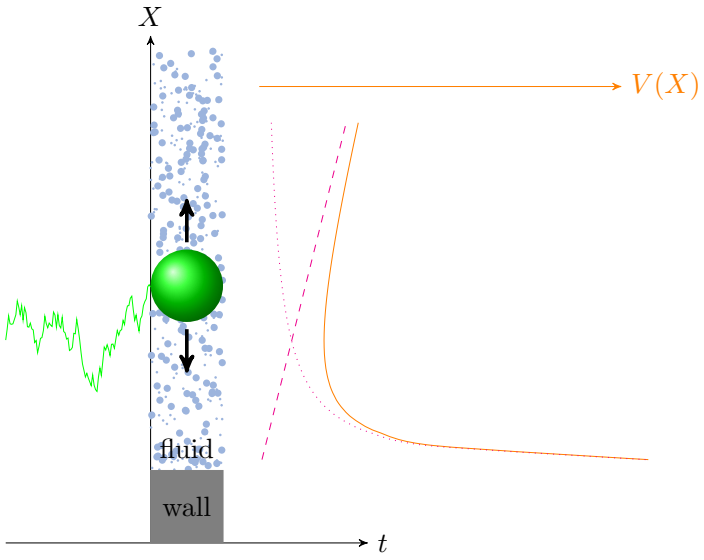

Figure 2.3: Random trajectory (green line) of a one-dimensional Brownian particle moving in a potential $V(X)$ (orange line). This potential is the sum of an attractive potential (purple, dashed line) and a repulsive potential (purple, dotted line). From a physical perspective, one would expect the EUR/CHF exchange rate between September 2011 and January 2015 to be controlled by such force potentials.

$V^{(2)}(r_{\text{eq}}) \equiv V''(r_{\text{eq}}) \equiv \frac{d^2V}{dr^2}\Big|_{r=r_{\text{eq}}}$ of the the potential V in equilibrium controls the volatility [3]

$$\dot{x} = -V''(r_{\text{eq}})x + g\eta. \tag{2.9}$$

Here, we have chosen g as a constant. Note that g is also called the *diffusion coefficient* [4] in physics or the volatility (coefficient) in finance. The problem with equation (2.9) is that it is symmetric under $x \mapsto -x$ and hence neglects the asymmetry of the potential (2.4) around its equilibrium position (see figure 2.2). The next simple process which respects this asymmetry can be obtained by considering a Taylor approximation of V up to third order:

$$V(X) = V(r_{\text{eq}} + x) = \underbrace{V(r_{\text{eq}})}_{\equiv 0} + \underbrace{V'(r_{\text{eq}})}_{=0} x + \frac{1}{2}V^{(2)}(r_{\text{eq}})x^2 + \frac{1}{6}V^{(3)}(r_{\text{eq}})x^3 + \mathcal{O}\left(x^4\right) \tag{2.10}$$

with $V^{(n)}$ the n-th order derivative of V. This leads us to a stochastic differential equation (SDE)

$$\begin{aligned}\dot{x} &= -\frac{d}{dX}V(X) \\ &\approx -V^{(2)}(r_{\text{eq}})x - \frac{1}{2}V^{(3)}(r_{\text{eq}})x^2.\end{aligned} \tag{2.11}$$

Setting the derivative of potential (2.4) to zero

$$0 \stackrel{!}{=} \frac{dV}{dr}\Big|_{r=r_{\text{eq}}} = -\frac{c}{r_{\text{eq}}^2} + F \tag{2.12}$$

[3] In finance, *volatility* is usually defined as the standard deviation of returns

[4] In a physical context, Brownian motion describes the movement of a particle that is suspended in a fluid. It can then be shown [21] that the diffusion coefficient depends on the size of the particle as well as on temperature and viscosity of the surrounding fluid.

we find that the equilibrium position satisfies

$$r_{\text{eq}} = \sqrt{\frac{c}{F}}. \tag{2.13}$$

The second derivative in equilibrium then reads

$$V^{(2)}(r_{\text{eq}}) = \left.\frac{d^2V}{dr^2}\right|_{r=r_{\text{eq}}} = 2\sqrt{\frac{F^3}{c}} \tag{2.14}$$

while for the third derivative we find

$$V^{(3)}(r_{\text{eq}}) = \left.\frac{d^3V}{dr^3}\right|_{r=r_{\text{eq}}} = -6\frac{F^2}{c}. \tag{2.15}$$

Finally, we have derived the following SDE for the EUR/CHF exchange rate:

$$\dot{x} = 3\frac{F^2}{c}x^2 - 2\sqrt{\frac{F^3}{c}}x + g\eta(t). \tag{2.16}$$

In particular, we have now an asymmetric distribution around the equilibrium point $x = 0$. However, this comes with a price: we have a non-linear stochastic differential equation. In the next section, we discuss a way to test our theory (2.16) without solving the actual equation.

2.3 Exchange rate dynamics: An empirical test

In the previous section we have set up a stochastic differential equation (2.16) modeling the EUR/CHF exchange rate after September 2011. In a next step, we must, of course, find a way to verify the theory empirically. Since the direct solution of (2.16) is difficult, we have set up an extensive framework which allows us to calculate the moments and cumulants of solutions to (2.16) perturbatively. This method relies heavily on the use of *Feynman path integrals* and *Feynman diagrams*. We thus present here just the results and give a detailed derivation in Appendix II.

We find that the variance $\mathbb{V}$ of the solution to (2.16) obeys

$$\mathbb{V}\left[x(t)\right] \sim r_{\text{eq}}^3. \tag{2.17}$$

Since (2.16) is asymmetric around its equilibrium position r_{eq} we can also find a non-vanishing *skewness*

$$\gamma\left[x(t)\right] \equiv \mathbb{E}\left[\left(\frac{x - \mathbb{E}\left[x\right]}{\sqrt{\mathbb{V}\left[x\right]}}\right)^3\right] \sim r_{\text{eq}}^2. \tag{2.18}$$

The idea is now to test the theory (2.16) by measuring variance and skewness of the time series. To this end, we proceed as follows:

(i) We download tick data [5] of the EUR/CHF exchange rate ranging from the 8th of April to the 6th of September 2012 from [1]. The time series consists of approximately 1.5 million data points. Furthermore, the data contains a bid and an ask column. We work with the mean $\frac{1}{2}\left(\text{bid} + \text{ask}\right)$ since it is the centre of the bid-ask-spread that incorporates all the information of the market and therefore changes randomly [70].

[5] *Tick data* denotes time series where the prices are not recorded in equal time intervals but every occurring price change is tracked.

(ii) We iterate over the data with a moving window of size n. Denote by $X_1, \ldots, X_n$ the data points (EUR/CHF exchange rate) in the i-th window. Then, we calculate r_{eq} of the i-th window as

$$r_{\text{eq}}[i] \equiv \text{median}\left\{X_1 - 1.20, X_2 - 1.20, \ldots, X_N - 1.20\right\}. \tag{2.19}$$

Furthermore, we calculate from $X_1 - 1.20, \ldots X_n - 1.20$ the variance $\mathbb{V}[i]$ and the skewness $\gamma[i]$.

(iii) Denote the amount of considered windows by k. We plot the data points $\big(r_{\text{eq}}[i], \mathbb{V}[i]\big)$ and $\big(r_{\text{eq}}[i], \gamma[i]\big)$ logarithmically for $i = 1, \ldots, k$. If (2.16) holds, we expect to see a straight line with a slope equal to three for the variance plot (equation (2.17)) and a straight line with a slope equal to two for the skewness plot (equation (2.18)).

(iv) We repeat steps (ii) and (iii) for several values of n. Concretely, we define the size of the moving window n in units of time: 10 minutes, 1 hour, 2 hours, 4 hours, 8 hours and 1 day.

Before this can be implemented we must clarify how to calculate the variance and skewness in step (ii) numerically. It is tempting to simply approximate the m-th moment by

$$\mathbb{E}\left[X^m\right] \approx \langle X^m \rangle \equiv \frac{1}{n} \sum_{i=1}^{n} X_i^m \tag{2.20}$$

However, not only is convergence of (2.20) slow for "large" values of m, it even turns out that this estimator is flawed when considering high-frequency data. We do not want to go into detail what the problems exactly are but we rather refer to specific literature [2, 34, 104, 105] instead. For the measurement of the variance we work with the *PARK estimator* [64]

$$\mathbb{V}_P \equiv \frac{(H - L)^2}{\log 16} \tag{2.21}$$

where H denotes the largest (highest) and L the smallest (lowest) value in the data. For the skewness, we work with the *Bowley coefficient* [9]

$$\gamma_B \equiv \frac{Q_{75\%} - 2Q_{50\%} + Q_{25\%}}{Q_{75\%} - Q_{25\%}} \tag{2.22}$$

where $Q_{p\%}$ stands for the empirical p-percent quantile of the considered dataset. We are now ready to implement the algorithm described above. The outcome for the variance is shown in figure 2.4 and the one for the skewness is depicted in figure 2.5 and figure 2.6. It can immediately be seen that the expected scaling laws do not even hold remotely. It seems that somewhere our reasoning went wrong. Lets see how we can elaborate on this.

2.4 The interfacial model

Since the simple idea of an entropic repulsive potential was not successful we have been thinking where it could have gone wrong. In fact, we will reveal section 4 that our ansatz is fundamentally wrong since we have not incorporated an important economic principle into our reasoning. But before we do so, let us - for purely didactical reasons - quickly present one more idea that we have examined. We do so because we think that although not applicable here, the method still has its merits. Readers who are only interested in results directly applicable to the EUR/CHF exchange rate can skip this section and keep on reading in section 3.

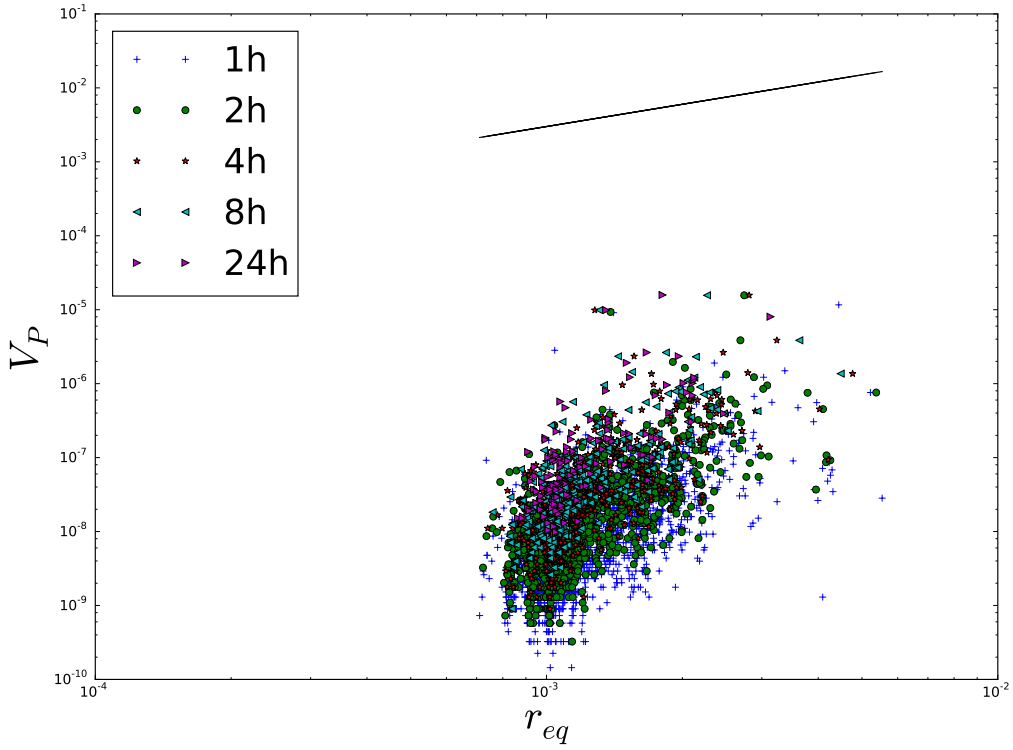

Figure 2.4: Logarithmic plot of the PARK variance (2.21) as a function of the empirically observed equilibrium (2.19). Several different window sizes are shown, as is described in the algorithm (i)-(iv) in the text above. According to (2.17) a linear relationship with a slope equal to three (see black slope as reference) is expected. This is not what is observed here.

As above, we will completely abstract from the problem of the EUR/CHF exchange rate and think purely physically in terms of a Brownian particle in presence of a barrier located at $X = 1.20$. The approach we take now is based on a method called *renormalization group* (RG). The RG is a very deep and rich model which is well-known in theoretical physics where it is used to describe systems at criticality. A qualitative introduction to the subject is provided by Nobel laureate Kenneth Wilson [101]. More quantitative introductions with applications to physics can be found for instance in [28, 36, 78, 88, 100]. For readers without a background in physics there is an introduction by Sornette [85] where the central limit theorem from statistics is proofed using arguments from renormalization group.

The repulsive part in potential (2.4) was derived under the assumption that we have a fixed barrier at 1.20 and a rigid interaction between the particle and the barrier. The particle moves freely until it touches the barrier. It is then repelled and keeps on moving freely until it touches the barrier again. This reasoning is similar to the interaction between, say, two billiard balls. Denote by r the distance between the two balls. Then, in *non-smooth mechanics* [11], their interaction is modeled by a *hard-core potential*

$$V_{\text{HC}}(r) = \begin{cases} 0, & r > 0 \\ \infty, & r = 0. \end{cases} \tag{2.23}$$

The billiard balls do not feel each other until they touch. Once they are in contact, energy and momentum is exchanged instantaneously and the balls keep on moving freely. While this rigid way

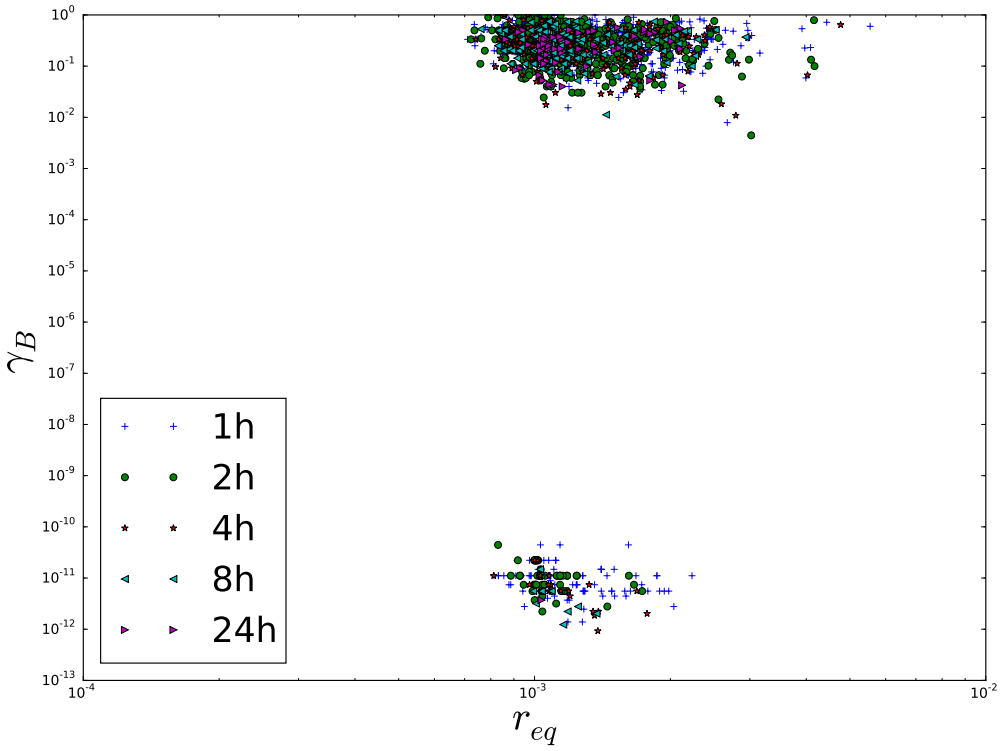

Figure 2.5: Logarithmic plot of the Bowley coefficient (2.22) as a function of the empirically observed equilibrium (2.19). Several different window sizes are shown, as is described in the algorithm (i)-(iv) in the text above. According to (2.18) a linear relationship with a slope equal to two is expected. This is not what is observed here. We note furthermore that there are two clusters. The lower cluster represents values where the skewness is basically zero. The reason is that there are times where the exchange rate remains unchanged for several hours. Figure 2.6 shows the upper cluster in more detail.

of modeling the interaction between two billiard balls is justified on a macroscopic scale, we know that microscopically the world is actually smooth. Assume that you look at the interaction between two billiard balls "under a magnifying glass". If you magnified sufficiently, you would see that the hard-core repulsion that is observed macroscopically is actually mediated through a smooth repulsive Coulomb potential V_C, governed by the laws of electrodynamics. In the language of RG we would say that upon renormalization ("zooming out") the smooth Coulomb potential V_C is renormalized into a hard-core repulsive potential V_{HC}. This reasoning forms the basis of our next idea. It seems unrealistic to assume that the SNB is waiting idle until the EUR/CHF is exactly at 1.20 and only then they start to interact. Much rather, the SNB starts trading against the Swiss franc already to a certain amount when EUR/CHF > 1.20 and they gradually increase their activity as the Swiss franc becomes stronger. Physically, this gives rise to a particle which feels a smoothly repelling potential V_{SNB}, for instance of exponential form. Roughly speaking, our idea is now the following: We assume that there is some microscopic potential V_{micro} in which the particle is undergoing a Brownian motion. This potential is the sum of the trading strategy of the SNB, V_{SNB}, and some exogenous potential, V_{ECO}, representing the economic distress. This microscopic potential is, however, not directly empirically accessible since it depends on many unknown details. What is accessible is the renormalized, macroscopic potential $V_{\text{micro}} \to \mathcal{R}\left[V_{\text{micro}}\right] \equiv V_{\text{macro}}$. The idea is then that we can

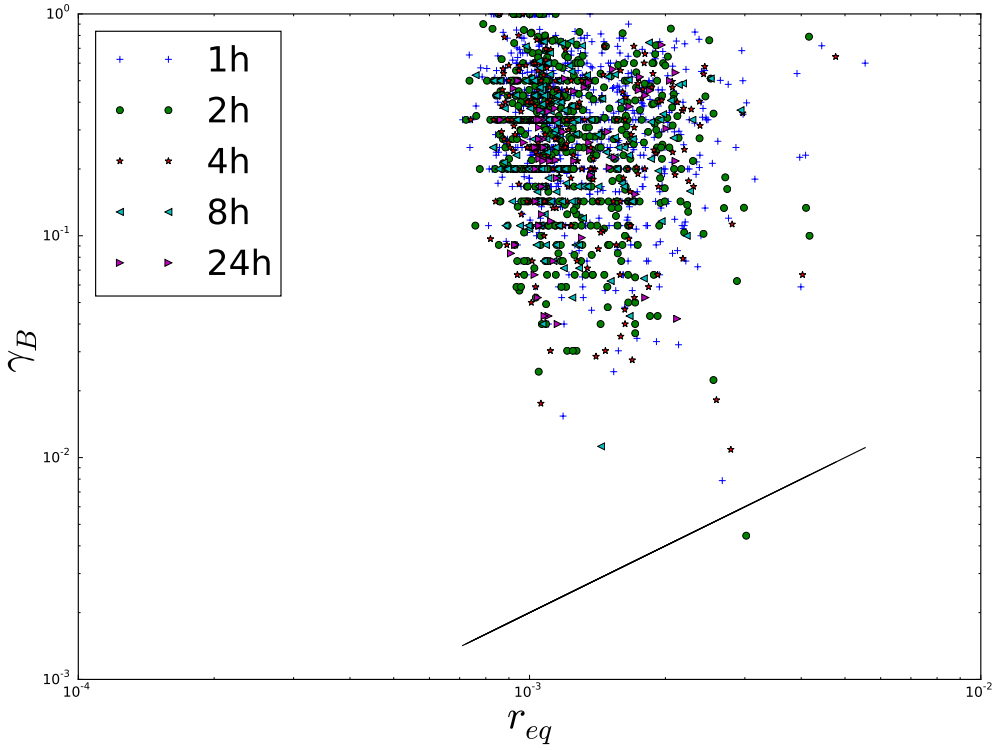

Figure 2.6: Logarithmic plot of the Bowley coefficient (2.22) as a function of the empirically observed equilibrium (2.19). Several different window sizes are shown, as is described in the algorithm (i)-(iv) in the text above. According to (2.18) a linear relationship with a slope equal to two (see black slope as reference) is expected. This is not what is observed here.

try several forms of microscopic potentials and see if the corresponding renormalized potential fits empirical observations. This allows us to gain insights into the underlying microscopic structure, such as the trading strategy of the SNB.

A random walk in the $(t, \vec{x})$ plane (t is the time-coordinate, $\vec{x}$ the $(D-1)$-dimensional space-coordinate) can also be modeled as a fluctuating $(D-1)$-dimensional interface in D-dimensional space with a non-zero *surface tension* σ [87]. This analogy enables us to rely on the extensive work that has been done on the interaction between fluctuating surfaces in statistical physics. Overviews are provided in [46, 51, 80, 87]. In our case we have $D = 2$ and the fluctuating surface is rather a fluctuating line than a surface. The surface (or line) tension σ controls the amplitude of the fluctuations. In the context of finance, σ can thus be related to the volatility. Without loss of generality we let D denote any dimension and set $D = 2$ only in the end.

We are working with the *interface displacement model* (IDM) in D dimensions where we consider the $z = 0$ plane as the $(D-1)$-dimensional hard wall. We denote points in this plane by the vector $\rho = (x_1, \ldots, x_{D-1})$. One configuration of a $(D-1)$-dimensional interface is given by the function $z(\rho)$ where z denotes the distance of the interface from the wall (height) at position ρ. The Hamiltonian of the IDM takes the form

$$\mathcal{H}(z) = \int \mathrm{d}^{D-1}\rho \, \left(\frac{\sigma}{2} \left| \nabla_\rho z(\rho) \right|^2 + V(z(\rho)) \right). \tag{2.24}$$

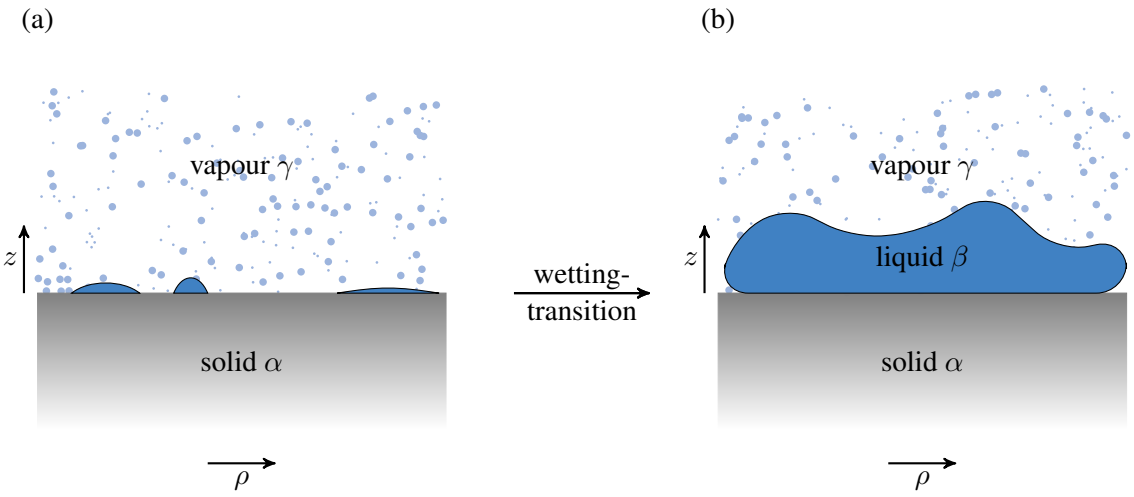

Figure 2.7: A typical physical application of the interface Hamiltonian (2.24) is the description of a wetting transition. In figure (a) we have what is called *partial wetting*, where the intermediate phase β is not fully covering the bulk phase α (e.g. a solid wall) such that the bulk phases α and γ (e.g. vapour) are in direct contact. A wetting transition occurs when the thickness of the intermediate phase β becomes infinite (macroscopic) and there is no more direct α-γ contact. We have then a *completely wetted surface* shown in (b). Such a phase transition from (a) to (b) can be described as the unbinding of the β-γ-interface from the wall.

The first term of (2.24) controls the fluctuations of a free surface. The second term of (2.24), the potential V (or V_{micro}), is the sum of all direct, i.e. "microscopic" interaction potentials between the wall and the interface. By microscopic we mean that these are the bare, in some sense "point-wise mediated" interactions that are independent of the interfaces as a whole. Physically, these are typically Van der Walls forces, Coulomb forces etc. In our case V consists of a repulsive part due to the SNB and of an attractive part due to economic distress.

In physics, the Hamiltonian (2.24) has many applications. It can be seen as the direct interaction of a fluctuating surface with a rigid wall or as the interaction of two fluctuating surfaces (where $z(\rho)$ then just denotes the relative distance between the two surface at a position ρ). One can then examine the highly non-trivial interplay between repulsive and attractive forces which lead to phase transitions from bound to unbound states, see for instance [52, 53, 83, 87]. Often, (2.24) is also used for the description of *wetting transitions*. When we think of wetting, we think of water, or any other liquid, in contact with a solid (e.g. dish or a piece of cloth). This is exactly one of the models one can always keep in mind: a solid, inert substrate covered with a film of liquid in equilibrium with its vapour. The word *wetting*, however, came to have a more general meaning, describing phenomena where no liquid is present. Wetting occurs whenever a phase, β, intrudes between phases α and γ with α, β and γ in coexistence (or one of them inert). If the thickness of the wetting layer is infinite (macroscopic) we say the phase β wets the $\alpha - \gamma$ interface (figure 2.7). It can happen that as the control parameters of the system (such as temperature) are changed we go from a non-wet to a wet situation. We say we went through a wetting transition [6]. See [6, 27, 50] for details.

The "interaction" between the EUR/CHF exchange rate and the 1.20 barrier is of course not that of two rigid straight lines. The EUR/CHF exchange rate as a function of time traces out a fluctuating line (surface). Due to these undulations, different parts of the random-walk-line are exposed to different repulsive and attractive forces, depending on their distance to the barrier. These complex interactions can be taken into account by renormalizing the potential V into a renormalized potential V_ℓ in which all the effects of fluctuations up to a certain scale ℓ are integrated out. In terms of the

visualization via billiard balls, this means that we "zoom out" by a factor of ℓ and calculate what the potential looks like at this magnification. For the interested reader, we present a thorough derivation of this renormalized potential in Appendix III where we work with a method known as *functional renormalization group*. In the end, the renormalized potential is found to be

$$V_\ell(z) = \frac{e^{(D-1)\ell}}{\sqrt{2\pi}\delta(l)} \int_{-\infty}^{\infty} dz'\, V_0(z')\, \exp\left(-\frac{(\gamma(\ell)z - z')^2}{2\delta^2(\ell)}\right) \tag{2.25}$$

where

$$\delta(\ell) = \frac{2\left(e^{(3-D)/\ell} - 1\right)}{(3-D)\bar{\sigma}} \tag{2.26}$$

denotes the width of the convolution,

$$\bar{\sigma} = \frac{(2\pi)^{(D-1)/2}\Gamma\left(\frac{D-1}{2}\right)\sigma\beta}{\Lambda^{D-3}} \tag{2.27}$$

is just a constant and

$$\gamma(\ell) = e^{\frac{3-D}{2}\ell} = b^{\frac{3-D}{2}} = b^{\zeta_b} \tag{2.28}$$

is called the *rescaling factor*. See Appendix III for a detailed explanation of all the variables involved. This is quite a neat close form solution since any microscopic potentials V can be plugged into (9.30) and we can readily read of its renormalized form. As practical as this result is in theory, it will not be useful in our further analysis. The reason is that we have taken the analogy between finance and physics too far and while doing so we have been neglecting fundamental economical principles. This will be explained in detail in section 4.

3 Extracting equations from financial time series

As already in the previous section, our goal is to find a suitable stochastic differential equation (2.5) which models the EUR/CHF exchange rate in the target zone enforced by the SNB since September 2011. Our previous analysis in terms of steric entropic interactions has not been successful. Therefore, in this section, we take a more direct approach by fitting the functions f and g in (2.5) to the time series of the EUR/CHF exchange rate. We start by deriving expressions for f and g as limits of realized observations. We then discuss an algorithm which allows us to extract f and g approximately from the data. Using a Monte-Carlo scheme, the validity of the algorithm is tested on a model equation. Next, the algorithm is applied to the EUR/CHF exchange rate. Finally, we discuss the numerical stability of the presented results.

3.1 Iteration of an Itô process

Motivated by the derivation of Risken [68] we want to express f and g in equation (2.5) as a limit of realized values X. It will be of crucial importance to make the distinction between Itô's and Stratonovich's definition for the stochastic integral. Hence, it is best to do the derivation with some mathematical rigor and we will therefore be working with the mathematician's notation. We start by writing (2.5) in the equivalent form

$$X(t+\tau) - X = \int_t^{t+\tau} dt'\, f(X(t'),t') + \int_t^{t+\tau} dW(t')\, g(X(t'),t') \tag{3.1}$$

where X is short for $X(t)$ and $W(t)$ is a Wiener process. In a physicist's notation, we have

$$w(\tau) \equiv W(t+\tau) - W(t) = \int_t^{t+\tau} dt'\, \eta(t'). \tag{3.2}$$

Since $\eta(t)$ is Gaussian distributed, so is $w(\tau)$. Using (2.6) and (2.7) we find furthermore

$$w(0) = 0 \tag{3.3}$$
$$\mathbb{E}\left[w(\tau)\right] = 0 \tag{3.4}$$
$$\mathbb{E}\left[w(\tau_1)w(\tau_2)\right] = 2\min\left\{\tau_1,\tau_2\right\}. \tag{3.5}$$

These are the defining properties of the Wiener process and so we see that the physicist's notation is consistent with the mathematician's.

Assume that f and g can be expanded in their first argument,

$$f(X(t'),t') = f(X,t') + f'(X,t')\left(X(t') - X\right) + \ldots \tag{3.6}$$

with

$$f'(X,t') \equiv \frac{\partial}{\partial X} f(X,t') \equiv \frac{\partial}{\partial X(t')} f(X(t'),t')\Big|_{X(t')=X} \tag{3.7}$$

and similar for g. We can plug this expansion both for f and g into (3.1) and obtain

$$X(t+\tau) - X = \int_t^{t+\tau} dt'\, f(X,t') + \int_t^{t+\tau} dW(t')\, g(X,t') \tag{3.8}$$

$$+ \int_t^{t+\tau} dt'\, f'(X,t') \left(X(t') - X\right) + \int_t^{t+\tau} dW(t')\, g'(X,t') \left(X(t') - X\right) \tag{3.9}$$

$$+ \dots$$

For the zeroth order approximation (3.8) we have just

$$\int_t^{t+\tau} dt'\, f(X,t') + \int_t^{t+\tau} dW(t')\, g(X,t') = f'(X, t+\Theta_1\tau)\tau + g(X, t+\Theta_2\tau) w(\tau) \tag{3.10}$$

for some $\Theta_{1,2} \in [0,1]$ which is a direct consequence of the *mean-value theorem* of integration theory and its stochastic analogon, see [44]. The first order approximation (3.9) can be iterated by expanding $X(t') - X$ as

$$X(t') - X = \int_t^{t'} dt''\, f(X(t''),t'') + \int_t^{t'} dW(t'')\, g(X(t''),t'')$$

$$= \int_t^{t'} dt''\, f(X,t'') + \int_t^{t'} dW(t'')\, g(X,t'') + \dots \tag{3.11}$$

$$+ \int_t^{t'} dt''\, f'(X,t'') \left(X(t'') - X\right) + \int_t^{t'} dW(t'')\, g'(X,t'') \left(X(t'') - X\right) + \dots \tag{3.12}$$

Plugging this expansion into (3.9), taking expectation values on both sides and using (3.3)-(3.5) we find in first order

$$\mathbb{E}\left[X(t+\tau) - X\right] = f(X, t+\Theta_1\tau)\tau$$

$$+ g'(X, t+\Theta_3\tau) g(X, t+\Theta_2\Theta_3\tau) \mathbb{E}\left[\int_0^{\tau} dW(\tau')\, w(\tau')\right]. \tag{3.13}$$

Now we use that

$$\mathbb{E}\left[\int_0^{\tau} dW(\tau')\, w(\tau')\right] \overset{\text{Itô}}{=} \mathbb{E}\left[\frac{w^2(\tau)}{2} - \tau\right] \overset{(3.5)}{=} 0 \tag{3.14}$$

from which we finally conclude

$$f(X,t) = \lim_{\tau\to 0} \frac{1}{\tau} \mathbb{E}\left[X(t+\tau) - X\right]. \tag{3.15}$$

Higher order corrections are at least of linear order in τ and hence negligible in the limit where $\tau \to 0$. Note that (3.14) is different in the Stratonovich interpretation where we have

$$\mathbb{E}\left[\int_0^{\tau} dW(\tau')\, w(\tau')\right] \overset{\text{Stratonovich}}{=} \mathbb{E}\left[\frac{w^2(\tau)}{2}\right] \overset{(3.5)}{=} \tau \tag{3.16}$$

and thus

$$f(X,t) + g'(X,t)g(X,t) \overset{\text{Stratonovich}}{=} \lim_{\tau\to 0} \frac{1}{\tau}\mathbb{E}\left[X(t+\tau) - X\right]. \tag{3.17}$$

We see that the distinction between Itô's and Stratonovich's definitions of stochastic integrals leads to non-trivial differences and hence it is important that we stick to Itô's definitions. In this thesis we are always using Itô's results (see also section 2.2).

In the same fashion that we have just derived (3.15) we can also find

$$g^2(X,t) = \lim_{\tau\to 0} \frac{1}{\tau}\mathbb{E}\left[(X(t+\tau) - X)^2\right]. \tag{3.18}$$

3.2 Extracting equations from empirical data

In the previous section we have found that the functions f and g in (2.5) can be written as the limits [6]

$$f(X,t) = \lim_{\tau\to 0} \frac{1}{\tau}\mathbb{E}\left[X(t+\tau) - X\right] \tag{3.19}$$

$$g(X,t) = \sqrt{\lim_{\tau\to 0} \frac{1}{\tau}\mathbb{E}\left[(X(t+\tau) - X)^2\right]}. \tag{3.20}$$

Let us now assume that we are examining a stationary process, $f(X,t) = f(X)$ and $g(X,t) = g(X)$. If we are given a time series with corresponding measured data of high frequency, i.e. τ is small, we can approximate

$$f(X) \approx \frac{1}{\tau}\left\langle X(t+\tau) - X\right\rangle \tag{3.21}$$

$$g(X) \approx \sqrt{\frac{1}{\tau}\left\langle (X(t+\tau) - X)^2\right\rangle} \tag{3.22}$$

with $\langle\cdot\rangle$ the sample mean which converges to the expectation value $\mathbb{E}[\cdot]$ according to the law of large numbers. On this basis, Friedrich et al. [31] have suggested an algorithm which takes a time series and returns numerical approximations of f and g. It works as follows:

(i) We start from any given time series `ts` that is a realization of an Itô process (2.5) for some unknown functions f and g. It is assumed that the data comes with equally spaced time stamps of distance τ. We denote by $\texttt{ts}_{\texttt{min}} = \min(\texttt{ts})$ the minimum value and by $\texttt{ts}_{\texttt{max}} = \max(\texttt{ts})$ the maximum value in `ts`.

(ii) Divide the value range $[\texttt{ts}_{\texttt{min}}, \texttt{ts}_{\texttt{max}}]$ into K bins $B_1, \ldots, B_K$. Take the middle of each bin to discretize the value range $[\texttt{ts}_{\texttt{min}}, \texttt{ts}_{\texttt{max}}]$ into K discrete points $x_1, \ldots, x_K$. These x_i will serve as arguments for the sampled functions f and g below.

(iii) Iterate over `ts` and each value $X(t)$ in `ts` is assigned to its bin. So for each bin B_i we then have a list of n_i values $X(t_1), \ldots, X(t_{n_i})$ for some timestamps t_k. Furthermore, we do not only store the values $X(t_k)$ but also the proceeding value $X(t_k + \tau)$.

[6] Actually, from (3.18) we can only infer that $|g| = \sqrt{\ldots}$ but with g the volatility we can assume that g is a positive function.

(iv) For each bin B_i, now calculate

$$f_i \equiv \frac{1}{\tau}\frac{1}{n_i}\sum_{k=1}^{n_i}\left(X(t_k+\tau)-X(t_k)\right) \tag{3.23}$$

and

$$g_i \equiv \sqrt{\frac{1}{\tau}\frac{1}{n_i}\sum_{k=1}^{n_i}\left(X(t_k+\tau)-X(t_k)\right)^2}. \tag{3.24}$$

(v) Plot (x_i, f_i) and (x_i, g_i) for $i = 1, \ldots, K$. The plotted points will then indicate the functional form of $f(X)$ and $g(X)$.

Note that this algorithm works by just considering one single time series. This is why the assumption of a stationary process was necessary. If we have an explicit time-dependence, we would require several data sets of repeated measurements.

3.3 Extracting equations: A Monte Carlo test

Before applying the above algorithm (i)-(v) to actual data we are going to verify its validity with Monte Carlo simulations [40]. Concretely, we want to estimate the equation

$$\dot{X} = -X^3 + \left(0.3 \cdot X^2 + 1\right)\eta(t) \tag{3.25}$$

with initial value $X(t=0) = 0$. To this end, we solve equation (3.25) $L = 1'000$ times numerically using a Milstein scheme [57]

$$X(t+\Delta t) = X(t) + f(X(t))\Delta t + g(X(t))\Delta W(t) + \frac{1}{2}g(X(t))g'(X(t))\left[\Delta W(t)^2 - \Delta t\right] \tag{3.26}$$

consisting of $M = 50'000$ discrete time steps of size $\Delta t = 1/360$ (= 10 seconds in units of hours). Here, $\Delta W(t)$ denotes the independently, identically and normally distributed random increments with zero expectation value and variance Δt. Figure 3.1 shows an exemplary solution. Solving equation (3.25) L times numerically yields L sets of discrete approximate solutions $\{X_k\}^{(j)}$ for $j = 1, \ldots, L$ and $k = 1, \ldots, M$. For each solution $\{X_k\}^{(j)}$ we run the algorithm (i)-(v) from which we obtain L sets of points $\{X_i, f_i\}^{(j)}$ and $\{X_i, g_i\}^{(j)}$ for $j = 1, \ldots, L$ and $i = 1, \ldots, K$ (compare with step (ii) from the above algorithm). Generally, of course, the $\{X_i\}^{(j)}$ differ for different realizations j. However, we can identify the arguments X_i from different numerical solutions by assigning them again to K bins $\tilde{B}_1, \ldots, \tilde{B}_K$ of equal size. For each bin $\tilde{B}_i$ we have now a set of values $\{f_j\}^{(B_i)}$ where the f_j are calculated from (3.23) and a set of values $\{g_j\}^{(B_i)}$ where the g_j are calculated from (3.24). For these two sets we can calculate median and 90% confidence interval. The outcome of this is shown in figure 3.2 and figure 3.3. We can see that the analytical solutions $f(X) = -X^3$ and $g(X) = 0.3X^2 + 1$ are indeed well-approximated. The confidence intervals widen with the distance from the origin. This effect is of statistical nature simply because data is more sparse towards the edges. We conclude that the algorithm (i)-(v) works well but results towards the edges should be considered more critically.

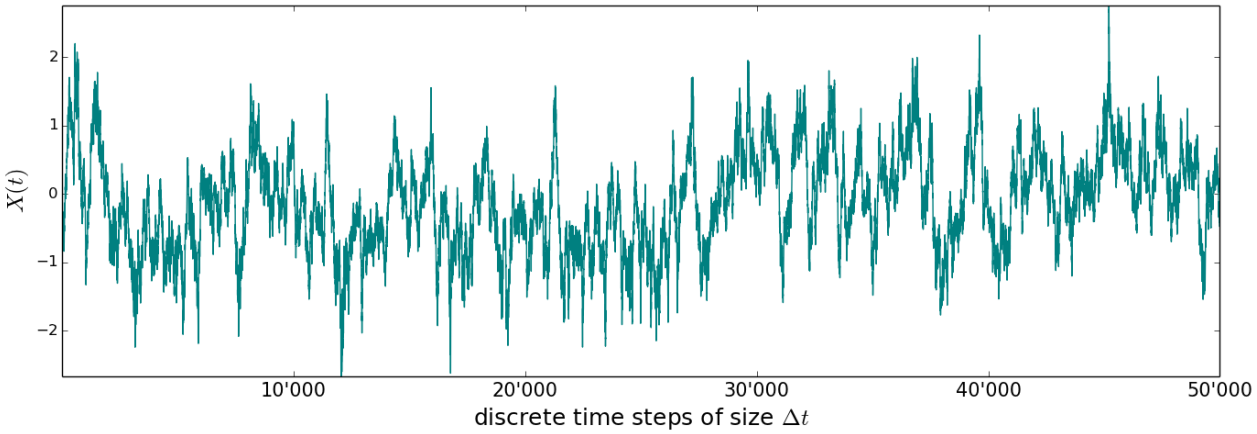

Figure 3.1: Example of a numerical solution to (3.25) using a Milstein scheme (3.26) with $M = 50'000$ steps and step size $\Delta t = 1/360$.

3.4 Empirical model for euro/Swiss franc exchange rate dynamics

We can apply the algorithm (i)-(v) from section 3.2 to the euro/Swiss franc exchange rate. To this end, we download tick-by-tick data of the EUR/CHF exchange rate between September 7,2011 and January 14, 2015 from [1] and upsample the data to ten second intervals by taking the median. This new time series of the EUR/CHF exchange rate in equally spaced 10 seconds intervals represents the time series that we have denoted by `ts` in the above algorithm (i)-(v). By definition, we have $\tau = 10$ seconds $= 1/360$ hours and we choose $K = 100$.

Of course, we must also analyze data before September 2011 in order to have a direct comparison between the dynamics before and after the barrier had been enforced. The target zone regime covers a time span of approximately 3 years. To examine a similar amount of data points, the analysis of other regimes should also cover about three years of data. Hence, we analyze data between 2005 and 2007 (figure 3.4) and between 2008 and 2010 (figure 3.5). We observe similar results for the 2005-2007 and for the 2008-2010 period for both f and g. Although there is considerable statistical noise, it can be inferred that f and g are both constant. More even, we can see that f is vanishing. This is in agreement with our reasoning in section 2 since there is no wall and hence no repulsive potential. Furthermore, there is no reason to assume a persistent one-sided economic distress (on small time-scales) which would justify the appearance of a short-term drift.

Now let us see how the results change during the target zone regime (figure 3.6). First of all, we notice that f is vanishing here as well (large fluctuations on the right edge are due to poor sampling). This is in direct contradiction to our reasoning in section 2 and explains why we were not successful. Indeed, we will argue in section 4 that from a theoretical point of view, f must necessarily be zero. This will reveal the fundamental error in our previous thinking. On the other hand, we observe a non-trivial behavior for g. Recall that in economic terms, g is equal to the volatility. We will sometimes also use nomenclature from random walk theory and interpret g as (proportional to) the average step length or mean free path. Hence, we see that the entire change in dynamics due to the barrier is hidden in g and not not in f. This is fundamentally different from the previous section where we have simply assumed the stochastic part g to be constant and focused purely on the deterministic f. We leave an interpretation of these findings for section 4.

The algorithm (i)-(v) from section 3.2 takes two parameters, the step size τ and the bin size K. Their

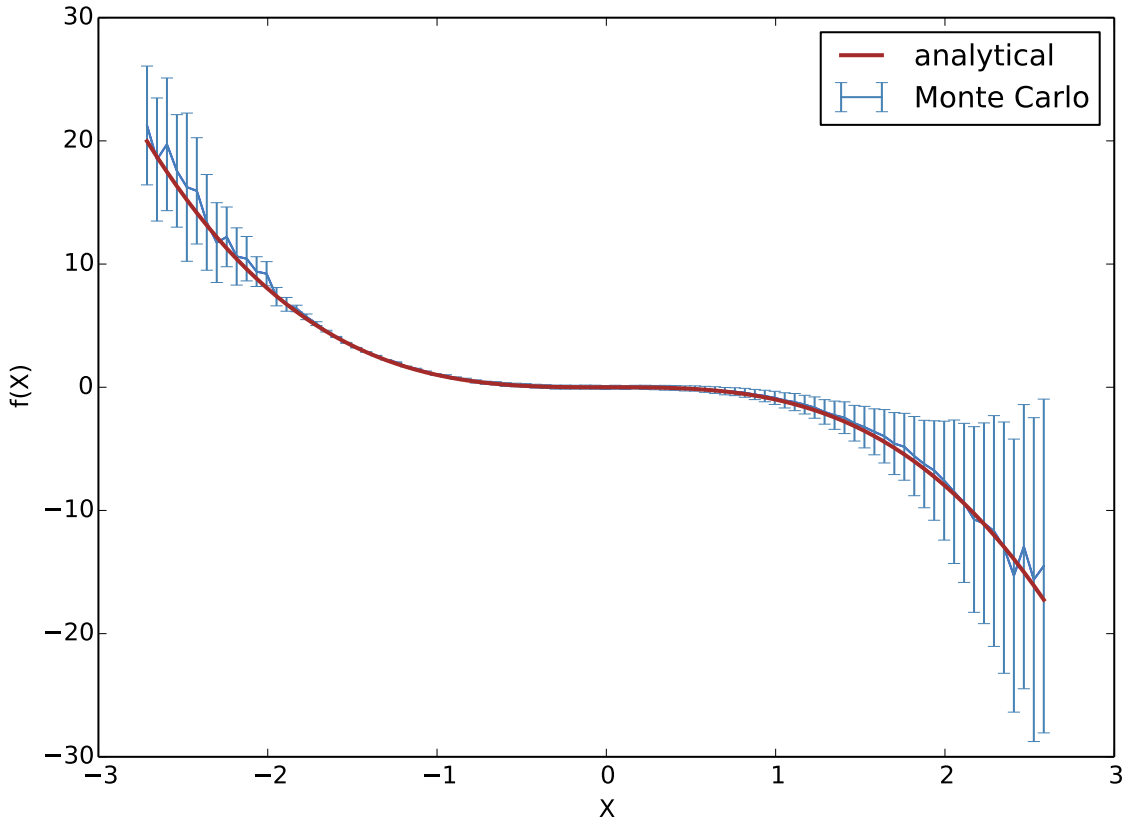

Figure 3.2: The red line shows the analytical form of $f(X)$ in equation (3.25). The blue line and error bars denote median and 90% confidence interval, respectively, as a result of solving equation (3.25) $L = 1'000$ times numerically using a Milstein scheme (3.26) with $M = 50'000$ steps and discrete time step $\Delta t = 1/360$. We can see that the analytical solution $f(X) = -X^3$ is indeed well-approximated. The confidence intervals widen with the distance from the origin (initial value). This effect is of statistical nature simply because data is more sparse towards the edges.

influence on the outcome should be discussed. The dependence on τ is quite subtle and is discussed in section 3.5 below. The dependence on K is intuitively clear: the larger K, the larger the bin size and consequently we have reduced statistical errors at the price of a less precise resolution of the shapes of f and g. So the choice of K is a trade-off situation. However, as figure 3.7 confirms, the result is not strongly dependent on the choice of K. The same holds for results of f and for other time spans.

3.5 Stability under first order corrections

When we have derived (3.15) and (3.18) we have dropped all corrections that were higher than zeroth order in τ since they would not contribute to the limit $\tau \to 0$ anyway. However, the algorithm that we have extracted from these results in section 3.2 is based on the approximation of finite, but small τ. We must thus ask if it was justified to neglect any correction terms coming from τ being finite.

Analytically, the correction terms can be derived in a straight forward manner as was outlined in

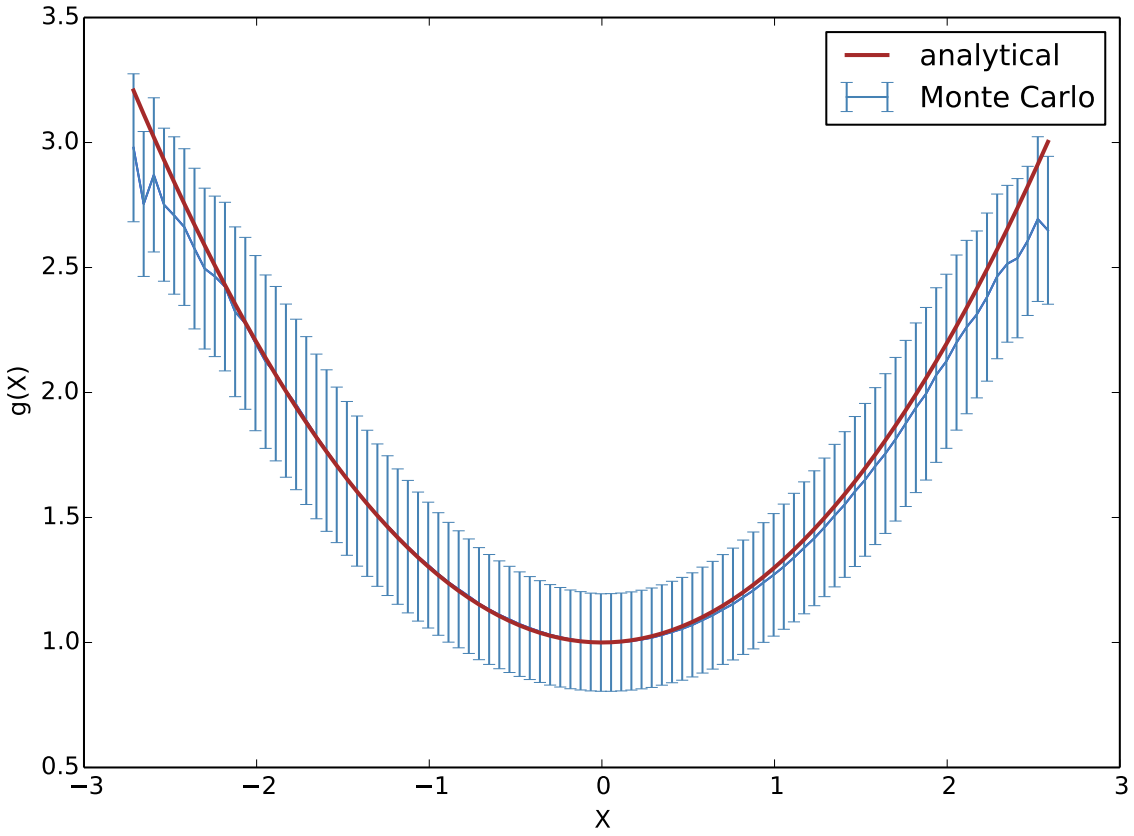

Figure 3.3: The red line shows the analytical form of $g(X)$ in equation (3.25). The blue line and error bars denote median and 90% confidence interval, respectively, as a result of solving equation (3.25) $L = 1'000$ times numerically using a Milstein scheme (3.26) with $M = 50'000$ steps and discrete time step $\Delta t = 1/360$. We can see that the analytical solution $g(X) = 0.3 \cdot X^2 + 1$ is indeed well-approximated. The further away from the origin (initial value) the more the blue line deviates from the red one. This effect is of statistical nature simply because data is more sparse towards the edges.

section 3.1. We simply have to iterate $X(t') - X$ in (3.9) and keep the terms of the next higher order. With some stochastic calculus and straight forward integral manipulations, one ends up with

$$\frac{1}{\tau}\mathbb{E}\left[X(t+\tau) - X\right] = f(X) + \left(\frac{1}{2}f(X)f'(X) + \frac{1}{4}f'(X)g^2(X)\right)\tau + \mathcal{O}\left(\tau^2\right) \tag{3.27}$$

$$\begin{aligned}\frac{1}{\tau}\mathbb{E}\left[\left(X(t+\tau) - X\right)^2\right] = g^2(X) + \Big(&f^2(X) + f'(X)g^2(X) + f(X)g(X)g'(X) \\ &+ \frac{1}{2}\left(g^2(X)\left(g'(X)\right)^2 + g^3(X)g''(X)\right)\Big)\tau + \mathcal{O}\left(\tau^2\right)\end{aligned} \tag{3.28}$$

We see that even simple forms of f and g give rise to non-trivial correction terms. Since f and g are a priori unknown we cannot use these analytical results to verify if the error is negligible. Therefore, Sura and Barsugli [90] suggest a method that they call *subsampling* the time series. Instead of running the algorithm on the entire time series, we skip every second value ($\tau \to 2\tau$) and consider if the results change significantly from the original sampling. This can be repeated several times ($2\tau \to 4\tau \to \ldots$). If the result (i.e. the shapes of f and g indicated by $\{(x_i, f_i\})$ and $\{(x_i, g_i)\}$) is

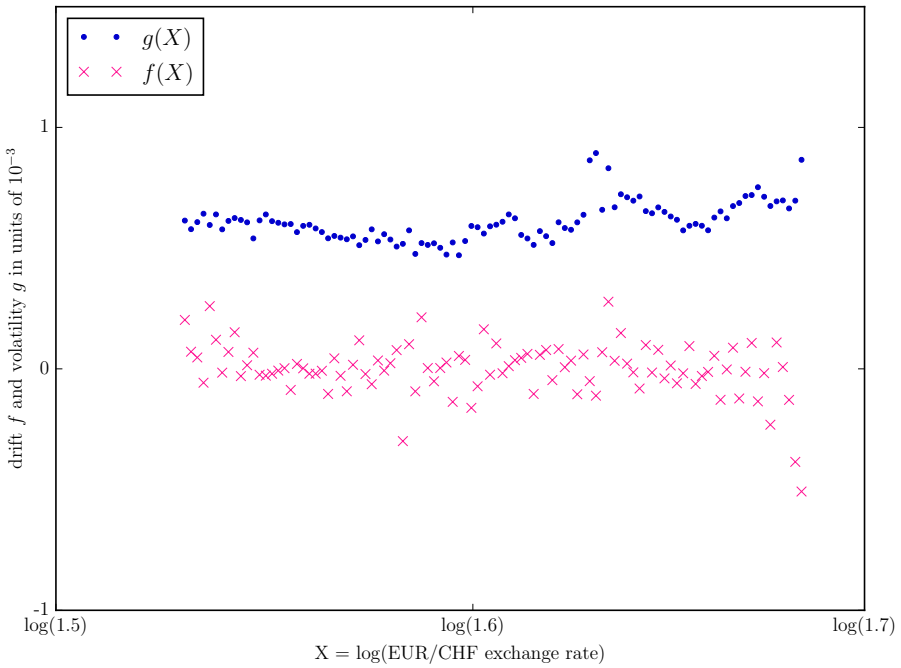

Figure 3.4: Approximation of the drift $f(X)$ and the volatility $g(X)$ from (2.5) using upsampled tick-by-tick data of the EUR/CHF exchange rate between January 2005 and December 2007. This figure is obtained by following faithfully the steps (i)-(v) described in section 3.2.

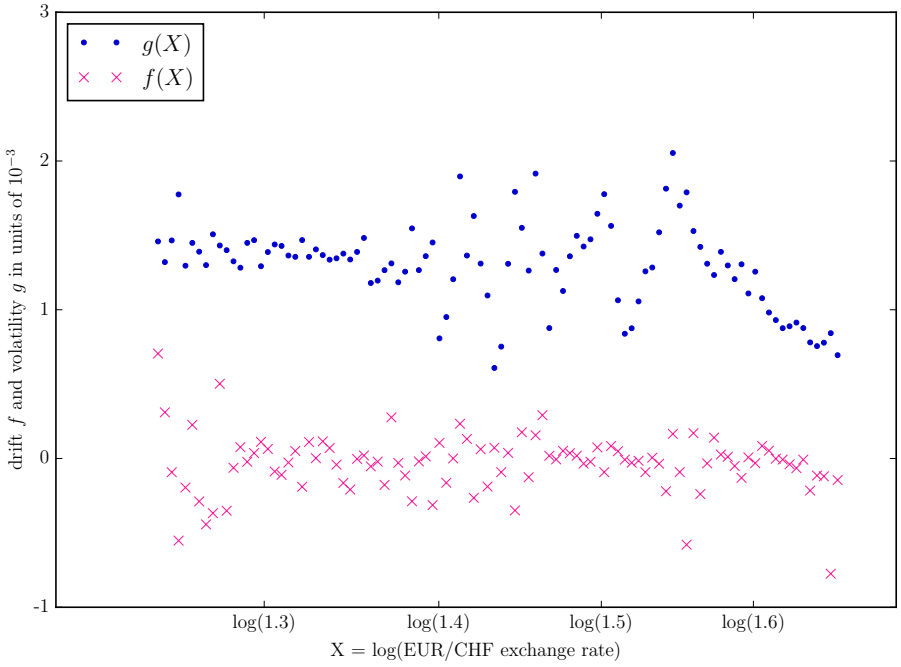

Figure 3.5: Approximation of the drift $f(X)$ and the volatility $g(X)$ from (2.5) using upsampled tick-by-tick data of the EUR/CHF exchange rate between January 2008 and December 2009. This figure is obtained by following faithfully the steps (i)-(v) described in section 3.2.

largely unaffected by this subsampling, we can be sure that the first order corrections in τ have little

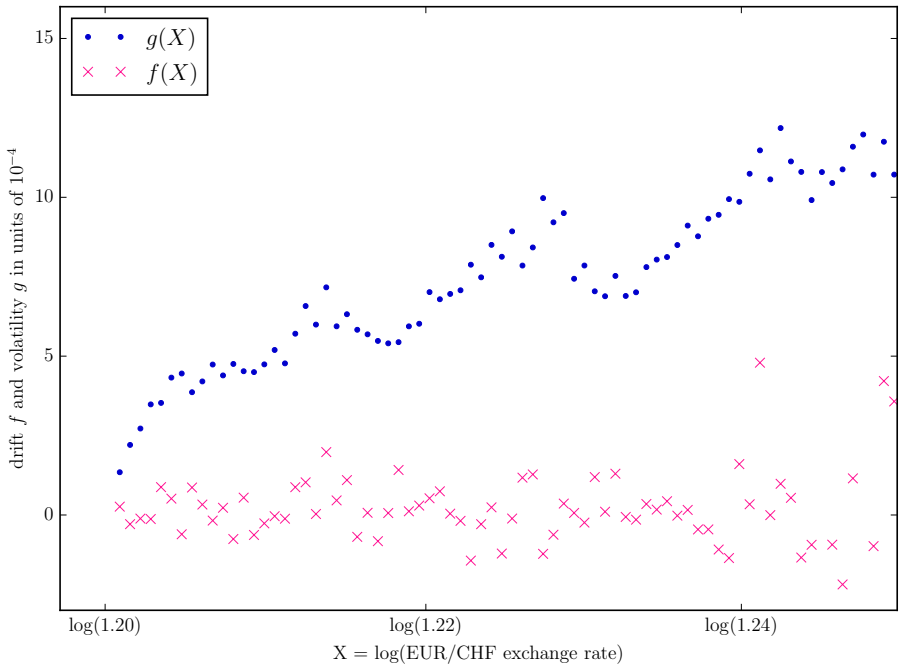

Figure 3.6: Approximation of the drift $f(X)$ and the volatility $g(X)$ from (2.5) using upsampled tick-by-tick data of the EUR/CHF exchange rate between September 7, 2011 and January 14,2015. This figure is obtained by following faithfully the steps (i) (v) described in section 3.2.

weight. Considering figure 3.8 shows that this is indeed the case. The same holds for results of f and for other time spans. We conclude that the first order approximations (3.21) and (3.22) are justified and the results reliable.

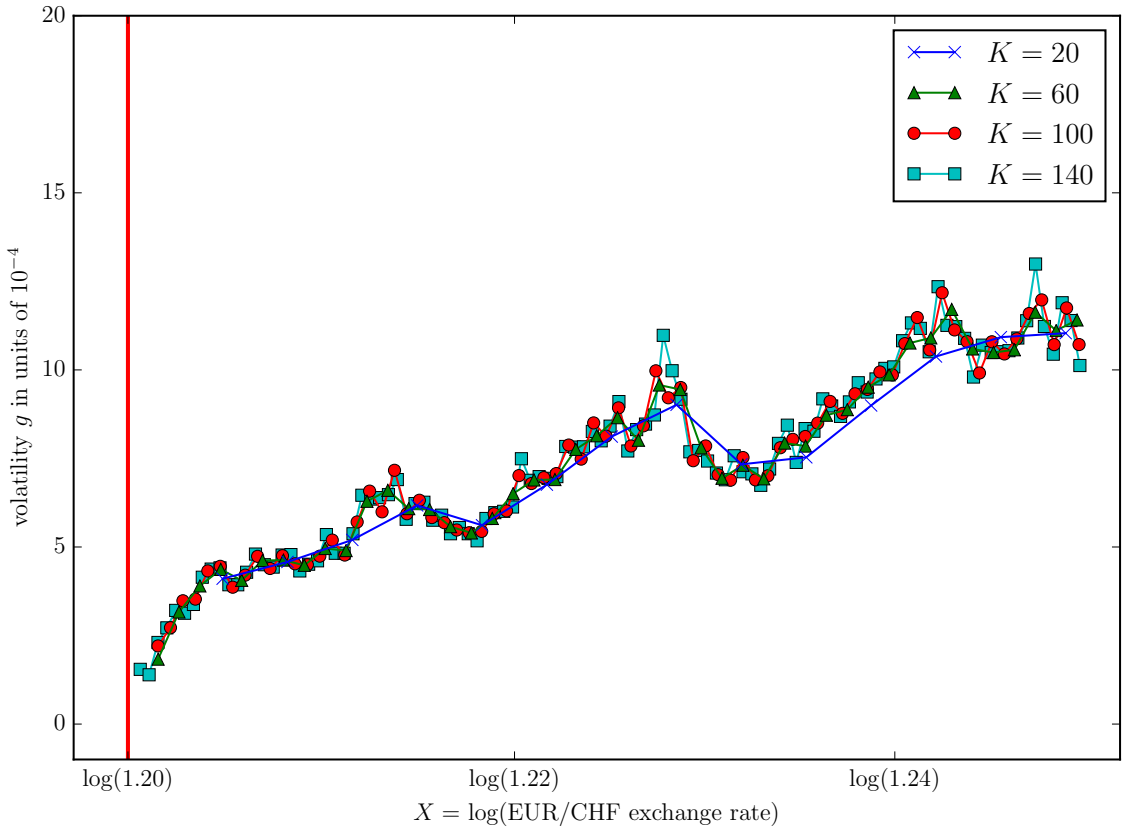

Figure 3.7: Approximation of the volatility $g(X)$ from (2.5) using upsampled tick-by-tick data of the EUR/CHF exchange rate between September 2011 and January 2015. This figure is obtained by following faithfully the steps (i)-(v) described in section 3.2. We see the choice of the number of bins K does not affect the indicated form of g.

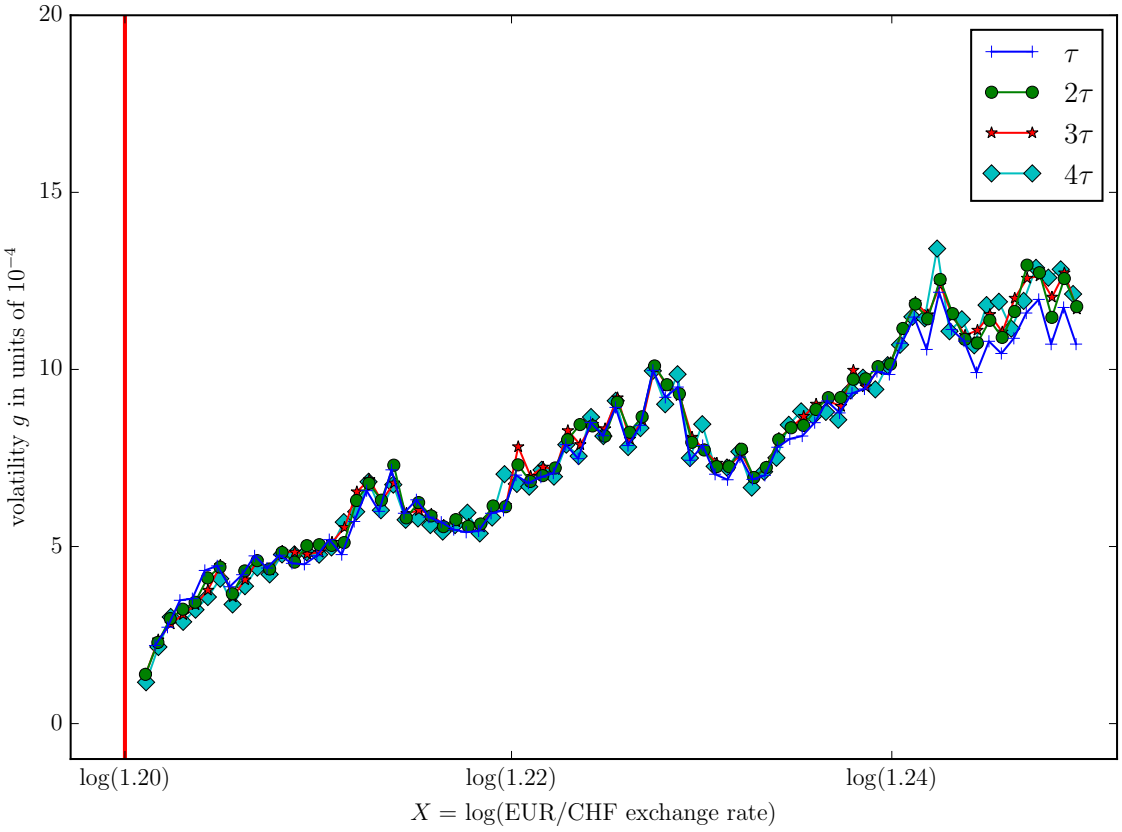

Figure 3.8: Approximation of the function $g(X)$ from (2.5) using upsampled tick-by-tick data of the EUR/CHF exchange rate between September 2011 and January 2015. This figure is obtained by following faithfully the algorithm described in section 3.2. Additionally, the algorithm is applied to subsampled time series as suggested by Sura and Barsugli [90]. We can see that the result is unaffected by this subsampling and conclude that the first order approximations (3.21) and (3.22) are justified.

4 Economic models for foreign-exchange markets

In our attempt to model the EUR/CHF exchange rate X after the enforcement of the 1.20-barrier in September 2011 as an Itô process

$$\dot{X} = f(X,t) + g(X,t)\eta(t) \tag{4.1}$$

we have first considered purely physical analogies in section 2. Since we had not been not successful, we have then turned to a more empirical approach in section 3 and presented an algorithm which fits the shapes of f and g to the observed data. Surprisingly, the outcome was fundamentally different from our physical intuition. While we have no deterministic part ($f \equiv 0$), all the dynamics is hidden in the stochastic g. It is the goal of this section to shine some light on these observations and justify them from a theoretical point of view. We start by reconsidering the analogy of exchange rates to a Brownian particle. We then give a concrete example which shows how from our physical description the exchange rate dynamics could be predicted, which makes it completely unrealistic from a financial view point. Next, we introduce the mathematical martingale property and discuss the Krugman target zone model, which incorporates the traders' expectations as a fundamental ingredient into its equations. It is shown that this model provides a suitable description for the EUR/CHF target zone.

4.1 Why physical analogies were inappropriate

In section 2 we have put great emphasis on the analogy between the dynamics observed in figure 1.4, i.e. the EUR/CHF exchange rate confined to lie above 1.20, and a constrained Brownian particle moving in a fluid. All the ideas that we have derived from this analogy were based on the simple logical chain

$$\text{random walk} + \text{barrier} \;\Rightarrow\; \text{repulsive potential}. \tag{4.2}$$

From a physical point of view these are all the ingredients to consider. We have a particle that is performing a random walk which, economically, ensures the no-arbitrage condition. Once a barrier is added we reduce the entropy of the system. Consequently, the statistical properties of the movement are changed, giving rise to an effective repulsive potential. Why does this reasoning not apply to the FX dynamics? The fundamental difference between the FX and the Brownian particle is that a financial market is a *complex system* whose various components and interdependences give rise to the emergence of new dynamics which cannot just be derived as the sum of contributions from each constituent (in Anderson's words: "more is different" [3]). After all, restricting the configuration space of a Brownian particle is very simple: the particle keeps on moving freely as if its movement was not restricted until it hits the barrier. It is then instantaneously repelled and keeps on moving freely. In particular, temporarily removing the barrier leaves the dynamics of the particle unchanged as long as it is not close to 1.20. Assume this was the same for the dynamics of the FX. This would mean that the market participants do not care at all about the SNB enforcing a minimum exchange rate. They keep on trading unaffectedly until one euro is traded for 1.20 Swiss francs, at which point the SNB intervenes, pushes the exchange rate up and the trading continues as before. The special dynamics of g that we have observed in the previous section proofs that this is not the case. Already when the exchange rate approaches the lower boundary the dynamics start to change, so there must be a more complex process behind.

The fact that the dynamics cannot be like its physical analog is also clear from an arbitrage point of view. Assume that indeed the dynamics was as suggested by equation (2.16). Taking expectation

values on both sides we can see that we have a non-vanishing conditional expectation value for price changes. This, in turn, results in a certain predictability and thus arbitrage opportunities. The efficient market hypothesis tells us that this opportunity must vanish. Hence, we see that imposing a barrier in an FX gives rise to more complex mechanisms which ensure that the market remains arbitrage-free:

$$\text{random walk} + \text{barrier} + \text{no-arbitrage} \;\Rightarrow\; \text{new dynamics}. \tag{4.3}$$

We will elaborate on this statement in more detail in subsection 4.3 and subsection 4.4. Before that, we want to give an example of the arbitrage opportunities that would prevail if our physically intuitive model held true.

4.2 Arbitrage potential

Assume that the EUR/CHF could be accurately described by the stochastic differential equation

$$\frac{dX}{dt} = 3\frac{F^2}{C}\left(X - X_{\text{eq}}\right)^2 - 2\sqrt{\frac{F^3}{C}}\left(X - X_{\text{eq}}\right) + g\eta(t). \tag{4.4}$$

We will now show how you can arbitrage based on a simple trading strategy.

4.2.1 Creating a suitable time series

To start, we have to create a reasonable time series obeying (4.4). For tick by tick data of the EUR/CHF exchange rate from the 8th of April and the 5th of September 2012 (the particularly stationary regime, see figure 1.4) the volatility is approximately $3 \cdot 10^{-4}$ and the average time step τ is around 1.5 seconds which is approximately equal to $4 \cdot 10^{-4}$ hours. Using a Milstein scheme [57], we then solve equation (4.4) with a discrete time step of $\tau = 4 \cdot 10^{-4}$ hours. The parameters F, C and g are chosen such that the simulated volatility is also approximately equal to $3 \cdot 10^{-4}$. This guarantees the creation of a "realistic" time series. Concretely, we have chosen $F = 0.04, C = 0.08$ and $g = 9 \cdot 10^{-5}$. Furthermore, looking at the empirical density of the EUR/CHF exchange rate (figure 4.1) indicates that $X_{\text{eq}} = 1.201$ is a reasonable choice for the equilibrium price. We have now all we need to simulate $6'000$ hours of price fluctuations (figure 4.2, left axis). This corresponds to approximately one year of data (there are about 250 trading days and the FX is open 24 hours).

4.2.2 A simple trading strategy

In the FX, trading costs TC are typically of the order of the bid-ask spread. Analysing the tick by tick data of the EUR/CHF exchange rate in regime IV we find that this spread is narrowly distributed around 1.2 pip $= 1.2 \cdot 10^{-4}$ Swiss francs per euro that is traded. Since $|X - X_{\text{eq}}| \ll 1$, the square term is small so that (4.4) is approximately an Ornstein-Uhlenbeck process with a slight tendency towards positive increments. This gives rise to the following trading strategy: We short sell euros whenever $X > X_{\text{eq}} + n \cdot \text{TC}$ (expected decrease in value) and we are long euros whenever $X < X_{\text{eq}} - n \cdot \text{TC}$ (expected increase in value) knowing that with probability one the exchange rate will eventually return to X_{eq}. Here, n denotes some positive number which can be adapted to optimize our gains. In principle, n can be chosen as small as $1/2$ which will just compensate for the transaction costs. If n is chosen too large, almost no trading will occur. Empirically, we have found that $n = 1$ yields

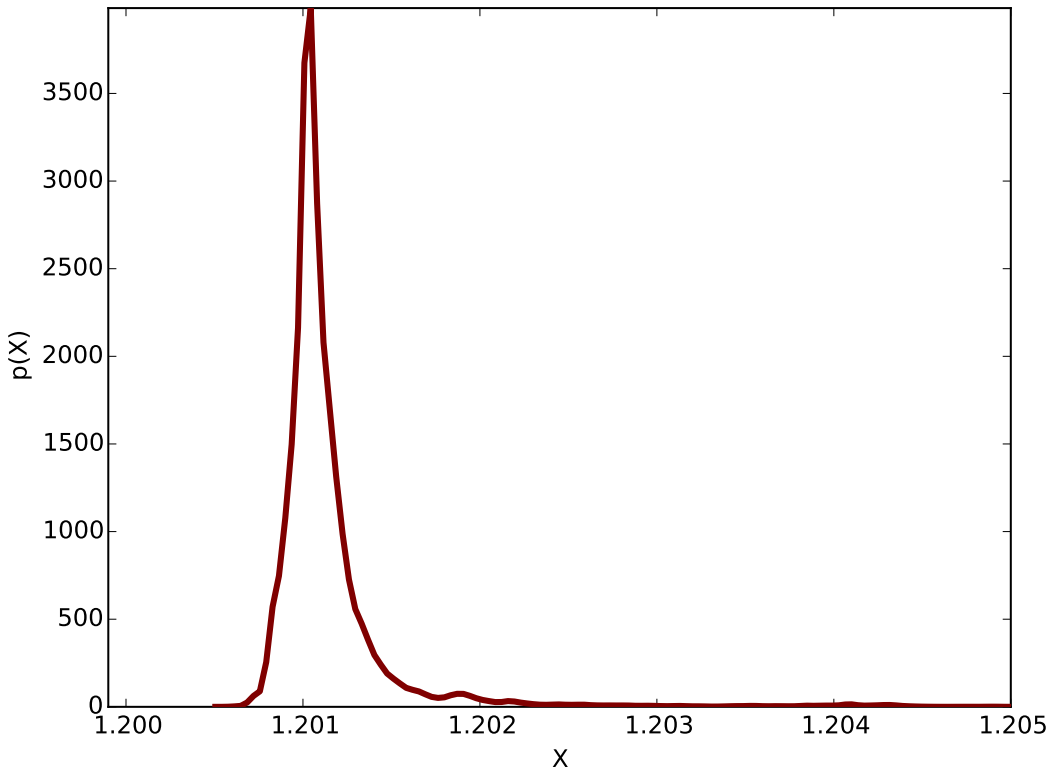

Figure 4.1: Empirical density distribution p obtained from a normalized histogram plot of the EUR/CHF exchange rate between the 8th of April and the 5th of September 2012. The peak is observed at $X = 1.201$ rather than at the location of the theoretical singularity $X = 1.20$. This is a typical finite-size effect.

steady gains. In practice, the parameters X_{eq}, F, C and g can be estimated from the data using a Bayesian framework for parameter estimation [16]. From the resulting gains, both mean return $\langle r_\tau \rangle$ and standard deviation σ_τ per time step τ can be calculated. The Sharpe ratio per time step is then given by $\langle r_\tau \rangle / \sigma_\tau$ (where we have neglected the subtraction of the risk free rate) through which we determine the annual Sharpe ratio (SR) by multiplying by the square root of the total number of time steps $6'000 \cdot 2'400$. Figure 4.2 shows the outcome for different choices of the transaction cost. We see that realistic transaction costs of 1 or 2 pip lead to Sharpe ratios which are more than 10 times times larger than what would already be considered a high Sharpe ratio. However, we have neglected slippage in this simple example (the fact that not all orders are executed at the ordered price). It is clear that the traded volume cannot grow arbitrarily. At some point, the orders would start to “eat" deep into the order book which increases the transaction costs and washes out the gains. On the other hand, it must be pointed out that the applied investment strategy is far from optimal. We could also make use of the strong correlation between returns. Approximating (4.4) as an Ornstein-Uhlenbeck process, the duration of temporal correlations is given by the inverse of the coefficient in front of the linear term which is in our case more than 17 hours. Implementing a linear predictor, it can be shown [8, 69] that even small temporal correlations can be exploited to arbitrage the market.

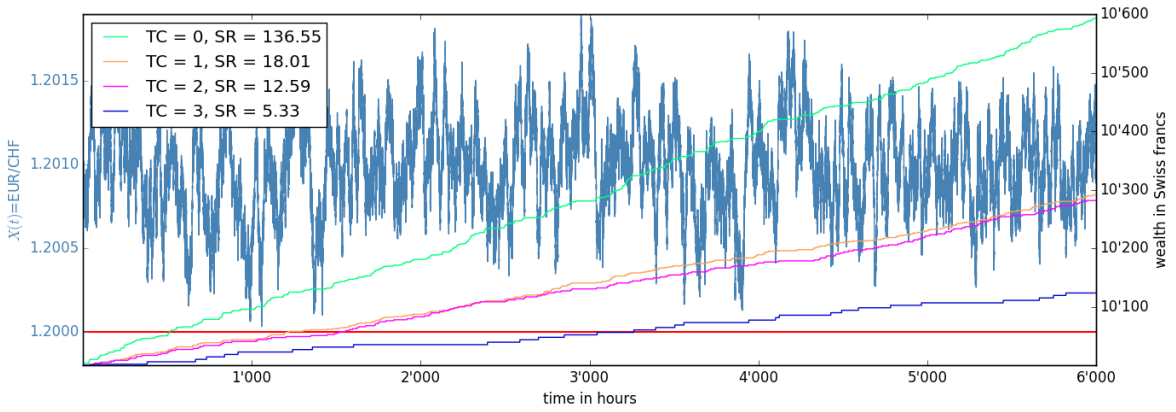

Figure 4.2: On the left axis we show one year of the simulated EUR/CHF exchange rate according to (4.4). On the right axis we show the wealth which results from the simple trading strategy described in the text and an initial investment of 10'000 CHF. The transaction costs TC are given in units of pip (= 10^{-4} Swiss francs per euro traded) and SR denotes the annual Sharpe ratio that is calculated from the risk-free trading strategy.

4.3 The martingale property

Starting from equation (4.1) we argue in this section why f has to vanish. This requires quite a bit of terminology and tools from stochastic calculus. Consult [39, 66] for in-depth mathematical introductions, [81, 82] for introductions with an emphasis on applications in finance and [33] for an emphasis on applications in natural sciences. However, more than a basic understanding of the concepts is not required and we will repeat the most important definitions and properties. Throughout this thesis we assume that f and g are (Itô-) integrable.

Let $\{X(t)\}$ denote a stochastic process on a filtered probability space $\left(\Omega, \mathcal{F}, (\mathcal{F}_t)_{t\geq 0}, \mathbb{P}\right)$ with, say, $t \in [0, \infty)$. Recall the following definition of a martingale from stochastic calculus:

A stochastic process $\{X(t)\}$ is called a *martingale* with respect to a filtration $\mathcal{F}_t$ if

(i) $X(t)$ is adapted to the filtration $\{\mathcal{F}_t\}_{t\geq 0}$,

(ii) for every $t \geq 0$

$$\mathbb{E}\left[|X(t)|\right] < \infty \tag{4.5}$$

and

(iii) for every X and t such that $0 \leq X < t$

$$\mathbb{E}\left[X(t)|\mathcal{F}_s\right] = X(X). \tag{4.6}$$

Whereas conditions (i) and (ii) are rather technical (see for instance [33] for a detailed explanation), condition (iii) is the characterizing property of the martingale. Its interpretation becomes evident once one realizes that $\mathcal{F}_s$ can be interpreted as "all the information that can be acquired from the process up to time X". The martingale property of a stochastic process then just says that the expectation value $\mathbb{E}\left[X(t)|\mathcal{F}_s\right]$ of $X(t)$ at a time $t > X$ conditional on all the available information from

the process up to time X is equal to the last observed value $X(X)$. Interpreting $X(t)$ as the time series of a traded asset this means that all the information about future price developments that could be extracted from the analysis of past prices is already incorporated in $X(X)$. Recalling the discussion of efficient markets from section 1.1 the following claim seems obvious: A stochastic process (a random walk) $X(t)$ describing the price movement of an asset (in particular exchange rates) must be a martingale. This is exactly what is proven more formally in Samuelson's paper [73] from 1965. Samuelson's reasoning is as follows:

Let $\{\ldots, X(t-1), X(t), X(t+1), \ldots, X(t+\tau), \ldots\}$ represent the time series of prices of any asset. Given knowledge of today's price and of past prices $\{X(t), X(t-1), \ldots, X(1)\}$, suppose we cannot know with certainty tomorrow's price $X(t+1)$ or any future price $X(t+\tau)$. Suppose there is at best a probability distribution for any future price, whose form depends solely on the number of periods ahead over which we are trying to forecast prices, given by

$$P(X) \equiv \text{Prob}\left(X(t+\tau) = X | X(t-1) = x_{t-1}, \ldots, X(1) = x_1\right). \tag{4.7}$$

These P's are assumed not to depend explicitly on historical calendar time, meaning that the probability distributions are stationary. Now consider today's *futures price quotation* for the actual spot price [7] that will prevail τ periods from now, i.e. the price quoted today at time t for a contract requiring delivery of the asset at time $t+\tau$. If the present spot price is $X(t)$, the relevant spot price that is to prevail later is given by $X(t+\tau)$. The newly defined futures price, quoted today, for that future $X(t+\tau)$ we denote by $Y(\tau, t)$. When another period passes, we shall know $\{X(t+1), X(t), X(t-1), \ldots X(1)\}$ instead of merely $\{X(t), X(t-1), \ldots, X(1)\}$ and the new quotation for the same futures price will be written as $Y(\tau-1, t+1)$. It in turn will be succeeded by the sequence

$$Y(\tau-2, t+2), Y(\tau-3, t+3), \ldots, Y(1, t+\tau-1), Y(0, t+\tau). \tag{4.8}$$

After $t+\tau$, there is no problem of pricing the particular futures contract. What relationship should be posit between the sequence $\{Y(\tau-n, t+n) \mid n = 0, 1, \ldots, \tau\}$ and the sequence $\{X(t)\}$? When the due date for the futures contract arrives, the no-arbitrage condition will ensure that (neglecting transaction costs)

$$Y(0, t+\tau) = X(t+\tau). \tag{4.9}$$

If this was not the case, we could immediately (i.e. instantaneously at time $t+\tau$) buy one, sell the other and pocket the difference. A period earlier, no one can know what $X(t+\tau)$ will turn out to be. If interest and risk-aversion can be ignored, it is tempting to assume that people in the market place make as full use as they can of the posited probability distribution P of next-period's price and bid by supply and demand $Y(1, t+\tau-1)$ to the expected level of tomorrow's price (which means that we assume fully informed, rational market participants). That way neither short-sellers nor long-buyers stand to make a positive gain or loss. Thus, Samuelson's postulates the *Axiom of Mathematically Expected Price Formation*: If spot prices $\{X(t)\}$ are subject to the probability distribution (4.7), a futures price is to be set by competitive bidding at the now-expected level of the terminal spot price. That is,

$$Y(\tau, t+\tau) = \mathbb{E}\left[X(t+\tau) \mid X(t), X(t-1), \ldots\right] \tag{4.10}$$

where the conditional expectation $\mathbb{E}$ is taken with respect to (4.7). With this axiom, it will be straight forward to proof Samuelson's *Theorem of Fair-Game Future Pricing*: If spot prices $\{X_t\}$ are subject to some probability law (4.7) and the futures price sequence (4.8) is subject to the axiom (4.10),

[7] The *Xpot price* of an asset is the price for the asset when payment and delivery follow immediately after concluding the contract. This is thus opposed to a *forward* or *future price* where payment and/or delivery can take place some time after concluding the contract. Note that often in this thesis we just talk about the *price* of an asset. It is then implicitly assumed that we mean the spot price.

then the later sequence is a martingale (also called *fair-game*) in the sense of having unbiased price changes

$$\mathbb{E}\left[Y(\tau-1,t+\tau-1)|X(t),X(t-1),\ldots\right]=Y(\tau,t). \tag{4.11}$$

All we need to proof this theorem is the *Law of Iterated Expectations* which states that

$$\mathbb{E}\left[R_1\right]=\mathbb{E}\left[\mathbb{E}\left[R_1|R_2\right]\right] \tag{4.12}$$

for any two random variables $R_{1,2}$ (in particular, for $R_1=R_2$ where this holds trivially). Now, just replace $Y(\tau-1,t+\tau-1)$ in (4.11) by (4.10) and apply (4.12) which already finishes the proof.

In terms of Fama's categorization (section 1.1), Samuelson proofs the weak form of market efficiency. There is a follow-up paper [74] from 1973 in which Samuelson shows that when historical price changes are properly adjusted for expected dividends paid out, they are more or less indistinguishable form a random walk. This can be shown to be equivalent to the semi-strong form of market efficiency since dividends can be seen as a proxy for information which is not incorporated in the market price.

Now that we know that $X(t)$ defined as a solution of (4.1) must be a martingale, we prove that f must vanish. Furthermore, we show that the martingale property does not restrict the form of g. First of all, note that (4.1) is equivalent to (or actually just a physicist's notation for)

$$X(t)-X_0=\int_0^t du\; f(X,u)+\int_0^t dW(u)\; g(X,u) \tag{4.13}$$

where $X_0\equiv X(t=0)$ is some initial value and the stochastic integral is interpreted in the Itô sense. It is a well-known property that $\mathbb{E}\left[R|\mathcal{F}_t\right]=R$ for any $\mathcal{F}_t$-measurable random variable R. Furthermore, $\mathbb{E}\left[R|\mathcal{F}_t\right]=\mathbb{E}\left[R\right]$ for any random variable R that is independent of $\mathcal{F}_t$. It follows that the Wiener process W_t is a martingale (with respect to the filtration $\mathcal{F}_t=\{W(X)\,|\,0\leq X\leq t\}$) since

$$\begin{aligned}\mathbb{E}\left[W_t|\mathcal{F}_s\right]&=\mathbb{E}\left[(W_t-W_s)+W_s|\mathcal{F}_s\right]\\&=\mathbb{E}\left[W_t-W_s|\mathcal{F}_s\right]+\mathbb{E}\left[W_s|\mathcal{F}_s\right]\\&=\mathbb{E}\left[W_t-W_s\right]+W_s\\&=W_s.\end{aligned} \tag{4.14}$$

In the last step we have used that the increments W_t-W_s of a Wiener process are independently and normally distributed with zero mean by definition. Recall from stochastic calculus that

$$\mathbb{E}\left[\int_a^b dW(u)\; h(u)\right]=0 \tag{4.15}$$

for any (sufficiently well-behaved) function h on a compact interval $[a,b]$. It follows immediately that any stochastic integral is a martingale:

$$\begin{aligned}\mathbb{E}\left[\int_0^t dW(u)\; g(X,u)\,\middle|\,\mathcal{F}_s\right]&=\mathbb{E}\left[\int_0^X dW(u)\; g(X,u)\,\middle|\,\mathcal{F}_s\right]+\mathbb{E}\left[\int_s^t dW(u)\; g(X,u)\,\middle|\,\mathcal{F}_s\right]\\&=\int_0^X dW(u)\; g(X,u)+\mathbb{E}\left[\int_s^t dW(u)\; g(X,u)\,\middle|\,\mathcal{F}_s\right]\\&=\int_0^X dW(u)\; g(X,u).\end{aligned} \tag{4.16}$$

In the second last step we have used that the Itô integrale is measurable. An immediate consequence of (4.16) is that the martingale property does not restrict the form of g. Thus, we see from (4.13) that

$$\begin{aligned}\mathbb{E}\left[X(t) - X_0 \middle| \mathcal{F}_s\right] &= \int_0^X dW(u)\, g(X,u) + \mathbb{E}\left[\int_0^t du\, f(X,u) \middle| \mathcal{F}_X\right] \\ &= \int_0^X dW(u)\, g(X,u) + \int_0^X du\, f(X,u) + \mathbb{E}\left[\int_s^t du\, f(X,u) \middle| \mathcal{F}_s\right] \end{aligned} \tag{4.17}$$

and deduce that (4.13) is a martingale if and only if

$$\mathbb{E}\left[\int_s^t du\, f(X,u) \middle| \mathcal{F}_s\right] = 0. \tag{4.18}$$

Since this has to hold for arbitrary times $X < t$ we conclude that (4.1) is a martingale process if and only if $f \equiv 0$.

4.4 Krugman's theoretical target zone model

Given the failure of our physically motivated model (4.4), we turn to the financial literature to find an explanation for figure 3.6. The work of Krugman [43] turns out to be the reference of a large part of the target zone literature. Following the original discussion by Krugman [43] and a review paper by Svensson [91], we are now going to summarise the basics of this model. Krugman's model starts from the following intuitive equation:

$$X = m + v + \gamma \frac{\mathbb{E}\left[dX\right]}{dt}. \tag{4.19}$$

All variables are expressed in natural logarithms and have the following interpretations:

- X is the (log of the) spot price of foreign exchange, also called the exchange rate. The exchange rate is the domestic price of foreign exchange, that is, the number of domestic currency units per foreign currency unit. From a Swiss perspective, we will thus describe the EUR/CHF exchange rate, such that EUR/CHF $=$ 1.20 means 1 euro is worth 1.20 Swiss francs. In a target zone, X is held inside the target zone band $\underline{X} < X < \overline{X}$. To simplify the mathematics, it is assumed that the target zone is symmetric around $X = 0$, i.e. $\underline{X} = -\overline{X}$. This is without loss of generality, since we only shift X by a constant. Obviously, this has no influence on its dynamics. In the following, we will discuss primarily the situation where $X \gtrsim \underline{X}$ which is the interesting case for us. Due to symmetry, all results immediately translate to the case where $X \lesssim \overline{X}$.
- m is the domestic money supply and controlled by the central bank. When the currency is strong (the exchange rate is low) the central bank can increase the money supply in order to weaken the domestic currency (increase the exchange rate). Krugman assumes that the monetary policy is passive, i.e. m is shifted only at (or infinitesimally close to) the exchange rate limits $\underline{X}$ and $\overline{X}$. As long as X lies within the target zone band $\underline{X} < X < \overline{X}$, m is held constant.

- v represents exogenous velocity shocks, i.e. economic and geopolitical events affecting the exchange rate that cannot be controlled by the (domestic) central bank. The velocity term is assumed to follow a simple Brownian motion

$$dv = \sigma dW_t \tag{4.20}$$

with $\sigma > 0$ constant. It follows $\mathbb{E}[dv] = 0$ in line with the no-arbitrage condition.

- $\mathbb{E}[dX]/dt$ is the expected change of the exchange rate. This is the ingredient of the model which contains the psychological component of market participants. In a credible target zone, when the exchange rate approaches its upper or lower limit, market participants anticipate the intervention by the central bank and act accordingly.

- $\gamma > 0$ is a constant which can be interpreted as the semi-elasticity of the exchange rate with respect to the instantaneous expected rate of currency depreciation. This can be understood from the definition of of semi-elasticity:

$$\text{Semi-elasticity of a function } f \text{ at a point } x := \frac{d \log f(x)}{dx}.$$

Indeed, we have

$$\frac{dX}{d\frac{\mathbb{E}[dX]}{dt}} = \gamma$$

and since X is the logarithm of the exchange rate this is consistent with the above definition of semi-elasticity.

- $m + v$ together represent the fundamental value of the exchange rate. We will sometimes also denote this quantity by $f \equiv m + v$. In particular, note that in absence of (or in the limit far away from) the exchange rate boundaries, where naturally $\mathbb{E}[dX]/dt = 0$, we have $X = f$.

4.4.1 Solution of the Krugman model

In order to proceed with the model (4.19) we must somehow rewrite the expectation term $\mathbb{E}[dX]/dt$. To this end, we simply apply Itô's Lemma

$$dX = dX(v) = \frac{\sigma^2}{2}\frac{\partial^2 X}{\partial v^2}dt + \sigma\frac{\partial X}{\partial v}dW_t, \tag{4.21}$$

take the expectation value,

$$\mathbb{E}[dX] = \frac{\sigma^2}{2}\frac{\partial^2 X}{\partial v^2}dt \tag{4.22}$$

and plug this into (4.19) in order to obtain

$$X = m + v + \frac{\gamma\sigma^2}{2}\frac{\partial^2 X}{\partial v^2}. \tag{4.23}$$

This simple, second order linear ODE has the general solution

$$X(m, v) = m + v + Ae^{\rho v} + Be^{-\rho v} \tag{4.24}$$

with $\rho \equiv \sqrt{2/\gamma\sigma^2}$. This result can be further simplified due to symmetry: Suppose that $m = 0$ at some point (again, without loss of generality, as only relative changes and not the absolute value of

m matter). We then expect to see $X(v=0)=0$. If this was not the case, we would have an offset and symmetry would be broken. We conclude that $A=-B$ and write

$$X(m,v)=m+v+A\left(e^{\rho v}-e^{-\rho v}\right)\equiv m+v+A\sinh\left(\rho v\right) \tag{4.25}$$

where we have absorbed a factor of 2 in the constant A. It is easy to see, and will be argued in more detail below, that only $A<0$ leads to a reasonably shaped $X(v)$-curve. Always remembering that $A<0$ is a brain teaser. Hence, let us write this right away as

$$X(m,v)=m+v-A\sinh(\rho v),\qquad (A>0). \tag{4.26}$$

Equation (4.26) constitutes the final functional form of the $X-v$ relation. However, the value of the constant A remains to be determined. This is what we discuss next.

4.4.2 The smooth-pasting condition

In this subsection we follow the ideas of [75] but we are more mathematically rigorous, working with limits and taking into account continuity conditions.

Assume that we are inside the band (so m is fixed) approaching the lower exchange rate limit $\underline{X}$ from above. Denote by $\underline{f}$ the value of the fundamental at which $X(\underline{f})=\underline{X}$. This condition must be understood as the limit $\lim_{f\downarrow\underline{f}}X(f)\equiv X\left(\underline{f}+0\right)$ because as soon as X touches $\underline{X}$, m will be changed, making it difficult to define a unique value $\underline{f}$.
We will now argue that A is determined by imposing the additional "smooth-pasting" condition

$$\left.\frac{\partial X}{\partial f}\right|_{f=\underline{f}}=0. \tag{4.27}$$

Smooth-pasting is based on a no-arbitrage argument, as can be seen from the following line of reasoning: Consider a point $f^*\gtrsim\underline{f}$ in the neighbourhood of $\underline{f}$ where the authorities intervene by increasing the money supply in such a way that f is pushed back into the band by a discrete amount Δf. Hence, whenever the exchange rate gets to $X\left(f^*\right)$ the authorities intervene by a discrete amount, resulting in the exchange rate becoming instantly equal to $X\left(f^*+\Delta f\right)$. As soon as X touches $X\left(f^*\right)$, then, the traders face a risk-free opportunity, since they can buy foreign currency just before the intervention and make a percentage profit equal to the difference between $X\left(f^*\right)$ and $X\left(f^*+\Delta f\right)$. This arbitrage opportunity is only eliminated if

$$X\left(f^*\right)=X\left(f^*+\Delta f\right) \tag{4.28}$$

By assumption, the central bank does not intervene at a point $f^*>\underline{f}$ but only infinitesimally close to $\underline{f}$. Hence, dividing (4.28) by Δf and considering the infinitesimal limit we find

$$\lim_{f^*\downarrow\underline{f}}\lim_{\Delta f\downarrow 0}\frac{X\left(f^*+\Delta f\right)-X\left(f^*\right)}{\Delta f}=0 \tag{4.29}$$

which - since X is a continuous function of f - is exactly the imposed smooth-pasting condition (4.27). Via $\lim_{f\downarrow\underline{f}}\equiv\underline{v}+m$ we can also define the value $\underline{v}$ at which $X\left(\underline{v}\right)=\underline{X}$, or, put more precisely, where $X\left(\underline{v}+0\right)=\underline{X}$.

We have now derived the following two conditions

$$X(\underline{v})=\underline{X}\quad\text{and}\quad\left.\frac{\partial X}{\partial f}\right|_{f=\underline{f}}=\left.\frac{\partial X}{\partial v}\right|_{v=\underline{v}}=0 \tag{4.30}$$

(understood as the limit $v \downarrow \underline{v}$) from which the two constants $\underline{v}$ and A can be determined uniquely (although only numerically). Assuming that we know $\underline{v}$, it is straight forward to derive formally an analytical expression for A:

$$0 \overset{!}{=} \left.\frac{dX}{dv}\right|_{v=\underline{v}} = 1 - A\rho\cosh(\rho\underline{v}) \quad \Rightarrow \quad A = \frac{1}{\rho\cosh(\rho\underline{v})}. \tag{4.31}$$

This completes our derivation of the Krugman model. The result is visualised in figure 4.3. When

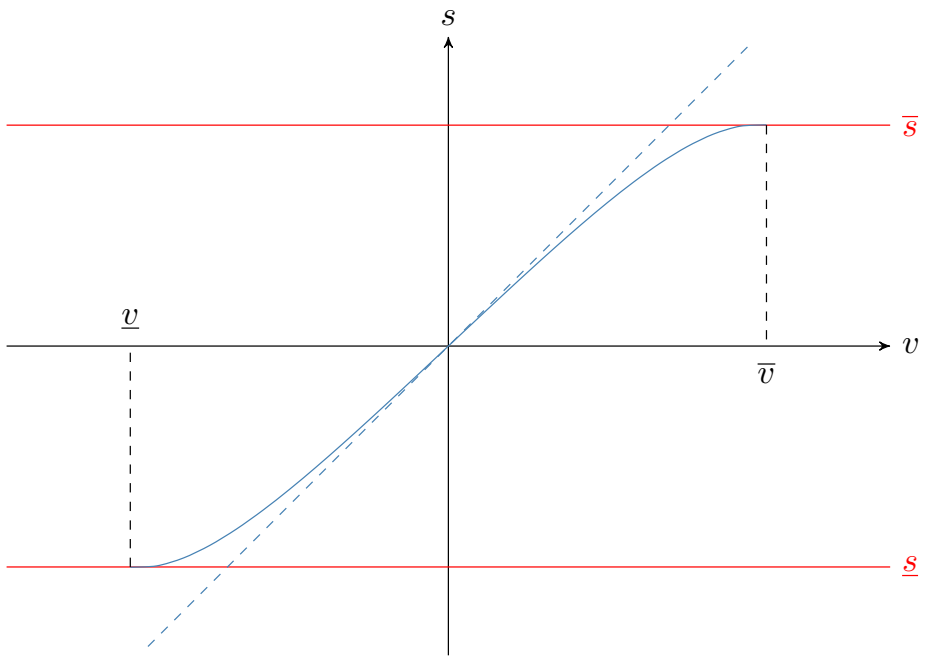

Figure 4.3: Schematic plot of Krugman's exchange rate model (4.26) showing the exchange rate X, bounded between $\underline{X}$ and $\overline{X}$ as a function of it's fundamental value v. The smooth-pasting condition (4.27) accounting for the no-arbitrage condition is clearly visible. Such a $X(v)$-line corresponds to one fixed amount of money supply m. Changing m shifts the entire line to the left or to the right as is explained in the text. The dashed line shows the trivial relation $X(f) = f$ that prevails under a freely floating exchange rate policy.

looking at figure 4.3, it is clearly visible that the closer X is to its upper or lower limit, the less it does react to external shocks v. Since this happens without active intervention of the central bank (which is only assumed to interact exactly at the limits) this shows that the sole announcement of a target zone renders the exchange rate less volatile. This is also known as the *Honeymoon effect*.

4.4.3 Money supply behavior

It remains to be described how m is changed when $X = \underline{X}$ or $X = \overline{X}$. Assume that we are at some point inside the band (point 1 in figure 4.4). Let $\underline{v}$ be the value of v at which a particular X-curve touches the bottom of the band (point 2). If v goes below $\underline{v}$, the money supply must be increased such that X remains at $\underline{X}$. As long as v continues to decrease, m is increased, shifting the curve from point 2 to point 3. Next, suppose that v starts to have positive shocks. Then the exchange rate will not retrace its steps since the monetary authority does not react to shocks that pushes X back into the band. Thus, the market will move back up a new X-curve, to a point like 4.

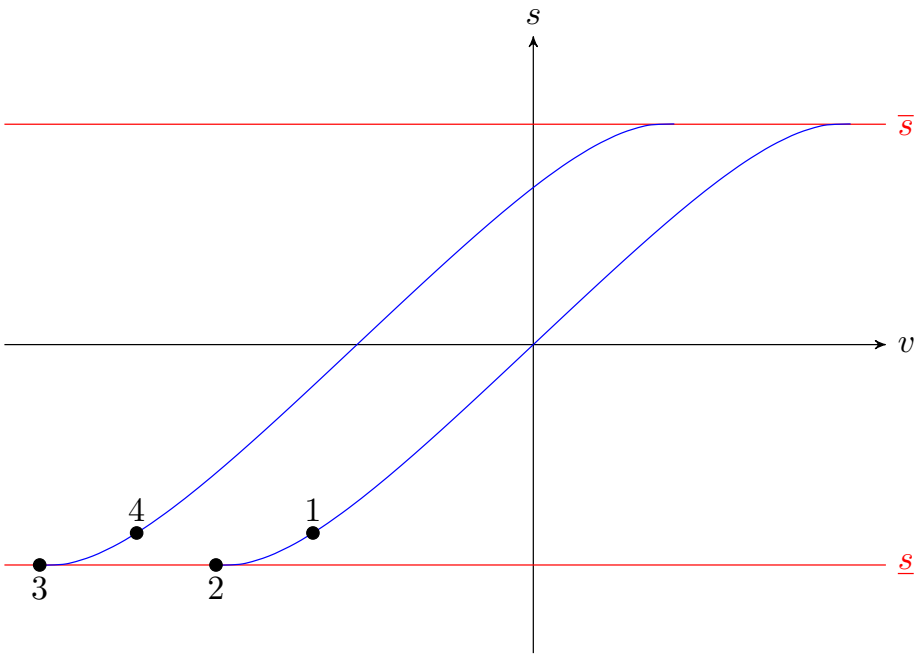

Figure 4.4: Marginal interventions by the central bank lead to a shift of the $X(v)$ curve. See text for a detailed explanation.

Similarly, the curve is shifted to the right if $v > \overline{v}$. The result is a family of X-curves. We can actually write a simple expression for the whole family of curves. Let A be determined so that the curve is tangent for some particular m. Then, the whole family of curves is defined by

$$X = m + v - A\sinh\left(\rho(m+v)\right) \tag{4.32}$$
$$= f - A\sinh(\rho f) \tag{4.33}$$

with the same A. Whenever negative shocks to v push (4.33) to $\underline{X}$, m will be reduced to keep $m+v$ constant. It follows that we can draw the whole family of X-curves as a single curve $X = X(f)$.

4.4.4 One-sided target zones

So far, we have kept the discussion very general and considered both a lower ($\underline{X}$) and an upper ($\overline{X}$) limit for the exchange rate X. All results apply equally for the single-sided (EUR/CHF) target zone in the sense that we always consider the regime $\overline{X} \gg X \gtrsim \underline{X}$ where the upper boundary $\overline{X}$ is not felt and hence negligible. More formally, the single-sided target zone can be described by demanding that the general solution (4.24) recovers $X \to v$ for $v \to \infty$. This implies $A = 0$ and $B > 0$ which is the formal solution for the one-sided target zone

$$X = m + v + Ae^{-\rho v} \tag{4.34}$$

For $X \gtrsim \underline{X}$ it is easy to verify that (4.34) asymptotically coincides with (4.26).

4.5 Assumptions and implications of the Krugman model

Krugman's target zone model has several important implications which allow us to test the model empirically. In this subsection we show that Krugman's model provides a suitable description of the EUR/CHF target zone.

4.5.1 Assumptions of Krugman's model

Krugman's target zone model is based on two crucial assumptions: First, the target zone is perfectly credible. This means that market participants belief at every time that the central bank will stick to its announced target zone. Second, the interventions by the central bank are marginal, meaning the monetary supply is held constant as long as X is within the target zone band. Only when X touches $\underline{X}$, the monetary supply is increased, just sufficiently to keep X at $\underline{X}$. These assumptions have been investigated specifically for the EUR/CHF exchange rate between 2011 and 2015 in [89] where it is found that the two assumptions hold sufficiently well so that Krugman's model can be applied. This sets the EUR/CHF target zone apart from many earlier empirical studies in which Krugman's model was already challenged on the basis of its assumptions. We refer to [75, 91] for detailed reviews.

4.5.2 Density distribution

A first implication of Krugman's model is that the distribution of the exchange rate within the band must be $\cup$-shaped, that is, the exchange rate must spend most of the time near the edges of the band [91]. To understand this implication, one must consider that the volatility vanishes smoothly as $X \to \underline{X}$ or $X \to \overline{X}$ (see derivation below). Hence, the exchange rate moves more and more slowly as it approaches its boundaries. The fundamental, in contrast, moves with a constant speed between its bounds, hence its distribution is uniform. Denote by $\tilde{p}(v)$ the probability density of the fundamental v (actually, $f = m + v$ but since m is constant inside the band we can also work with v instead of f). Since the fundamental is distributed (asymptotically) uniformly within the exchange rate band, we have trivially

$$\tilde{p}(v) = \frac{1}{2\underline{X}}. \tag{4.35}$$

We are interested in the density $p(X)$ as a function of the exchange rate X. Changing variables,

$$p(X)dX \overset{!}{=} \tilde{p}(v)dv = \tilde{p}(v(X))\frac{dv}{dX}dX, \tag{4.36}$$

gives

$$p(X) = \tilde{p}(v)\frac{dv}{dX} \overset{(4.35)}{=} \frac{1}{2\underline{X}}\frac{dv}{dX} \sim \frac{dv}{dX}. \tag{4.37}$$

Below we show that for X close to $\underline{X}$,

$$v \sim \sqrt{X - \underline{X}} + \underline{v}. \tag{4.38}$$

Consequently, we predict

$$p(X) \sim \frac{1}{\sqrt{X - \underline{X}}} \tag{4.39}$$

close to the lower barrier $\underline{X}$ which is in good agreement with the data (figure 4.5).

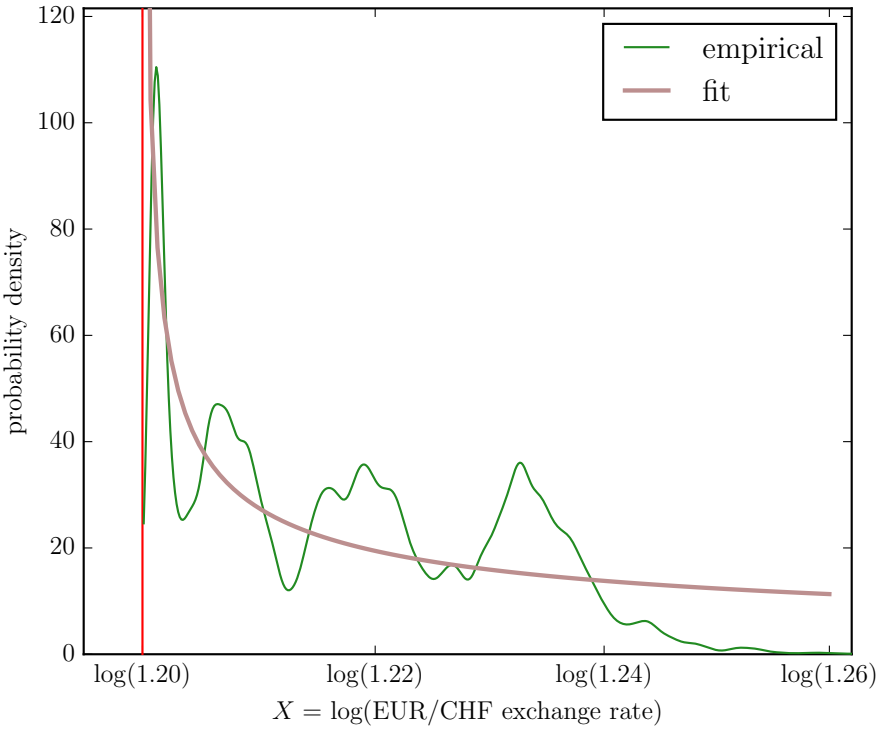

Figure 4.5: The green line indicates the empirical density distribution of EUR/CHF exchange rate tick-by-tick data between September 2011 and January 2015. The brown line represents the result of a one-parameter ordinary least-squares fit with(4.39) determining $C \approx 2.5$.

4.5.3 Drift and volatility in Krugman's model

By applying Itô's lemma to (4.26), we derive the following drift f and volatility g in the Krugman framework:

$$f(v) = \frac{1}{2} A\sigma^2\rho^2 e^{-\rho v} \tag{4.40}$$

$$g(v) = \sigma - \sigma A\rho e^{-\rho v}. \tag{4.41}$$

For practical purposes, working with (4.40) and (4.41) is cumbersome because v cannot be measured but only estimated [29]. Nevertheless, testing directly the non-linear $X(v)$ relation (4.26) by estimating v is the method that has been widely applied in the empirical literature. The reported results have then either rejected Krugman's target zone model entirely or have shown only a very noisy evidence for (4.26). We refer again to [75, 91] for a broad overview and to [89] for EUR/CHF specific results. Our strategy is different: Instead of relying on v, we invert the $X(v)$ relation (4.26) locally to lowest order in $v - \underline{v}$ (it is easy to see that (4.26) has a well-defined, global inverse $v(X)$ which, however, has no analytical closed form expression). Since we only care about the regime $X \gtrsim \underline{X}$ it is sufficient to invert a Taylor-expanded approximation of $X(v)$ expanded around $\underline{v}$ with $v > \underline{v}$. We find

$$\begin{aligned} X(v) &= \underbrace{X(\underline{v})}_{=\underline{X}} + \underbrace{X'(\underline{v})}_{=0}(v-\underline{v}) + \frac{1}{2}X''(\underline{v})(v-\underline{v})^2 + \mathcal{O}\left((v-\underline{v})^3\right) \\ &\sim \underline{X} - \frac{1}{2}A\rho^2\sinh(\rho\underline{v})(v-\underline{v})^2. \end{aligned} \tag{4.42}$$

Since $\sinh(\rho\underline{v}) < 0$ we see that $-\frac{1}{2}A\rho^2\sinh(\rho\underline{v})$ is a positive constant which I shall denote by C. Hence, we have found that

$$X \sim \underline{X} + C(v - \underline{v})^2 \quad \Rightarrow \quad v \sim \sqrt{\frac{1}{C}(X - \underline{X})} + \underline{v}. \tag{4.43}$$

Redefining $C \mapsto C^{-1/2}$ for convenience, we end up with

$$v \sim C\sqrt{X - \underline{X}} + \underline{v}. \tag{4.44}$$

Plugging (4.44) into (4.40) and (4.41) the following expressions derive for drift and volatility:

$$f(X) = \alpha \tag{4.45}$$

$$g(X) = \beta\sqrt{X - \underline{X}}. \tag{4.46}$$

Here $\alpha = \sigma/\sqrt{2\gamma}$ and $\beta = 2^{3/4}\sqrt{\sigma}/\gamma^{1/4}$. In particular, we note that $\sqrt{\alpha}/\beta = 1/2$. There are higher order terms leading to corrections to (4.45) and (4.46). It is easy to check that for our data where $s < \log(1.26)$ these corrections are negligible. Comparing (4.45) and (4.46) with figure 3.6, one can check that the data conform very well to Krugman's theory. For the volatility, we can apply a one parameter least-squares fit which determines $\beta = (5.42 \pm 0.06) \cdot 10^{-3}$. Another least-squares fit determines $\alpha = (1.40 \pm 0.8) \cdot 10^{-5}$ (figure 4.6). Basic error propagation calculations yield

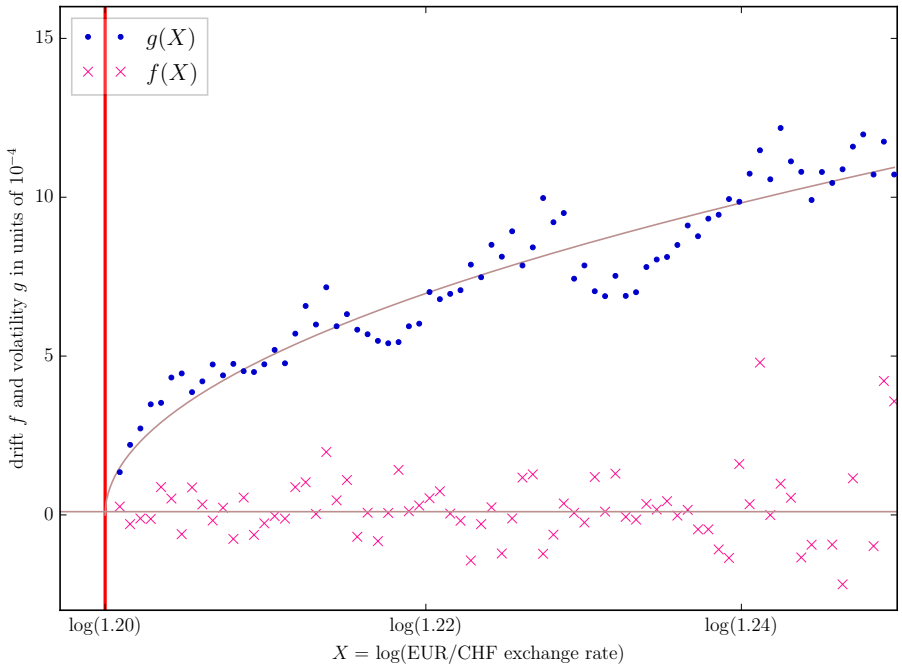

Figure 4.6: We show the parameter free estimate of drift $f(X)$ and volatility $g(X)$. The result is fundamentally different from the Brownian particle analogy (4.4) but well described by the Krugman model (4.26). The straight lines represent the best non-linear least-squares fit for the drift (4.45) and volatility (4.46), respectively.

$\sqrt{\alpha}/\beta = 0.68 \pm 0.22$. Despite the relatively large fluctuations for $s \gtrsim \log(1.24)$, the data agrees with the theoretical value $1/2$ within one standard deviation. Ignoring the large fluctuations around $s \gtrsim \log(1.24)$ leads to even better correspondence between data and theory. This confirms that Krugman's target zone model provides a suitable description of the constrained EUR/CHF exchange rate.

5 Hindered diffusion in an order-book fluid

We have started this thesis by pointing out a seeming analogy between physics and finance that turned out to be wrong. As was pointed out by Krugman [43], the naive view that the exchange rate behaves as if the regimes were one of free floating until the rate hits the edge of the authorised band are incorrect. The principal issue in modelling exchange rate dynamics under a target zone regime is the formation of expectations, so that investors adapt their strategies as a function of the proximity to the band edges according to their anticipation of the central bank actions. These expectations and their observable consequences turn out not to be described by the entropy reduction (2.4) associated with the forbidden paths that would cross the rigid barrier.

5.1 Physical hindered diffusion

Interestingly, it turns out that Krugman's model gives rise to a physical parallel after all. Indeed, using the analogy with a Brownian particle embedded in a fluid of small colliding particles, the presence of a barrier translates into the decrease due to hydrodynamic forces of the diffusion coefficient of the Brownian particle upon its approach to the wall. As we will show now, the volatility $g(X)$ is thus, at least semi-quantitatively, related to the physical problem of hindered diffusion. Financial price fluctuations has been recently shown to be more deeply anchored in the physics-finance analogy of a colloidal Brownian particle embedded in a fluid of molecules as shown in figure 2.3 (omitting the previously shown incorrect potentials), where the surrounding molecules reflect the structure of the underlying order book [103].

It turns out that this analogy can be extended even further to incorporate the case in which the motion is restricted by a wall (or target zone, respectively). Consider a physical Brownian particle in a fluid. The presence of a wall leads to a modification of the hydrodynamic flow of the molecules trapped between the wall and the Brownian particle. The closer the Brownian particle to the wall, the thinner the lubrification layer between them and the more hindered is the diffusion of the Brownian particle. In physics, it is more common to work with the diffusion coefficient $D(X)$ which is related to our volatility via $g = \sqrt{2D}$. In the bulk of a fluid (where the wall is not felt), the diffusion coefficient D is a constant D_0. The Einstein-Stokes equation predicts for a spherical particle with radius R

$$D_0 = \frac{k_B T}{6\pi\nu R} \tag{5.1}$$

with k_B the Boltzmann constant, T the temperature and ν the viscosity of the fluid. In presence of a wall at $X = \underline{X}$, the diffusion coefficient must be modified by $D(X) = D_0/\lambda$ [10] where λ is given by

$$\lambda_\perp = \frac{4}{3}\sinh(\alpha)\sum_{n=1}^{\infty}\left[\frac{n(n+1)}{(2n-1)(2n+3)}\frac{2\sinh((n-1)\alpha)+(2n+1)\sinh(\alpha)}{4\sinh^2((n+1/2)\alpha)-(2n-1)^2\sinh^2(2\alpha)}\right] \tag{5.2}$$

and $\alpha = \operatorname{arcosh}(X/R)$. The result is depicted in figure 5.1. An approximation of this result had already been found decades before by Lorentz [55] who predicted

$$\lambda \sim 1 + \frac{9}{8}\frac{R}{X-\underline{X}}. \tag{5.3}$$

From (5.3) we infer that close to the wall $D(X) = D_0/\lambda$ is, to first order, linear in $X - \underline{X}$. It follows immediately that close to the wall, the volatility of the particle increases like the square-root of $X - \underline{X}$, in correspondence with Krugman's prediction (4.46) from finance.

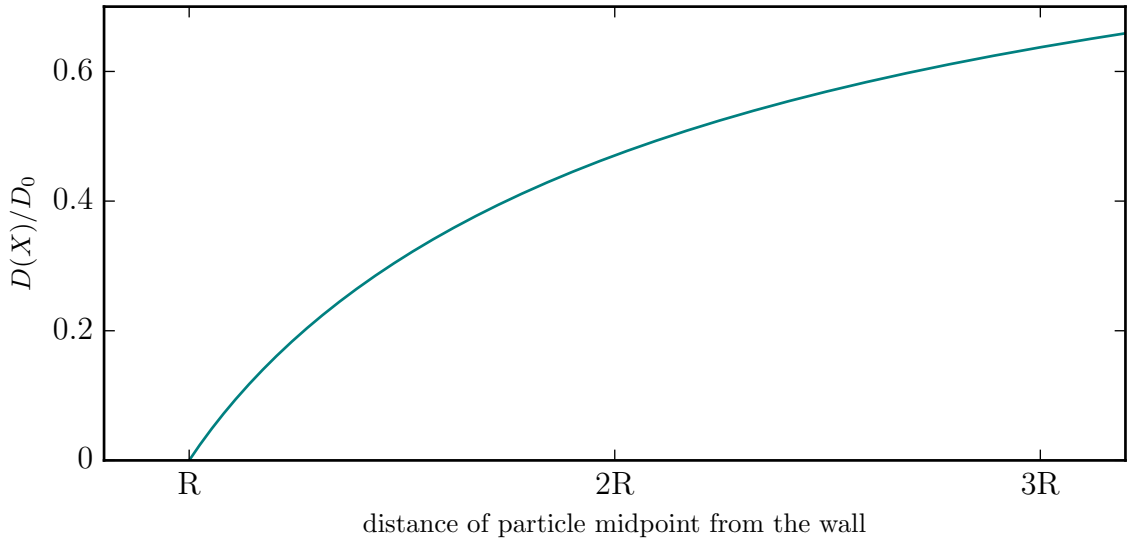

Figure 5.1: Physical diffusion coefficient as a function of particle distance from the wall. To first order and close to the wall, $D(X)$ is a linear function of $X - \underline{X}$.

5.2 Thermal equilibrium in finance?

In absence of any external forces, what is the stochastic process that describes a physical Brownian particle? Naively, one is led to propose $dX/dt = g(X) \cdot \eta(t)$. However, this implies not only that we are working in Itô's interpretation of stochastic calculus, but can furthermore be shown to be inconsistent with convergence towards thermal equilibrium. For an equilibrium system, the probability density $p(X,t)$ must have a steady state solution with the canonical form $p(X) \sim \exp(-\mathcal{H}/k_BT)$ with $\mathcal{H}$ the Hamiltonian of the system. If we insist on working in Itô's interpretation as is customary in finance to ensure causality of financial strategies, it has recently been shown [45] than an additional drift term $g(X)\frac{dg(X)}{dX}$ must be added to the stochastic differential equation in order to be consistent with the physical steady state distribution. From (4.46), we then derive the following stochastic equation for a Brownian particle close the a wall and in absence of external forces:

$$\begin{aligned} \frac{dX}{dt} &= g(X)\frac{dg(X)}{dX} + g(X) \cdot \eta(t) \\ &= \frac{\beta^2}{2} + \beta\sqrt{X - \underline{X}} \cdot \eta(t). \end{aligned} \tag{5.4}$$

Remarkably, the square-root shaped volatility is exactly the function which induces a constant positive drift in agreement with Krugman's prediction (4.45). The correspondence between physical hindered diffusion and Krugman's target zone model is only semi-quantitative in the sense that here $\sqrt{\text{"drift term"}}/\beta = 1/\sqrt{2}$. For Krugman, on the other hand, we have derived $\sqrt{\text{"drift term"}}/\beta = 1/2$, thus revealing a key difference between Krugman's constant drift term and the one resulting from a noise-induced drift of the form (5.4). We attribute this difference of the numerical values of $\sqrt{\text{"drift term"}}/\beta$ to the global condition of thermal equilibrium $p(X) \sim \exp(-\mathcal{H}/k_BT)$, which is absent in finance. Lévy and Roll [49] have recently proposed to impose the constraint that the global market portfolio is mean-variance efficient, i.e, that it obeys the predictions of the Capital Asset Pricing Model (CAPM). This global condition can be shown to lead to a reassessment and an improved estimation of the expected returns of the stocks constituting the global market [59]. But it

is not known what could be other consequences, in particular in exchange rate dynamics. Indeed, in finance, the existence of an economic equilibrium distribution similar to Boltzmann, and its relation to detailed balance is highly debated and far from trivial. We refer to [25] for a recent discussion of this topic and to [7, 23, 86] for further details on the interplay and coevolution of physics and economics in general.

5.3 Diffusion close to a wall

Let us end this section by pointing out that, also from a purely physical perspective, our result (5.4) has interesting implications. It reveals the special role played by the linearly increasing diffusion coefficient. In this subsection we want to give a less rigorous but simple heuristic derivation of Lorentz' approximate result (5.3). What is nice about our derivation is that no detailed knowledge about hydrodynamic interactions is required.

Working with Itô's interpretation of stochastic calculus, it can be shown [45] that a Brownian particle with general diffusion coefficient $D(X) = g(X)^2/2$ and in absence of any external forces is described by the stochastic differential equation

$$\frac{dX}{dt} = g(X)\frac{dg(X)}{ds} + g(X)\cdot\eta(t). \tag{5.5}$$

We want to determine the volatility $g(X)$ of a Brownian particle at position X close to a wall located at $X = \underline{X}$. Without loss of generality, we set now $\underline{X} = 0$ and make the fairly general approximation that, close to the wall, $g(X) = \beta X^\gamma$ for some $\gamma > 0$ (it is easy to see that $\lim_{X\downarrow 0} D(X) = 0$ is a necessary condition). Plugging this into (5.5) gives

$$\frac{dX}{dt} = \beta^2\gamma X^{2\gamma-1} + \beta X^\gamma\cdot\eta(t). \tag{5.6}$$

In the limit $X \downarrow 0$, we can distinguish three cases:

$$\text{the drift } g(X)\frac{dg(X)}{ds} \quad \begin{cases} \text{diverges} & \text{if } \gamma < 1/2, \\ \text{is constant} & \text{if } \gamma = 1/2, \\ \text{vanishes} & \text{if } \gamma > 1/2. \end{cases}$$

If $\gamma < 1/2$, the particle will be repelled with infinite force and can never touch the wall. Furthermore, placing initially the particle at the wall is ill-defined. If $\gamma > 1/2$, the particle, once it has reached the wall, will stay there forever (more precisely, it can be shown that a particle starting from $X > 0$ can never exactly reach the wall, but approach it arbitrarily close [32]). Also, a particle placed at the the wall will simply stay there forever. We deduce that $\gamma = 1/2$, and hence $D(X) \sim s$ is the only physically reasonable choice. In this case, a particle starting from $X \geqslant 0$ has non-zero probability to reach the boundary in finite time, upon which it will be repelled. These arguments can be formalised by solving analytically the Fokker-Planck equation corresponding to (5.6) in terms of an eigenfunction expansion [68, 71].

6 Summary and Conclusions

In this thesis we have examined the dynamics of the EUR/CHF exchange rate that arose from the SNB enforcing a minimum value of 1.20 Swiss francs per euro between September 2011 and January 2015. The overall goal was to set up a suitable stochastic differential equation (2.5) for this process.

Section 1 served as an introduction. The reasoning behind the efficient market hypothesis and the functioning of the foreign-exchange market were summarized. Different regimes in the development of the EUR/CHF exchange rate were highlighted.

In an initial approach, in section 2, we have relied on an apparent analogy from physics: A freely moving, one-dimensional Brownian particle whose motion is restricted only by a hard, repulsive wall. With arguments from statistical physics we have derived a long-range repulsive potential and set up the stochastic differential equation (2.16) that was thought to capture the dynamics of the EUR/CHF exchange rate. Numerical tests have shown that this is not the case. It turned out that equation (2.16) is ill-suited for the description of the FX since it focuses too much on the deterministic drift f in (2.5) that violates the no-arbitrage condition. Rather, the dynamics must be hidden in the stochastic volatility g. This section came with three appendices. In Appendix I we have derived several important random walk properties. In particular, we have derived the partition function of a random walker in presence of a barrier. Using Feynman path integrals and diagrams, Appendix II provides a general framework for the perturbative calculation of cumulants of solutions of stochastic differential equations. This is then applied to (2.16) and its validity is discussed. A functional renormalization group calculation of the interaction between a D-dimensional fluctuating surface and a hard wall is shown in Appendix III.

In section 3 we have abandoned the physical analogies. We have presented an algorithm that allowed us to extract both drift and volatility in a parameter-free way. After testing the accurateness of the algorithm by applying a Monte-Carlo scheme to a model equation, we have applied it to tick data of the EUR/CHF exchange rate. We found that the drift f is essentially constant, whereas the volatility g exhibits non-trivial behavior, increasing non-linearly as a function of the distance to the barrier.

The purpose of section 4 was to back all the previous empirical findings from a new theoretical perspective. In a first part, we have justified why the physical analogy of the Brownian particle from section 2 is too simplistic. In particular, we have shown how a rather naive trading strategy would lead to immense gains on the costs of the SNB. We have also explained this more formally in terms of the martingale condition. Consequently, we turned our attention to the famous Krugman target zone model which, as we could show, provides an accurate description of the EUR/CHF target zone regime.

By describing the exchange rate as a colloidal Brownian particle embedded in an “order book fluid", we could show in section 5 that there is a formal analogy to the physical hindered diffusion problem in the sense that both systems can be described by the same stochastic differential equation. This provides novel empirical support for the recently introduced model of a “financial Brownian particle in a layered order book fluid” [103], which generalises the standard random walk model of financial price fluctuations. We have also pointed out two fundamental differences between physical and economic hindered diffusion: First, in finance, market participants’ expectations must be taken into consideration. And their dedicated actions lead in aggregate to a quasi-absence of arbitrage opportunities. This is a typical feature of a complex human system that the physicist should always keep in mind when applying methods from natural sciences to model social dynamics. Second, in physics, we have an additional constraint in terms of a thermal equilibrium based on detailed balance. In finance, the existence of such a global equilibrium is a priori not clear and must be investigated further.

7 Appendix I: A Random Walker and a Wall

In this appendix we derive the partition function of a random walker in presence of a wall. Knowledge of the partition function is needed in order to derive the effective repulsive potential that a random walker feels due to that wall. Note that "wall" and "barrier" obviously mean the same in this context. We start by considering a free random walk and setting up proper nomenclature. We can then describe the presence of a wall with the help of *mirror paths*. This is similar to the method of *mirror charges* known from electrostatics which was originally developed by Maxwell [56] already around 1870. The presented calculations are built on the discussions by Chandrasekhar [14].

7.1 A Free Random Walker

Let us start with the most simple of all random walks: an unbiased, one-dimensional free random walk with all steps of equal length. Unbiased means that the walker chooses the direction of its next step (up or down) both with probability $p = 1/2$. Without loss of generality we set the constant step length to $\ell = 1$. We are now asking for $W(m, N)$, the probability to be at position m after N steps when starting at the origin. Note that m must be even (odd) when N is even (odd). In the following, we are always assuming that this is the case (otherwise, we have trivially $W(m, N) = 0$).

The probability for any given random walk consisting of N steps is $(1/2)^N$. This is because there are 2^N distinct walks each of which having equal probability. Hence, we know that

$$W(m, N) = \text{number of distinct walks from 0 to } m \cdot \left(\frac{1}{2}\right)^N. \tag{7.1}$$

It is easy to see that we must take $(N+m)/2$ steps into the positive and $(N-m)/2$ into the negative direction (where the 'positive'-direction is defined by the sign of m). Hence, we have found that

$$W(m, N) = \begin{pmatrix} N \\ (N+m)/2 \end{pmatrix} \left(\frac{1}{2}\right)^N \tag{7.2}$$

which corresponds to a Bernoullian distribution. Clearly, due to symmetry it must hold that the expectation value of m vanishes:

$$\mathbb{E}[m] = 0. \tag{7.3}$$

Since the increments are independent, the variance is additive and we find

$$\mathbb{E}\left[m^2\right] = \sum_{i=1}^{N} 1 = N \tag{7.4}$$

which implies the following result for the root mean square displacement:

$$\sqrt{\mathbb{E}[m^2]} = \sqrt{N}. \tag{7.5}$$

We can simplify (7.2) in the case of $N \gg m$ by using Stirling's formula

$$\log N! = \left(N + \frac{1}{2}\right) \log N - N + \frac{1}{2} \log 2\pi + \mathcal{O}\left(N^{-1}\right) \quad (N \to \infty). \tag{7.6}$$

We find

$$\log W(m,N) \sim \left(N+\frac{1}{2}\right)\log N - \frac{1}{2}(N+m+1)\log\left(\frac{N}{2}\left(1+\frac{m}{N}\right)\right) - \frac{1}{2}(N-m+1)\log\left(\frac{N}{2}\left(1-\frac{m}{N}\right)\right) - \frac{1}{2}\log 2\pi - N\log 2. \tag{7.7}$$

A first order Taylor approximation yields

$$\log\left(1\pm\frac{m}{N}\right) = \pm\frac{m}{N} - \frac{1}{2}\frac{m^2}{N^2} + \mathcal{O}\left(\frac{m^3}{N^3}\right). \tag{7.8}$$

Thus, our expression simplifies further to

$$\log W(m,N) \sim -\frac{1}{2}\log N + \log 2 - \frac{1}{2}\log 2\pi - \frac{m^2}{2N} \tag{7.9}$$

and finally

$$W(m,N) \sim \sqrt{\frac{2}{\pi N}}e^{-m^2/2N}. \tag{7.10}$$

A simple numerical analysis shows that this approximation is very accurate already for small parameters such as $N = 10$ and $m < 7$.

Changing nomenclature, we can make rewrite (7.10) such that taking the continuous limit will be straight forward. We write $x = m\ell$ where ℓ is now a constant step size of any length. Then, x is simply the net displacement from the origin. In particular, we can now ask for the probability $W(m,N)\Delta x$ that we are in the interval $[x, x+\Delta x]$ after N steps for $\Delta x \gg \ell$. We have

$$W(x,N)\Delta x = W(m,N)\frac{\Delta x}{2\ell} \tag{7.11}$$

where the factor 2 stems from the fact that m can take only even (odd) values when N is even (odd). Combining all this, we can write

$$W(x,N) = \frac{1}{\sqrt{2\pi N\ell^2}}e^{-x^2/2N\ell^2}. \tag{7.12}$$

Moreover, if we assume that we make n steps per unit time and we define the *diffusion coefficient* $D \equiv \frac{1}{2}n\ell^2$ we can write

$$W(x,t)\Delta x = \frac{1}{2\sqrt{\pi Dt}}e^{-x^2/4dt}\Delta x. \tag{7.13}$$

7.2 A Random Walker and a Reflective Wall

Let us assume that there is a perfectly *reflecting wall* at $m_0 > 0$ (the case $m_0 < 0$ is analogous). This means that whenever the particle arrives at m_0 it is retracing its step to $m_0 - 1$ with probability 1. We ask for the probability $W^{(\text{refl})}(m,N;m_0)$, i.e. the probability that a particle arrives at m after N steps under the condition that there is a reflecting boundary positioned at m_0. Obviously, we have $W^{(\text{refl})}(m,N;m_0) = 0$ for all $m > m_0$ since we assume that (without loss of generality) the walk starts at the origin. To derive an expression if $m \leqslant m_0$ we have to modify (7.2) by accounting for the fact that whenever the walker is at m_0 he or she turns with probability 1. Formally, this means that a path which is reflected k times at m_0 before reaching m must be weighted by a factor of 2^k since

we have falsely multiplied the probability of this path by a probability of $(1/2)^k$. At this point, it is usually argued that we can account for these factors 2^k by considering also all the *mirrored paths*, hence, that we have

$$W^{(\text{refl})}(m, N; m_0) = W(m, N) + W(2m_0 - m, N) \tag{7.14}$$

$$\overset{N \gg m}{\approx} \sqrt{\frac{2}{\pi N}} \left(e^{-m^2/2N} + e^{-(2m_0-m)^2/2N} \right). \tag{7.15}$$

This is indeed true, but let us derive this in some more detail. Let $k_{\max}$ denote that maximal possible number of reflections that a path starting at the origin and arriving at m after N steps can have. Also, "# DP" stands for "number of distinct paths" and "RW" stands for "random walk". We find

$$\begin{aligned}
W^{(\text{refl})}(m, N; m_0) &= \sum_{k=0}^{k_{\max}} \sum_{\substack{\text{RW } i \text{ with} \\ k \text{ reflections}}} \underbrace{\begin{pmatrix}\text{probability for a RW } i \\ \text{with } k \text{ reflections}\end{pmatrix}}_{\text{equal } \forall\ i} \\
&= \sum_{k=0}^{k_{\max}} \begin{pmatrix}\#\text{ DP with} \\ k \text{ reflections}\end{pmatrix} \cdot \begin{pmatrix}\text{probability for a RW } i \\ \text{with } k \text{ reflections}\end{pmatrix} \\
&= \sum_{k=0}^{k_{\max}} \begin{pmatrix}\#\text{ DP with} \\ k \text{ reflections}\end{pmatrix} \cdot 2^k \begin{pmatrix}\text{probability for the same RW } i \\ \text{but in absence of the wall at } m_0\end{pmatrix} \\
&= \sum_{k=0}^{k_{\max}} \begin{pmatrix}\#\text{ DP with} \\ k \text{ reflections}\end{pmatrix} \cdot 2^k \left(\frac{1}{2}\right)^N
\end{aligned} \tag{7.16}$$

Now the idea of mirror paths comes into play. We claim that for each path with k reflections at m_0 there exist $2^k - 1$ forbidden paths (i.e. paths that cross the reflective wall) that lead either to m or to its image (i.e. its reflection at m_0) $2m_0 - m$. This can be justified inductively:

(i) All the paths that arrive at m without ever being reflected are trivially accounted for by $W(m, N)$. There are $2^k - 1 = 2^0 - 1 = 0$ mirrored paths.

(ii) Now, consider a path that leads to m and is reflected exactly $k = 1$ time at m_0. It is easy to see (figure 7.1) that for every path that is reflected just once there is exactly one mirrored path that leads to $2m_0 - m$. Hence, we have $2^k - 1 = 1$ additional forbidden path.

(iii) If we draw a path that is reflected $k = 2$ times at the wall m_0 before arriving at m (blue line in figure 7.2) we can see that there are two alternative paths that lead to $2m_0 - m$ (red and red dashed line) and that there is one additional path that crosses the wall twice and leads back to m (green line). Hence, we have $2^k - 1 = 3$ additional forbidden paths.

(iv) This reasoning can be continued inductively. One has then shown that for a path with k reflections there are $2^k - 1$ additional forbidden paths which lead either to m or to $2m_0 - m$. We omit showing this step explicitly here since the idea is intuitively clear.

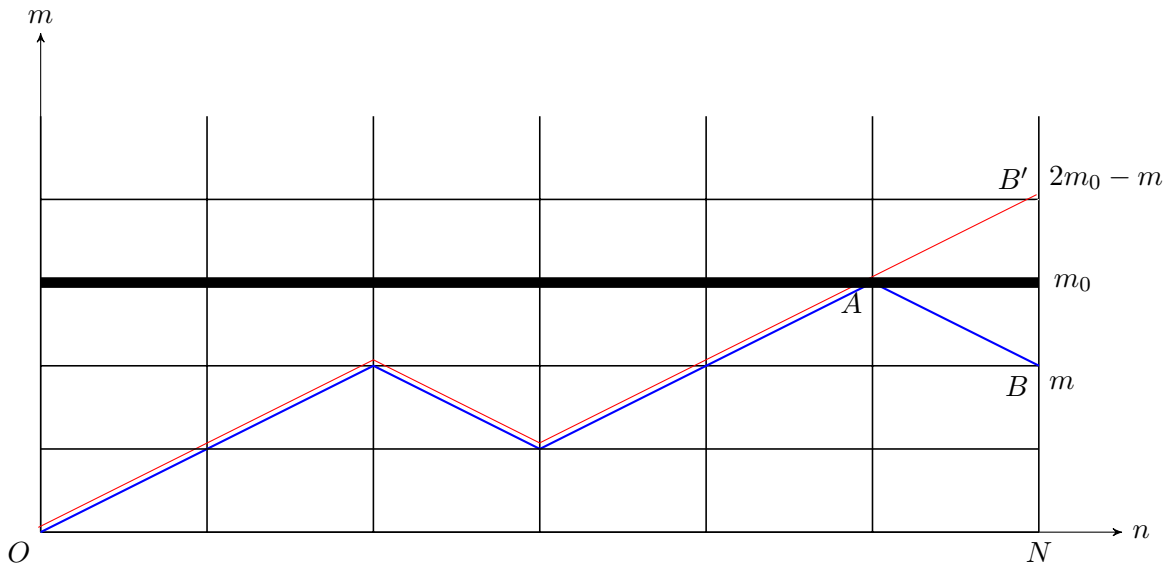

Figure 7.1: The blue line denotes the path of a random walk with $N = 6$ steps, $k = 1$ reflections at a reflective wall wich is located at $m_0 = 3$ and ending at $m = 2$. For $k = 1$ reflections we have to account for $2^k = 2$ distinct walks (blue and red line) that lead to the same path if there is a wall present.

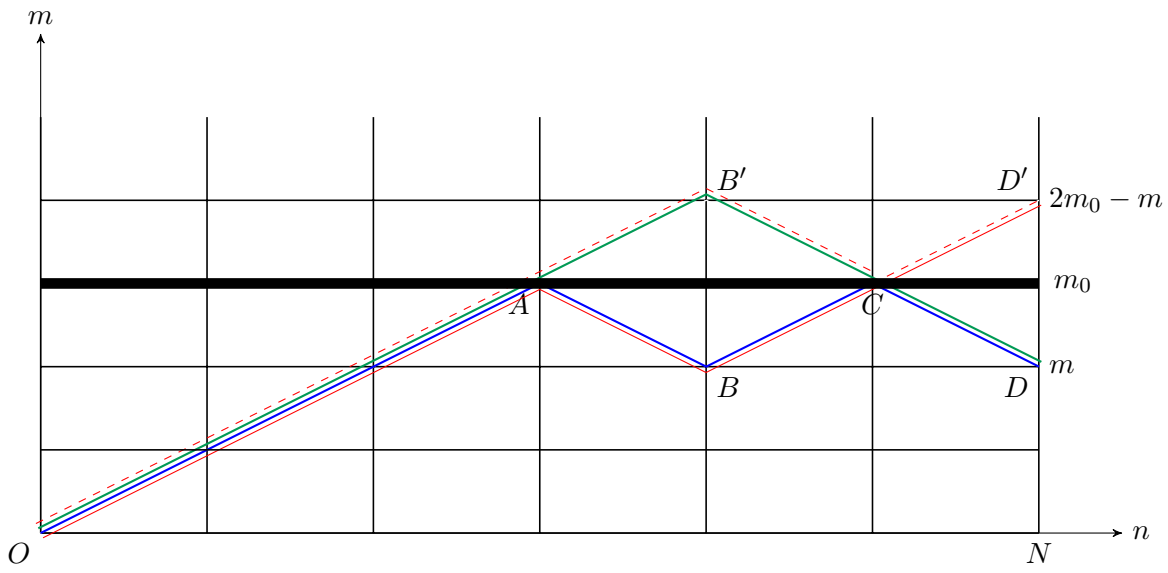

Figure 7.2: The blue line denotes the path of a random walk with $N = 6$ steps, $k = 2$ reflections at a reflective wall wich is located at $m_0 = 3$ and ending at $m = 2$. For $k = 2$ reflections we have to account for $2^k = 4$ distinct walks (blue, red, red dashed and green line) that lead to the same path if there is a wall present.

With this claim, we can write further

$$\begin{aligned} W^{(\text{refl})}(m,N;m_0) &= \sum_{k=0}^{k_{\max}} \binom{\#\text{ DP with}}{k\text{ reflections}} \cdot 2^k \left(\frac{1}{2}\right)^N \\ &= \sum_{k=0}^{k_{\max}} \binom{\#\text{ DP with}}{k\text{ reflections}} \cdot \left[\binom{\text{probability for RW with } k \text{ reflections}}{\text{or its mirrored paths to } m} + \right. \\ &\qquad \left. \binom{\text{probability for mirrored paths of RW}}{\text{with } k \text{ reflections to } 2m_0 - m}\right] \\ &= W(m,N;m_0) + W(2m_0 - m, N; m_0) \end{aligned} \tag{7.17}$$

which proofs (7.14).

Changing again to the notation $x = ml$ the probability $W^{(\text{refl})}(x,t,x_1)\Delta x$ hat a particle is between x and $x + \Delta x$ after a time t (during which it takes $n \cdot t$ steps) in the presence of a reflecting wall at $x_0 = m_0\ell$ we have

$$W^{(\text{refl})}(x,t;x_0) = \frac{1}{2\sqrt{\pi D t}} \left(e^{-x^2/4Dt} + e^{-(2x_0-x)^2/4Dt}\right). \tag{7.18}$$

Note that this implies

$$\left.\frac{\partial W^{(\text{refl})}}{\partial x}\right|_{x=x_0} = 0, \tag{7.19}$$

i.e. the probability flux through the hard wall at m_0 is vanishing, as anticipated.

7.3 A Random Walker and an Absorbing Wall

Let us assume that there is a perfectly *absorbing wall* at $m_0 > 0$, i.e. whenever the random walker arrives at m_0 he or she becomes trapped and cannot keep on walking. We ask for $W^{(\text{abs})}(m,N;m_0)$ which is the probability that the particle is at position m after N steps in presence of the absorbing wall at m_0. As already for the reflecting wall we can solve this problem with the method of images. Obviously, we have $W^{(\text{abs})}(m,N;m_0) = 0$ for all $m > m_0$ since we assume that (without loss of generality) the walk starts at the origin. When counting the number of distinct walks in order to derive $W^{(\text{abs})}(m,N;m_0)$ for some $m \leqslant m_0$ we must be careful to exclude all sequences which include even a single arrival at m_0. Hence, we must exclude all the *forbidden sequences*. From our discussion above we know now that every forbidden sequence uniquely defines another sequence leading to the image point $2m_0 - m$. This can be seen by reflecting the path at $m = m_0$ once the trajectory hits m_0 for the first time. Conversely for every trajectory leading to $2m_0 - m$ we obtain by reflection a forbidden trajectory leading to m since any trajectory to $2m_0 - m$ must necessarily cross the absorbing wall at m_0. Hence,

$$W^{(\text{abs})}(m,N;m_0) = W(m,N) - W(2m_0 - m, N) \tag{7.20}$$

$$\overset{N\gg m}{\sim} \sqrt{\frac{2}{\pi N}} \left(e^{-m^2/2N} - e^{-(2m_0-m)^2/2N}\right) \tag{7.21}$$

$$\sim \frac{1}{2\sqrt{\pi D t}} \left(e^{-x^2/4Dt} - e^{-(2x_0-x)^2/4Dt}\right). \tag{7.22}$$

In particular, $W^{(\text{abs})}(m_0,t;m_0) \equiv 0$.

7.4 Scaling of the Partition Function

We are interested in the partition function

$$Z_N^{(\text{refl/abs})} = \sum_{m=-N}^{m_0} W^{(\text{refl/abs})}(m, N; m_0) \tag{7.23}$$

of a random walk starting at the origin and consisting of N steps with a reflecting or absorbing wall located at $m_0 > 0$. Formally, this is of course just equal to unity (the walker certainly has to end up somewhere) since all our probabilities have been properly normalized by 2^{-N} in (7.2). However, we are rather interested in the leading scaling behavior of Z_N as a function of the number of steps N. For this, note that in leading order in N it holds

$$(7.15) \sim N^{-3/2} e^{-m^2/2N}. \tag{7.24}$$

Comparison with (7.21) shows that the same scaling behavior applies for an absorbing wall. Therefore, we can drop this distinction in the following. The number of terms in the partition function (7.23) is of order N and so we find that

$$Z_N \sim \frac{1}{\sqrt{N}}. \tag{7.25}$$

Finally, we also note that the most probable distance and the mean distance from the wall after N steps scale as

$$\mathbb{E}[m] \sim \sqrt{N}. \tag{7.26}$$

which can be seen from (7.2) and (7.23) by setting the corresponding derivatives (in the continuous limit) to zero. Alternatively, this can also be seen from (7.5) using symmetry arguments. This is all we need for the derivation of the repulsive force acting on a random walker in presence of a wall.

8 Appendix II: Path Integral Methods for Stochastic Differential Equations

In section 2.2 we have encountered a stochastic differential equation (SDE) of the form

$$\dot{X}(t) = -aX(t) + bX(t)^2 + \sqrt{D}\eta(t). \tag{8.1}$$

where a, b, D are some constants and η is white noise. Let $X_0 \equiv X(t=0) \in \mathbb{R}$ denote some initial value. We are interested in calculating the (time-dependent) moments and cumulants of X. A first step to do so could consist of solving (8.1) which is, however, not so simple. Alternatively solving the corresponding Fokker-Planck equation is not any easier. Luckily, it turns out that we do not have to solve any of these equations. We can use a path integral formalism to obtain perturbative results of all the moments and cumulants.

The following discussion relies on the work of Chow and Buice [15]. The entire discussion presented here displays close similarities to the path integral treatment of (quantum) field theories (QFT). This includes the usage of mathematical tools such as *Feynman diagrams* and *functional derivatives* but also nomenclature that is directly adopted from physical analogies. Readers unfamiliar with the topic are referred to more didactical introductions. See the standard textbooks by Peskin & Schröder [65] or Ryder [72] for an introduction in the context of quantum field theory. See Kleinert [41] for an introduction which also includes applications to finance.

8.1 Motivation

For a one-dimensional, real random variable X we define the *moment generating function* Z as

$$Z[\lambda] = \left\langle e^{\lambda X} \right\rangle = \int dX P(X) e^{\lambda X} \tag{8.2}$$

where P is the density distribution function of X and $\lambda \in \mathbb{R}$ some dummy variable. Via

$$\langle X^n \rangle = \frac{1}{Z[0]} \frac{d^n}{d\lambda^n} Z(\lambda)\bigg|_{\lambda=0} \tag{8.3}$$

we can then calculate the n-th moment of X as can be seen immediately by applying the derivative directly on the integrand in (8.2). [8] Note that usually in this context $Z[0] = 1$ since P is normalized. However, we must not insist on this condition since this factor cancels out in (8.3) anyway. Furthermore, the *cumulant generating function* Z_C is defined as

$$Z_C[\lambda] = \log Z[\lambda]. \tag{8.4}$$

By definition, the n-th cumulant is then given by

$$\langle X^n \rangle_C = \frac{d^n}{d\lambda^n} W(\lambda)\bigg|_{\lambda=0}. \tag{8.5}$$

It is now clear that having a closed-form expression for Z presents a convenient way of calculating moments and cumulants: It is then just a matter of taking derivatives.

[8] Mind the change in notation. In this thesis, we usually denote theoretical expectation values by $\mathbb{E}$ and empirical mean values by $\langle\cdot\rangle$. However, in this appendix we choose to denote theoretical expectation values also by $\langle\cdot\rangle$ to highlight the formal equivalence between the following calculations and the formalism know from field theories.

Let us now consider the special case of a Gaussian distributed variable X with mean a and standard deviation σ. We find

$$\begin{aligned} Z[\lambda] &= \frac{1}{\sqrt{2\pi}\sigma} \int dX \; e^{-\frac{\left(X-\lambda\sigma^2-a\right)^2}{2\sigma^2}+\lambda X} \\ &= Z[0] e^{\lambda a + \frac{\lambda^2\sigma^2}{2}} \end{aligned} \tag{8.6}$$

with $Z[0] = \sqrt{2\pi}\sigma$. The second equality follows from completing the square in the exponent.

This method generalizes to an n-dimensional random variable $\vec{X} = (X_1, \ldots, X_n)$ in a natural way through

$$\begin{aligned} Z\left[\vec{\lambda}\right] &= \frac{1}{(2\pi)^{n/2}\sqrt{|\det(K)|}} \int \prod_{i=1}^{n} dX_i \exp\left(-\frac{1}{2}\sum_{j,k} X_j K^{-1}_{jk} X_k + \sum_j \lambda_j X_j\right) \\ &= Z[0] \exp\left(\sum_{j,k} \frac{1}{2}\lambda_j K_{jk} \lambda_k\right) \end{aligned} \tag{8.7}$$

with $Z[0] = (2\pi \det K)^{n/2}$ and K is the inverse of the covariance matrix.

It is now intuitive to consider the generalization to an "infinite-dimensional random variable" $X_i \to X(t)$ where $t \in [0, T]$. This yields the "infinite-dimensional generalization"

$$Z[\lambda] \propto \int \mathcal{D}X(t) \; \exp\left(-\frac{1}{2}\int ds\, dt\; X(s) K^{-1}(s,t) X(t) + \int dt\; \lambda(t) X(t)\right) \tag{8.8}$$

$$= Z[0] \exp\left(\int ds\, dt\; \frac{1}{2}\lambda(s) K(s,t) \lambda(t)\right) \tag{8.9}$$

where $\mathcal{D}X(t) \equiv \lim_{n\to\infty} \prod_{i=0}^{n} dx_i$ and $Z[0] = \lim_{n\to\infty} (2\pi \det K)^{n/2}$. In the last step we have again "completed the square". Integrals of type (8.8) which integrate over an entire functional space are commonly called *(Feynman) path integrals*. Note that $Z[0]$ is formally infinite but as already argued above, we will see that this divergent pre-factor cancels out in the calculation of moments and cumulants.

8.2 From Differential Equations to Path Integrals

The above was just a special case for an "infinite-dimensional Gaussian distributed stochastic process". Let us have a look now at how we can generalize this idea in order to apply it to a general SDE of the form

$$\dot{X} = f(X,t) + g(X,t)\eta(t) \quad \Leftrightarrow \quad dX(t) = f(X,t)dt + g(x,t)dW(t) \tag{8.10}$$

where $W(t)$ is a Wiener process and the equation is interpreted in the Itô sense (see section 2.2 for a discussion of Itô vs. Stratonovich) Moreover, we have the initial condition $X_0 = X(t=0) \in \mathbb{R}$. Let us now rewrite this initial value problem as a probability density

$$P[X(t)|X_0, \eta(t)] = \delta\left[\dot{X}(t) - f(X,t) - g(X,t)\eta(t) - X_0\delta(t-t_0)\right] \tag{8.11}$$

where δ is the delta functional, i.e. the functional generalization of Dirac's delta distribution. The definition of the density P via (8.11) is actually a trivial statement since all we do is writing a

probability distribution that is constrained at the solution of the SDE. Recall that the δ-functional has the path-integral representation

$$\delta(X(t)) = \mathcal{N} \int \mathcal{D}K(t)\, e^{-\int dt\; iK(t)X(t)} \equiv \mathcal{N} \int \mathcal{D}\tilde{K}(t)\, e^{-\int dt\; \tilde{K}(t)X(t)} \tag{8.12}$$

where we have defined $\tilde{K}(t) := iK(t)$. Moreover, we denote by $\mathcal{N}$ some pre-factor in which we will collect all the (possibly diverging) pre-factors that occur in the following calculations. Using that η is white noise we find

$$\begin{aligned} P[X(t)|X_0] &= \mathcal{N} \int \mathcal{D}\eta\; P[X(t)|X_0,\eta]\; e^{-\eta^2(t)} \\ &= \mathcal{N} \int \mathcal{D}\eta\, \mathcal{D}\tilde{K}\; \exp\left(-\int dt\; \left[\tilde{K}(t)\left(\dot{X}(t) - f(X,t) - X_0\delta(t-t_0)\right)\right.\right. \\ &\qquad \left.\left. + \tilde{K}(t)g(x,t)\eta(t) - \eta^2(t)\right]\right) \\ &= \mathcal{N} \int \mathcal{D}\tilde{K}(t)\; \exp\left(-\int dt \left[\tilde{K}(t)\left(\dot{X}(t) - f(x,t) - X_0\delta(t-t_0)\right) + \frac{1}{2}\tilde{K}^2(t)g^2(x,t)\right]\right) \end{aligned} \tag{8.13}$$

where in the last step we have completed the square and integrated out the η-dependence. We will drop $\mathcal{N}$ in the following for simplicity and since it would cancel out in final-results anyway. Now we can write the moment and cumulant generating functionals for the solution of (8.1) as

$$\begin{aligned} Z[J,\tilde{J}] &= \left\langle \exp\left(\int dt\; \left(\tilde{J}(t)X(t) + J(t)\tilde{K}\right)\right)\right\rangle \\ &= \int \mathcal{D}X(t)\, \mathcal{D}\tilde{K}(t)\; \exp\left(-S[X,\tilde{K}] + \int dt\; \tilde{J}(t)X(t) + \int dt\; J(t)\tilde{K}(t)\right) \end{aligned} \tag{8.14}$$

with the *action*

$$S[X,\tilde{K}] \equiv \int dt \left[\tilde{K}(t)\left(\dot{X}(t) - f(X(t),t) - X_0\delta(t-t_0)\right) - \frac{1}{2}\tilde{K}^2(t)g^2(X(t),t)\right]. \tag{8.15}$$

The terms proportional to $\tilde{J}X$ and $J\tilde{K}$ in (8.14) are the so-called *source terms*. Since J and $\tilde{J}$ will be set to zero in any final result we have introduced them without loss of generality. Working with functional derivatives, the source terms turn out useful because the moments can be obtained via

$$\left\langle \prod_{i=1}^{m}\prod_{j=1}^{n} X(t_i)\tilde{K}(t_j)\right\rangle = \frac{1}{Z[0,0]} \prod_{i=1}^{m}\prod_{j=1}^{n} \frac{\delta}{\delta\tilde{J}(t_i)}\, \frac{\delta}{\delta J(t_j)} Z\Big|_{J=\tilde{J}=0} \tag{8.16}$$

whereas the cumulants obey

$$\left\langle \prod_{i=1}^{m}\prod_{j=1}^{n} X(t_i)\tilde{K}(t_j)\right\rangle_C = \frac{1}{Z[0,0]} \prod_{i=1}^{m}\prod_{j=1}^{n} \frac{\delta}{\delta\tilde{J}(t_i)}\, \frac{\delta}{\delta J(t_j)} \log Z\Big|_{J=\tilde{J}=0}. \tag{8.17}$$

Now, let us apply this formalism specifically to (8.1). The expression for the action (8.15) then reads

$$S[X,\tilde{K}] = \int dt\; \left[\tilde{K}\left(\dot{X} + aX - bX^2 - X_0\delta(t-t_0)\right) - \frac{D}{2}\tilde{K}^2\right]. \tag{8.18}$$

We see immediately that this does not correspond to a *free* action, meaning that X and $\tilde{K}$ appear in such a way that we cannot complete the square and perform the integration as before but we will require perturbative methods instead. We thus separate $S = S_F + S_I$ where S_F denotes the free part

$$S_F[X,\tilde{K}] = \int dt\; \tilde{K}\left(\dot{X} + aX\right) = \int dt\; \tilde{K}\left(\frac{d}{dt} + a\right) X \tag{8.19}$$

and the rest of the action belongs to the *interaction* part S_I. Now we only have to determine the inverse (or rather Green's function) G of the operator $\left(\frac{d}{dt}+a\right)$, i.e. solve for

$$\left(\frac{d}{dt}+a\right)G(t,t')=\delta(t-t'). \tag{8.20}$$

Once we know G, we add source terms to S_F, i.e. define $S_0 := S_F + \int dt\ \tilde{J}(t)X(t) + \int dt\ J(t)\tilde{K}(t)$. This yields the generating functional of the free action with source terms

$$Z_F[J,\tilde{J}] = Z_0 \exp\left(\int ds\ dt\ \tilde{J}(s)G(s,t)J(t)\right) \tag{8.21}$$

where we have completed the square such that all the source terms become independent of X and $\tilde{K}$. In this way the path integral becomes nothing but a (diverging) pre-factor $Z_0 \equiv Z[J=0]$ which cancels out when we calculate moments and cumulants. The generating functional of the entire theory including the interaction part is given as

$$Z[J,\tilde{J}] = \exp\left(S_I\left[\frac{\delta}{\delta J},\frac{\delta}{\delta \tilde{J}}\right]\right) Z_F[J,\tilde{J}]. \tag{8.22}$$

By expanding the exponential up to an arbitrary order and using (8.16) and (8.17), respectively, we can calculate any moment or cumulant with arbitrary precision.

It is important to note that a perturbative expansion makes only sense if we can make sure that the *coupling constants* are small. In our case, this means that we must make sure that b, D and X_0 (a belongs to the free action) are small. We discuss the validity of this assumption in section 8.4. For now, let us assume that this is indeed the case.

Before we can start calculating moments and cumulants we must solve equation (8.20). This is done best by transforming the equation into Fourier-space (variables denoted with a hat) where we use that $\widehat{\frac{d}{dt}} = -iE$ and $\widehat{\delta} = 2\pi$. In Fourier-space we have nothing but a simple polynomial equation

$$(a-iE)\,\hat{G}(E) = 2\pi \quad \Rightarrow \quad \hat{G}(E) = \frac{2\pi}{a-iE}. \tag{8.23}$$

In order to transform back to $G(t) = \frac{1}{2\pi}\int dE\ 2\pi e^{iEt}/(a-iE)$ we can use the residue theorem (see for instance [12]) together with a distinction of cases for $t \leq 0$ and $t > 0$ to find

$$G(t,t') = \Theta(t-t')e^{-a(t-t')} \tag{8.24}$$

where

$$\Theta(t) = \begin{cases} 0, & t \leqslant 0 \\ 1, & t > 0 \end{cases} \tag{8.25}$$

is the left-continuous Heaviside function. [9]

We have now all we need to calculate the moments and cumulants. We expand the interacting part of the action as

$$\begin{aligned}\exp\left(S_I[X,\tilde{K}]\right) = 1 - X_0\tilde{K}(t_0) - b\int dt\ \tilde{K}(t)X^2(t) - \frac{D}{2}\int dt\ \tilde{K}^2(t) \\ + \frac{1}{2}\left(X_0\tilde{K}(t_0) + b\int dt\ \tilde{K}(t)X^2(t) + \frac{D}{2}\int dt\ \tilde{K}^2(t)\right)^2 + \ldots,\end{aligned} \tag{8.26}$$

replace X by $\delta/\delta J$ and $\tilde{K}$ by $\delta/\delta\tilde{J}$, plug this into (8.22) and then calculate the cumulants via (8.17).

[9] Left-continuity is an important detail in order to be consistent with our interpretation of the stochastic process according to Itô's definition.

8.3 Feynman Diagrams

The above technique for calculating cumulants is possible but also rather tedious. There is a much more convenient way to keep track of the necessary terms by introducing *Feynman diagrams*. A technical introduction to the use of Feynman diagrams can be found in [65, 72]. With some practice, one can quickly derive the Feynman diagrams and the corresponding *Feynman rules* from the action (8.18). There may be some additional subtleties to the rules when the fields involved in the theory have vectorial or tensorial structure as for instance in quantum chromodynamics (QCD). For (8.18) the derivation is straight forward:

The *propagator* G corresponds to the free part of (8.18) and is graphically denoted by a straight line:

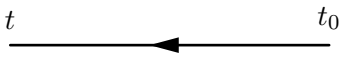

$$= \left\langle \tilde{K}(t)X(t_0) \right\rangle_F = G(t,t_0) \quad (t > t_0). \tag{8.27}$$

The subscript F means averaging with respect to the free partition function (8.21). We work in the convention that time flows from right to left. The right end of a line then denotes a time t_i and the left end point denotes a time t_f with $t_f > t_i$.
Each summand in the interacting part in (8.18) now constitutes one additional Feynman rule, a so-called *vertex*. In a simple theory like (8.18) a vertex is drawn according to the following rules: For each X-field we draw an ingoing and for each K-field we draw an outgoing line. Consequently, the corresponding Feynman rule for this vertex is nothing but the term in the action but with the opposite sign since $Z \propto e^{-S}$. For the first vertex, we read from (8.18)

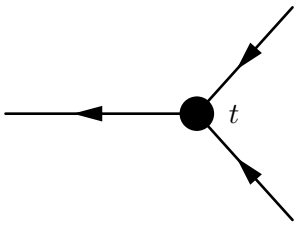

$$= bX^2(t)\tilde{K}(t). \tag{8.28}$$

Time t denotes any time between the time t_i to the right of the incoming lines and the time t_f to the left of the outgoing line. Since t can denote any point with $t_i < t < t_f$ we will see below that we have to integrate over t, i.e. consider a superposition of all possibilities $t \in (t_i, t_f)$.
The second vertex in (8.18) reads

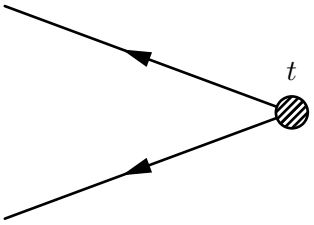

$$= \frac{D}{2}\tilde{K}^2(t) \tag{8.29}$$

and finally we have a *tadpole*, i.e. a vertex with no ingoing line,

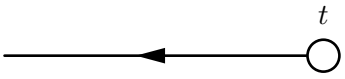

$$= X_0 \tilde{K}(t)\delta(t - t_0). \tag{8.30}$$

The δ arises because this node cannot be connected to the right. Hence, it must denote the "right-most" point in time, i.e. the initial time t_0. The usefulness of these diagrams is due to the following statement:

Expression (8.16) is equal to the sum of all (topologically distinct) Feynman diagrams with m ingoing and n outgoing lines which can be drawn with only the above nodes (8.28)-(8.30). Furthermore, the cumulants (8.17) are given by the sum of all *fully connected* Feynman diagrams. Here, fully connected means just that all nodes are connected to each other (either directly or via other nodes).

This is a powerful statement. It tells us that instead of working with multiple functional derivatives and a myriad of product and chain rules, we can simply draw intuitive diagrams which then correspond to certain mathematical expressions. However, two questions naturally arise: What are distinct diagrams? For a given m and n, there seems to be in general an infinite amount of diagrams with m incoming and n outgoing lines. Do we have to consider an infinite amount of diagrams? As will become more clear below, there is a 1:1 correspondence between the number of nodes in a diagram and the order of the expansion in (8.26). We can see from (8.26) that if the *coupling constants* y, b and D are small, only the diagrams with the least amount of nodes will contribute significantly. We will argue in section 8.4 that indeed these coupling constants are small and hence we are safe to consider only the diagrams with the smallest amount of nodes.
Regarding the first question, we can look for instance at the node (8.28). We see that there are two possibilities for the two incoming lines to connect to the node. (Line coming from top right going to the top right "plug" of the node or line coming from top right going to the bottom right "plug" of the node. Only the first possibility is depicted in (8.28).) Indeed, these are two topologically distinct diagrams and so they have to be considered as two different diagrams. However, they represent the same mathematical expression. It is therefore easier to just consider each such diagram as one, and than multiply it by its *symmetry factor* $\mathcal{S}$. The symmetry factor accounts exactly for the number of topologically distinct diagrams that represent the same mathematical expression. Another ambiguity arises from the choice t of the node which must be between t_i and t_f. Since each such choice corresponds to a different diagram, we must integrate over all such choices of t. This leads us finally to the following set of *Feynman rules* which tell us exactly what mathematical expression we must assign to each diagram:

(i) Each line between two points of time t_i and t_j corresponds to a propagator $G(t_i, t_j)$ where $t_i > t_j$. [10]

(ii) For $\mathcal{S}$ distinct ways of connecting edges to vertices that lead to the "same" diagram we account a symmetry factor $\mathcal{S}$.

[10] The case $t_i = t_j$ (e.g. in loops) drops automatically out since $\Theta(0) = 0$.

(iii) For each vertex we multiply by the corresponding pre-factor (X_0, b or $D/2$) and integrate each vertex over the time-domain (t_0, ∞).

It is easy to verify, that these rules yield exactly the same as the approximation of (8.16) and (8.17) via (8.26). Note that for an expansion up to k-th order in (8.26) we have to consider a factor of $1/k!$ from the expansion of the exponential. This factor does not show up in our Feynman rules because it cancels exactly with the number of permutations of the vertices that lead to the same diagram.

We are now ready to calculate the cumulants of $X(t)$ from (8.1). For the variance and skewness of $X(t)$ we will need to know $\langle X^n(t)\rangle_C$ for $n = 2, 3$. Let us start with $\langle X^3(t)\rangle_C$. A first straight forward idea which comes to mind is

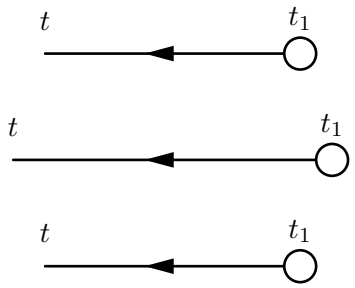

(8.31)

This diagram contributes to $\langle X^3(t)\rangle$. However, as argued above, only the fully connected diagrams contribute to the cumulants. (Thinking in terms of (8.17) and (8.26) this can easily be seen as a consequence of the product rule for the functional derivative.) Hence, we can already discard all the diagrams that are not fully connected and find for the lowest order contribution to $\langle X^3(t)\rangle_C$ the following diagram:

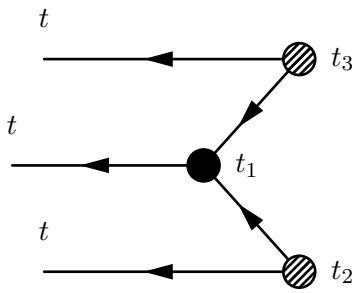

(8.32)

For all the three vertices we have 2 possibilities each to connect the lines to the vertices. This yields a symmetry factor of 8. Hence, we find that

$$\begin{aligned}(8.32) &= 8b\frac{D^2}{4}\int dt_1 \int dt_2 \int dt_3\, G(t,t_1)G(t,t_2)G(t,t_3)G(t_1,t_2)G(t_1,t_3) \\ &= \frac{2bD^2}{3a^3}e^{-4at}\left(e^{at}-e^{at_0}\right)^3\left(e^{at}+3e^{at_0}\right). \end{aligned} \tag{8.33}$$

In the limit of large t we have thus found that the third cumulant is given up to third order by

$$\langle X^3(t)\rangle_C = \frac{2bD^2}{3a^3}. \tag{8.34}$$

The next higher contribution term is of the form

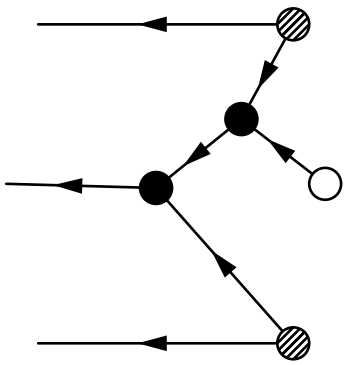

(8.35)

and so forth. If necessary, we can expand the third cumulant up to arbitrary precision. However, we argue in section 8.4 that this is not necessary in our case.

To have everything in the same order we calculate the second cumulant $\left\langle X^2(t)\right\rangle_C$ (which is equal to the variance $\mathbb{V}\left[X(t)\right]$) also up to third order:

$\mathbb{V}\left[X(t)\right] =$ 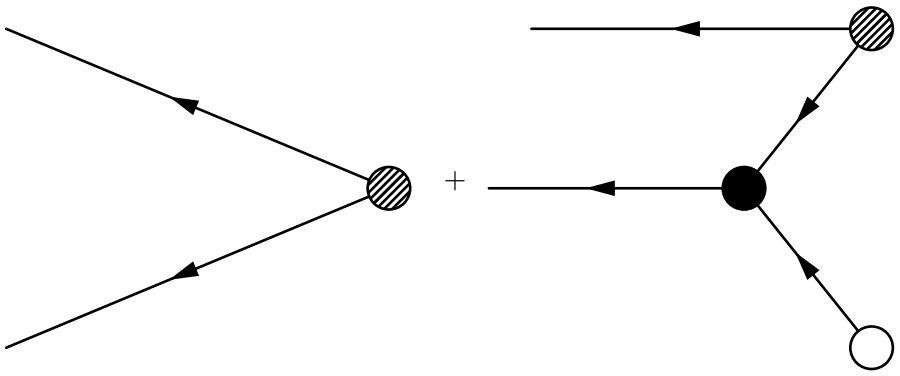

(8.36)

For the first diagram we calculate

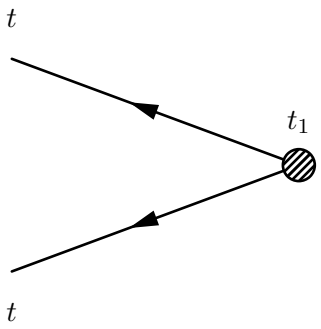

$$= D \int dt_1 \, G(t,t_1)^2 = \frac{D}{2a}\left(1 - e^{2a(t_0-t)}\right) \tag{8.37}$$

and for the second one we have

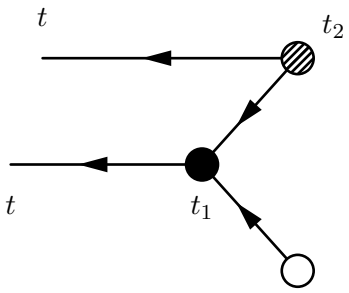

$$= 2byD \int dt_1 \int dt_2 \, G(t,t_1)G(t,t_2)G(t_1,t_0)G(t_1,t_2)$$

$$= \frac{bX_0D}{a^2} e^{a(t_0-3t)} \left(e^{at} - e^{at_0}\right)^2 . \tag{8.38}$$

Thus, we have found that up to third order

$$\left\langle X^2(t) \right\rangle_C = \mathbb{V}(X(t)) = \frac{D}{2a}\left(1 - e^{2a(t_0-t)}\right) + \frac{bX_0D}{a^2} e^{a(t_0-3t)} \left(e^{at} - e^{at_0}\right)^2 \overset{t\to\infty}{\longrightarrow} \frac{D}{2a}. \tag{8.39}$$

The skewness γ of a random variable X is defined as

$$\gamma(X) = \mathbb{E}\left(\left(\frac{X - \mathbb{E}[X]}{\sqrt{\mathbb{V}[X]}}\right)^3\right) = \frac{\left\langle X^3(t) \right\rangle_C}{\mathbb{V}^{3/2}}, \tag{8.40}$$

thus

$$\gamma(X(t)) = \frac{\sqrt{2}}{3}\frac{b\sqrt{D}}{a^{3/2}} \frac{e^{-4at}\left(e^{at} - a^{at_0}\right)^3 \left(e^{at} + 3e^{at_0}\right)}{\left(1 - e^{2a(t_0-t)} + \frac{2by}{a} e^{a(t_0-t)}\left[e^{a(t_0-t)} - 1\right]^2\right)^{3/2}}. \tag{8.41}$$

In the limit of $t \to \infty$ the time dependence cancels out and we are left with

$$\gamma(X(t)) = \frac{\sqrt{2}}{3}\frac{b\sqrt{D}}{a^{3/2}}. \tag{8.42}$$

8.4 Higher Order Expansions

The method presented in the previous section delivers perturbative results in b, X_0 and D (however, not in a which is part of the free action) for moments and cumulants of X. In order to work with the first order result (8.32) for the skewness we have to argue that it is justified to neglect higher order diagrams. This means that we have to argue that the "coupling constant" b, X_0 and D are indeed small. Let us consider D first. Analyzing the time series of the stationary region (figure 1.4) we see that the fluctuations are of order 10^{-3}. Since the random fluctuations scale with $\sqrt{D}\eta$ and η is normally distributed with standard deviation equal to unity we see that we must choose D of order 10^{-6}. Hence, perturbation in D is clearly justified. It is only reasonable to choose an initial value of similar order such that X_0 must also be of magnitude 10^{-3} or smaller. So perturbation in X_0 is justified. Finally, we have that $b = 6F^2/c$. We have shown in section 2.2 that $F \sim 1/r_{\text{éq}}^2$ and since $r_{\text{eq}} \gtrsim 1.20$ we see that F^2 is of order $1/2$. For b to be small, we must show that c is small. This is problematic, since c is a parameter from the model that we cannot influence or estimate a priori. However, we will show now that perturbation is still justified, as long as c is reasonably "small".

The third cumulant $\left\langle X^3(t) \right\rangle_C$ is given in first approximation by (8.32). This means first order in b, second order in D and zeroth order in X_0. Since $D \ll X_0$, the order of D is the one that must be kept

the lowest since one order higher in D will already make the diagram several orders of magnitude less important. We can keep D in second order and expand up to arbitrary order in b and X_0 according to:

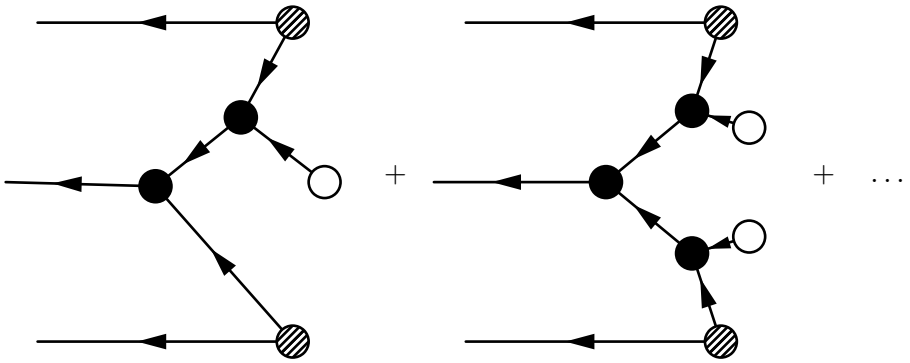

(8.43)

Expanding in this manner we see that if we expand up to n-th order in b we are at $(n-1)$-th order in X_0. However, we know that X_0 is of order 10^{-3} and so as long as c is of order 10^2 or smaller perturbation is still justified. We can also expand in higher orders of D. In third order of D we have for instance

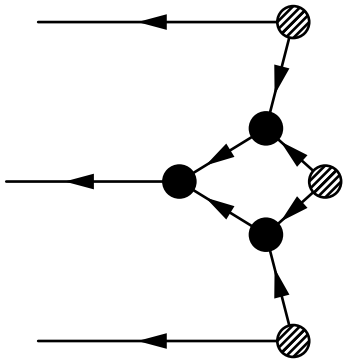

(8.44)

and so forth. However, since D is of order 10^{-6} we can safely neglect higher order expansions in D. It is therefore completely justified to consider only contributions from (8.32) to the calculation of $\left\langle X^3(t)\right\rangle_C$ as long as the value of b is of order 100 or lower because then multiplication with X_0 shows that each higher order is still one order of magnitude less significant. We could even set $X_0 = 0$ (and loose some generality) and then c could take values of order 10^5 and the expansions would still be justified. By nature of the problem, we can assume that b will not exceed such large values since $b \sim 1/c$ and c is a constant in the potential $V = \frac{c}{r} + Fr$.

A similar discussion holds for the variance. With every b vertex that we add to the diagram we have to add at least one X_0 or D vertex which makes it immediately a few orders of magnitude less important. Therefore, it is in good approximation justified to consider only (8.37) for the contribution to the variance.

9 Appendix III: Functional Renormalization Group

In section 2.4 we have proposed an analogy between the constrained EUR/CHF exchange rate and the renormalized potential V describing the interaction of a D-dimensional surface embedded in a $(D+1)$-dimensional space. Applying a method known as *functional renormalization group* (FRG) we want to show in this appendix how the potential V can be renormalized. FRG is a special type of the general renormalization group (RG) framework, see [18] for an in-depth introduction.

We are working with the *interface displacement model* (IDM) in D dimensions where we consider the $z = 0$ plane as the $(D-1)$-dimensional hard wall. We denote points in this plane by the vector $\rho = (x_1, \ldots, x_{D-1})$. One configuration of a $(D-1)$-dimensional interface is given by the function $z(\rho)$ where z denotes the distance of the interface from the wall (height) at position ρ. The Hamiltonian of the IDM takes the form

$$\mathcal{H}(z) = \int \mathrm{d}^{D-1}\rho \, \left(\frac{\sigma}{2} \left| \nabla_\rho z(\rho) \right|^2 + V(z(\rho)) \right). \tag{9.1}$$

The first term of (9.1) controls the fluctuations of a free surface. The second term of (9.1), the potential V (or V_{micro}), is the sum of all direct, i.e. "microscopic" interaction potentials between the wall and the interface. By microscopic we mean that these are the bare, in some sense "point-wise mediated" interactions that are independent of the interfaces as a whole. Physically, these are typically Van der Walls forces, Coulomb forces etc. In our case, V consists of a repulsive part due to the SNB and of an attractive part due to economic distress, as was have discussed above. See section 2.4 for a discussion of physical interpretations of the Hamiltonian (9.1).

It is implicitly assumed that the Hamiltonian (9.1) has a short distance cutoff at some length scale $1/\Lambda$. In terms of wetting transitions, $1/\Lambda$ is of the order of the bulk correlation lengths. Economically, it can be seen as the time scale over which quotes are correlated.

The "interaction" between the EUR/CHF and the 1.20 barrier is of course not that of two rigid straight lines. The time evolution of the EUR/CHF exchange rate traces out an irregular, fluctuating surface. Due to these undulations different parts of the random-walk-line are exposed to different repulsive and attractive forces, depending on their distance to the 1.20 line. These complex interactions can be taken into account by renormalizing the potential V into a renormalized potential V_ℓ in which all the effects of fluctuations up to a certain scale ℓ are integrated out.

In the following, we set up a renormalization of the interfacial Hamiltonian (9.1). There exists a variety of approaches to this problem. We will follow here the approach by Fisher & Huse [26] since it offers a neat closed form solution for which we can try out several forms of potentials without any additional effort. We present a more detailed derivation, borrowing also from [84] as well as from more didactical RG review papers [18, 42, 99]. It would be far beyond the scope of this thesis to give a fundamental introduction to the methods of RG. Consult the references given in section 2.4 for this purpose.

It is convenient to work in Fourier transformed coordinates

$$\hat{z}(k) = \int \mathrm{d}^{D-1}\rho \; z(\rho) e^{ik\cdot\rho} \tag{9.2}$$

such that (9.1) becomes

$$\mathcal{H}(\hat{z}) = \int\limits_{|k|<\Lambda} \mathrm{d}^{D-1}k \, \left(\frac{\sigma}{2} |k|^2 \, |\hat{z}(k)|^2 + V(\hat{z}(k)) \right). \tag{9.3}$$

The partition function can be written as the functional integral

$$Z_\Lambda = \int\limits_{|k|<\Lambda} \mathcal{D}z\, e^{-\beta\mathcal{H}} \equiv \prod_{|k|<\Lambda} \int \mathrm{d}z(k)\, e^{-\beta\mathcal{H}} \tag{9.4}$$

where β is some parameter (physically, $\beta = 1/k_B T$ with T the temperature and k_B the Boltzmann constant). Quite generally, a RG-cycle consists of three steps:

(i) Integrating out the degrees of freedom (here z) within the thin momentum shell $\Lambda/b < |k| < \Lambda$ with $b > 1$ the *rescaling factor*. We set $b = 1 + \ell$ with ℓ infinitesimal. Generally, this step is also called *decimation* since we coarse grain our system (not necessarily always through integration). Intuitively, this step corresponds to "zooming out". Next, all the quantities that are affected by this procedure must be rescaled in such a manner that the Hamiltonian reclaims its original form.

(ii) Rescaling of the coordinates (here ρ or k, respectively). Interpretatively, this amounts to "blowing up" the radius of integration back to its original value Λ so that the system looks again like the previous one. It is then clear that

$$k \to k' = bk \qquad \Leftrightarrow \qquad \rho \to \rho' = \rho/b \tag{9.5}$$

which is essentially just a change of coordinates.

(iii) The last step is normalization which means the rescaling of the the field z according to [11]

$$z'(k') = \zeta_b^{-1} z(k). \tag{9.6}$$

The *field rescaling factor* ζ_b depends in general also on more system specific quantities such as the scaling of the correlation function. Its specification is not necessarily unique and depends on the problem at hand. This rescaling leads to a rescaling of the Hamiltonian $\mathcal{H} \to \mathcal{H}'$. We must now change all the parameters (coupling constants) of the system in such a way that $\mathcal{H}'$ has the same structure as $\mathcal{H}$ and such that the partition function does not change

$$Z_{\Lambda/b}(\mathcal{H}') = Z_\Lambda(\mathcal{H}). \tag{9.7}$$

Insisting on (9.7) is necessary to ensure that the physical properties of the system are unchanged. In fact, note that Z may change up to a multiplicative constant since this contributes just an additive constant to the energy.

Before performing the integration (i), we can split $z(\rho)$ into two parts: the "fast" part

$$z_f(\rho) = \int\limits_{\Lambda/b<|k|<\Lambda} \mathrm{d}^{D-1}k\, \hat{z}(k) e^{-ik\cdot\rho} \tag{9.8}$$

which will be integrated out and the remaining "slow" part $z_s(\rho) = z(\rho) - z_f(\rho)$. Notice that $\Lambda/b = \Lambda/(1+\ell) = \Lambda(1-\ell) + \mathcal{O}\left(\ell^2\right) \sim \Lambda(1-\ell)$ so that

$$\begin{aligned} z_f(\rho) &= \int\limits_{\Lambda(1-\ell)<|k|<\Lambda} \mathrm{d}^{D-1}k\, e^{-i\rho\cdot k}\hat{z}(k) = \int d\Omega \int\limits_{\Lambda(1-\ell)<|k|<\Lambda} \mathrm{d}|k|\, |k|^{D-2} e^{-i\rho\cdot k}\hat{z}(k) \\ &\sim \int\limits_{\Lambda(1-\ell)<|k|<\Lambda} \mathrm{d}|k|\, |k|^{D-2} e^{-i\rho\cdot k}\hat{z}(k) \;\sim\; \Lambda\ell\cdot\left(\Lambda^{D-2} e^{-i\rho\Lambda}\hat{z}(\Lambda)\right) \\ &\sim \ell\cdot const(\rho) \end{aligned} \tag{9.9}$$

[11] Often, in literature, normalization is also counted to (ii) so that RG consists of two steps only: decimation and rescaling.

is arbitrarily small. This justifies the expansion

$$V(z) = V(z_s) + z_f \frac{dV}{dz_s} + z_f^2 \frac{1}{2} \frac{d^2V}{dz_s^2} + \dots \tag{9.10}$$

where the ρ dependence of all the arguments is implicitly assumed and $\frac{dV}{\mathrm{d}z_s}$ is short for $\frac{dV(z)}{dz}\Big|_{z=z_s}$ etc. Keeping only terms up to second order in z_f we can plug this into the partition function (9.4) and obtain

$$\begin{aligned}
Z_\Lambda &= \prod_{0<|k|<\Lambda} \int \mathrm{d}z(k)\ \exp\left(-\beta \int \mathrm{d}^{D-1}\rho\ \left[\left|\frac{\sigma}{2}\nabla_\rho\left(z_s + z_f\right)\right|^2 + V(z_s) + z_f \frac{dV}{\mathrm{d}z_s} z_f^2 \frac{1}{2}\frac{d^2V}{\mathrm{d}z_s^2}\right]\right) \\
&= \prod_{0<|k|<\Lambda/b} \int \mathrm{d}z_s(k)\ \exp\left(-\beta \int \mathrm{d}^{D-1}\rho\ \left[\frac{\sigma}{2}\left|\nabla_\rho z_s\right|^2 + V(z_s)\right]\right) \cdot \\
&\qquad \cdot \prod_{\Lambda/b<|k|<\Lambda} \int \mathrm{d}z_s(k)\ \exp\left(-\beta \int \mathrm{d}^{D-1}\rho\ \left[\frac{\sigma}{2}\left|\nabla_\rho z_f\right|^2 + z_f \frac{dV}{\mathrm{d}z_s} + z_f^2 \frac{1}{2}\frac{d^2V}{\mathrm{d}z_s^2}\right]\right) \\
&= \prod_{0<|k|<\Lambda/b} \int \mathrm{d}z_s(k)\ \exp\left(-\beta\mathcal{H}_s\right) \cdot \\
&\qquad \cdot \prod_{\Lambda/b<|k|<\Lambda} \int \mathrm{d}z_f(k)\ \exp\left(-\beta \int \mathrm{d}^{D-1}\rho\ \left[\frac{\sigma}{2}\left|\nabla_\rho z_f\right|^2 + z_f \frac{dV}{\mathrm{d}z_s} + z_f^2 \frac{1}{2}\frac{d^2V}{\mathrm{d}z_s^2}\right]\right)
\end{aligned} \tag{9.11}$$

where we have defined

$$\mathcal{H}_s = \int \mathrm{d}^{D-1}\rho\ \left[\frac{\sigma}{2}\left|\nabla_\rho z_s\right|^2 + V(z_s)\right]. \tag{9.12}$$

Identifying furthermore

$$\begin{aligned}
\exp\left(-\beta\mathcal{H}'\right) = \exp\left(-\beta\mathcal{H}_s\right) \cdot \\
\prod_{\Lambda/b<|k|<\Lambda} \int \mathrm{d}z_f(k)\ \exp\left(-\beta \int \mathrm{d}^{D-1}\rho\ \left[\frac{\sigma}{2}\left|\nabla_\rho z_f\right|^2 + z_f \frac{dV}{\mathrm{d}z_s} + z_f^2 \frac{1}{2}\frac{d^2V}{\mathrm{d}z_s^2}\right]\right)
\end{aligned} \tag{9.13}$$

we can rewrite (9.11) simply as

$$Z_{\Lambda/b} \equiv \prod_{0<|k|<\Lambda/b} \int \mathrm{d}z_s(k)\ \exp\left(-\beta\mathcal{H}'\right) \tag{9.14}$$

Note that the mixed term $\sim \nabla_\rho z_s \cdot \nabla_\rho z_f$ that would appear in (9.11) vanishes since Fourier components of different wavelengths are orthogonal. So far, we have done nothing but restructuring the partition function. In order to continue, we must actually integrate out the high momentum shell. If it was not for the terms proportional to $z_f dV/dz_s$ and $z_f^2 d^2V/dz_s^2$ this would be trivial since the components z_s and z_f are then uncoupled. Integrating out the second part of (9.11) yields then merely a multiplicative constant which we can ignore. In fact, let us go even one step further and assume for the moment that we have turned off all the interactions, $V \to 0$. This will serve us to determine ζ_b. Performing the path integral between Λ/b and Λ then just yields

$$Z_{\Lambda/b} = \prod_{0<|k|<\Lambda/b} \int \mathrm{d}z_s(k)\ \exp\left(-\beta \underbrace{\int \mathrm{d}^{D-1}\rho\ \left|\frac{\sigma}{2}\nabla_\rho z_s\right|^2}_{=:\mathcal{H}_0}\right). \tag{9.15}$$

We also call $\mathcal{H}_0$ a *Gaussian Hamiltonian*. It represents a freely fluctuating surface. In (9.15) we have have dropped the multiplicative constant that arose from integrating out the momentum shell (see it as absorbed into the integration measure). Following faithfully the three steps of FRG we must now rescale the coordinates. From (9.5) we infer

$$d\rho \to b^{1-D} d\rho' \qquad \text{and} \qquad \nabla_\rho \to b \nabla_{\rho'} \tag{9.16}$$

such that

$$\mathcal{H}_0 \to \mathcal{H}_0' = \int \mathrm{d}^{D-1}\rho'\, b^{3-D} \left| \frac{\sigma}{2} \nabla_{\rho'} z_s(\rho') \right|^2 . \tag{9.17}$$

According to step (iii) above we must now rescale z_s. But how do we choose ζ_b? Thinking about this problem physically, it becomes clear that the free Hamiltonian $\mathcal{H}_0$ ought to be a fixed point of the RG transformation. It is the fixed point of the complete interface unbinding transition. Insisting on $\mathcal{H}_0$ (and hence its only parameter σ) being invariant under the RG transformation finally leads to

$$\zeta_b = b^{(D-3)/2}. \tag{9.18}$$

Now back to the evaluation of

$$(9.11) \propto \prod_{\Lambda/b<|k|<\Lambda} \int \mathrm{d}z_f(k)\ \exp\left(-\beta \int \mathrm{d}^{D-1}\rho\ \left[\frac{\sigma}{2} |\nabla_\rho z_f|^2 + z_f \frac{dV}{dz_s} + z_f^2 \frac{1}{2} \frac{d^2V}{dz_s^2} \right] \right). \tag{9.19}$$

Since z_f and z_f^2 are small, we can expand the exponential to first order [12]

$$(9.11) \propto \prod_{\Lambda/b<|k|<\Lambda} \int \mathrm{d}z_f(k)\ \left(1 + z_f \frac{dV}{dz_s} + z_f^2 \frac{1}{2} \frac{d^2V}{dz_s^2} + \dots \right) \exp\left(-\beta \int \mathrm{d}^{D-1}\rho\ \frac{\sigma}{2} |\nabla_\rho z_f|^2 \right). \tag{9.20}$$

It is common practice to interpret the exponential of the free part of the Hamiltonian in (9.20) as probability weight such that we can write furthermore

$$(9.11) \propto \langle 1 \rangle_{f;0} + \frac{dV}{dz_s} \langle z_f \rangle_{f;0} + \frac{d^2V}{dz_s^2} \frac{1}{2} \langle z_f^2 \rangle_{f;0} + \dots \tag{9.21}$$

where we have used linearity of the functional integral and the subscript "$f;0$" denotes averaging with respect to the free (0) Hamiltonian over the fast (f) modes. The term proportional to $\langle 1 \rangle_{f;0}$ can be ignored since it represents just a constant. The term proportional to $\langle z_f \rangle_{f;0}$ drops out by symmetry. [13] We are thus left with the determination of

$$\begin{aligned} \langle z_f^2 \rangle_{0;f} &= \prod_{\Lambda/b<|k|<\Lambda} \int \mathrm{d}z_f\ z_f^2\ \exp\left(-\int \mathrm{d}^{D-1}\rho\ \frac{\beta\sigma}{2} |\nabla_\rho z_f|^2 \right) \\ &= \prod_{\Lambda/b<|k|<\Lambda} \int dz_f(\rho)\ z_f^2 \exp\left(-\int \mathrm{d}^{D-1}\rho\ \frac{\beta\sigma}{2} |\nabla_\rho z_f|^2 \right) \end{aligned} \tag{9.22}$$

Readers familiar with the path integral formulation of (quantum) field theories will note immediately that this functional integral can be solved exactly by *completing the square*. In fact, this is the same

[12] Since (9.19) is quadratic in z_f we could also solve this integral by completing the square as we have done in Appendix II.

[13] The probability weight is symmetric under $z_f \to -z_f$. The reason for the vanishing is thus the same as for instance in

$$\int_{-\infty}^{\infty} dx\ x e^{-x^2} = 0.$$

technique that we have used in Appendix II in order to evaluate path integrals. What follows is a standard procedure in field theories: Using integration by parts we bring the exponential in (9.22) into a standardized form. We then introduce a *source term* $J(\rho)$ in order to express z^2 in terms of functional derivatives. Finally we solve the integral by completing the square. Working with the notation from (9.4) we now perform the actual calculation:

$$\begin{aligned}
(9.22) &= \int\limits_{\Lambda/b<|k|<\Lambda} \mathcal{D}z_f \; z_f^2 \exp\left(-\int \mathrm{d}^{D-1}\rho \, \frac{\beta\sigma}{2} \, |\nabla_\rho z_f|^2\right) \\
&= \int\limits_{\Lambda/b<|k|<\Lambda} \mathcal{D}z_f \; z_f^2 \exp\left(\int \mathrm{d}^{D-1}\rho \, \frac{\beta\sigma}{2} z_f \Delta_\rho z_f\right) \\
&= \frac{\delta^2}{\delta J(\rho)^2} \int\limits_{\Lambda/b<|k|<\Lambda} \mathcal{D}z_f \; \exp\left(\int \mathrm{d}^{D-1}\rho \, \frac{\beta\sigma}{2} z_f \Delta_\rho z_f + J(\rho) z_f(\rho)\right)\Bigg|_{J=0} \\
&= \frac{\delta^2}{\delta J(\rho)^2} \exp\left(-\int \mathrm{d}^{D-1}\rho \, G(\rho) J^2(\rho)\right)\Big|_{J=0} \\
&= -G(\rho).
\end{aligned} \tag{9.23}$$

In the second-last step we have introduced the Green's function G of the Laplacian operator $\frac{\sigma\beta}{2}\Delta_\rho$. It is straight forward to figure out the form of G in Fourier space since the Fourier transform of the delta-functional is proportional to unity (compare also with our discussion in Appendix II):

$$\frac{\sigma\beta}{2}\Delta_\rho G(\rho) = \delta(\rho) \quad \Rightarrow -\frac{\sigma\beta}{2} \, |k|^2 \, \hat{G}(k) = (2\pi)^{-(D-1)}. \tag{9.24}$$

We can easily solve for $\hat{G}$ and transform back to find

$$\begin{aligned}
(9.22) = -G(\rho) &= \frac{2}{(2\pi)^{D-1}\sigma\beta} \int_{\Lambda/b<|k|<\Lambda} \mathrm{d}^{D-1}k \, \frac{1}{|k|^2} \\
&= \frac{2}{(2\pi)^{D-1}\sigma\beta} \int d\Omega \int\limits_{\Lambda/b}^{\Lambda} \mathrm{d}|k| \; |k|^{D-2} \frac{1}{|k|^2} \\
&= \frac{2}{(2\pi)^{D-1}\sigma\beta} \frac{(2\pi)^{(D-1)/2}}{\Gamma\left(\frac{D-1}{2}\right)} \int\limits_{\Lambda/b}^{\Lambda} \mathrm{d}|k| \; |k|^{D-4} \\
&\sim \frac{2}{(2\pi)^{D-1}\sigma\beta} \frac{(2\pi)^{(D-1)/2}}{\Gamma\left(\frac{D-1}{2}\right)} \; (\ell\Lambda) \, \Lambda^{D-4} \\
&\sim \frac{2(2\pi)^{(1-D)/2}}{\Gamma\left(\frac{D-1}{2}\right)} \frac{(b-1)\Lambda^{D-3}}{\sigma\beta}
\end{aligned} \tag{9.25}$$

Plugging this result into (9.21) and from there back into (9.11) we find that, after rescaling and normalizing $\mathcal{H}_s$, this gives rise to a change in the potential

$$V(z_s) \to V_\ell(z_s) \equiv b^{D-1} V\left(b^{(3-D)/2} z_s\right) + \frac{b-1}{\bar{\sigma}} \frac{d^2 V}{dz_s^2} \tag{9.26}$$

with

$$\bar{\sigma} = \frac{(2\pi)^{(D-1)/2} \Gamma\left(\frac{D-1}{2}\right) \sigma\beta}{\Lambda^{D-3}}. \tag{9.27}$$

Keeping only terms linear in ℓ yields

$$V_\ell(z_s) = V(z_s) + (D-1)V(z_s)\ell + \frac{3-D}{2}\frac{dV}{dz_s}dl + \frac{1}{\bar{\sigma}}\frac{d^2V}{dz_s}\ell \tag{9.28}$$

and since ℓ is infinitesimal we can write this as an effective change in the potential according to

$$\frac{\partial V(z)}{\partial l} = (D-1)V(z) + \frac{3-D}{2}z\frac{dV}{dz} + \frac{1}{\bar{\sigma}}\frac{d^2V}{dz}. \tag{9.29}$$

In the last step we have set z_s back to z since we have now completed the above steps (i)-(iii) and hence one (functional) RG cycle. From here on, we can iteratively repeat these steps up to any scale giving us the typical renormalization group flow. However, the "parameter" V is a function, and hence infinite-dimensional itself. This explains why the method goes by the name *functional* RG. Equation (9.29) is just the one-dimensional *Fokker-Planck equation* with constant coefficients. Its solution is known analytically (for constant coefficients) and discussed for instance in [68]. Essentially, it boils down to finding the corresponding Green's function and then convoluting with the bare potential $V_0(z)$ at $\ell = 0$. Explicitly, we have

$$V_\ell(z) = \frac{e^{(D-1)\ell}}{\sqrt{2\pi}\delta(l)}\int_{-\infty}^{\infty} dz'\, V_0(z')\, \exp\left(-\frac{(\gamma(\ell)z - z')^2}{2\delta^2(\ell)}\right) \tag{9.30}$$

where

$$\delta(\ell) = \frac{2\left(e^{(3-D)/\ell} - 1\right)}{(3-D)\bar{\sigma}} \tag{9.31}$$

denotes the width of the convolution and

$$\gamma(\ell) = e^{\frac{3-D}{2}\ell} = b^{\frac{3-D}{2}} = b^{\zeta_b} \tag{9.32}$$

is nothing but the rescaling factor of the field- (i.e. z-) direction (9.18). This determines uniquely the FRG-flow of the potential V up to linear order in V. Higher order corrections (possibly leading also to corrections for σ) arise by taking into account additional terms from (9.20).

Declaration of originality

ETH

Eidgenössische Technische Hochschule Zürich
Swiss Federal Institute of Technology Zurich

Declaration of originality

The signed declaration of originality is a component of every semester paper, Bachelor's thesis, Master's thesis and any other degree paper undertaken during the course of studies, including the respective electronic versions.

Lecturers may also require a declaration of originality for other written papers compiled for their courses.

I hereby confirm that I am the sole author of the written work here enclosed and that I have compiled it in my own words. Parts excepted are corrections of form and content by the supervisor.

Title of work (in block letters):

Master Thesis: Constrained Random Walk Models

Authored by (in block letters):

For papers written by groups the names of all authors are required.

Name(s):	**First name(s):**
Lera	Sandro

With my signature I confirm that

- I have committed none of the forms of plagiarism described in the 'Citation etiquette' information sheet.
- I have documented all methods, data and processes truthfully.
- I have not manipulated any data.
- I have mentioned all persons who were significant facilitators of the work.

I am aware that the work may be screened electronically for plagiarism.

Place, date	**Signature(s)**
Zurich, 02.02.2015	

For papers written by groups the names of all authors are required. Their signatures collectively guarantee the entire content of the written paper.

References

[1] HistDatalFree Forex Historical Data.

[2] Andersen, T. G., Bollerslev, T., Diebold, F. X., and Labys, P. Modeling and Forecasting Realized Volatility. *Econometrica 71*, 2 (March 2003), 579–625.

[3] Anderson, P. More Is Different. *Science 177*, 4047 (August 1972), 393–396.

[4] Bachelier, L. Théorie de la Spéculation. *Annales Scientifiques de l'École Normale Supérieure 17* (1900), 21–86.

[5] Baghdjian, A., and Koltrowitz, S. Swiss Central Bank Stuns Market with Policy U-Turn. Reuters, January 2015.

[6] Bernardino, N. F. R. *The Nonlocal Model of Short-Range Wetting*. PhD thesis, Department of Mathematics - Imperial College, March 2008.

[7] Bouchaud, J.-P. Power laws in economics and finance: some ideas from physics. *Quantitative Finance 1*, 1 (2001), 105–112.

[8] Bouchaud, J.-P., and Potters, M. *Theory of Financial Risks: From Statistical Physics to Risk Mangement*. Cambridge University Press, 2000.

[9] Bowley, A. L. S. *Elements of Statistics*. London: P.S. King, 1901.

[10] Brenner, H. The Slow Motion of a Sphere Through a Viscous Fluid Towards a Plane Surface. *Chemical Engineering Science 16*, 3-4 (December 1961), 242–251.

[11] Brogliato, B. *Nonsmooth Mechanics: Models, Dynamics and Control*, second ed. Communications and Control Engineering. Springer, 2002.

[12] Cain, G. *Complex Analysis*. Georgia Tech, 2009, ch. 5. Cauchy's Theorem.

[13] Chaboud, A. P., Chernenko, Sergey, V., Howorka, E., Krishnasami, I., Liu, D., and Wright, J. H. The High-Frequency Effects of U.S. Macroeconomic Data Releases on Prices and Trading Activity in the Global Interdealer Foreign Exchange Market. *International Finance Discussion Papers*, 823 (November 2004).

[14] Chandrasekhar, S. Stochastic Problems in Physics and Astronomy. *Rev. Mod. Phys. 15* (Jan 1943), 1–89.

[15] Chow, C. C., and Buice, M. a. Path integral methods for stochastic differential equations. *Journal of mathematical neuroscience 5*, 8 (2015), 1–35.

[16] Coelho, F. C., Codeço, C. T., and Gomes, M. G. M. A Bayesian Framework for Parameter Estimation in Dynamical Models. *PLoS ONE 6*, 5 (2011), e19616.

[17] Cox, S. The Three Big Misconceptions about the Swiss Franc. The Economist, January 2015.

[18] Demalotte, B. *Renormalization Group and Effective Field Theory Approaches to Many-Body Systems*, vol. 852 of *Lecture Notes in Physics*. Springer Berlin-Heidelberg, 2012, ch. An Introduction to the Nonperturbative Renormalization Group, pp. 49–132.

[19] Draghi, M. *Speech by Mario Draghi at the Global Investment Conference in London*. European Central Bank, 2012.

[20] EASLEY, D., LÓPEZ DE PRADO, M., AND O'HARA, M., Eds. *High-Frequency Trading - New Realities for Traders, Markets and Regulators*. Risk Books, 2013.

[21] EINSTEIN, A. Ueber die von der Molekularkinetischen Theorie der Wärme geforderte Bewegung von in Ruhenden Flüssigkeiten suspendierten Teilchen. *Annalen der Physik 322*, 8 (May 1905), 549–560.

[22] FAMA, E. F. Efficient Capital Markets: A Review of Theory and Empirical Work. *The Journal of Finance 25*, 2 (May 1970), 383–417.

[23] FARMER, J., AND LUX, T. Applications of statistical physics in economics and finance. *Journal of Economic Dynamics and Control 32*, 1 (2008), 1–320.

[24] FELLER, W. *An Introduction to Probability Theory and its Applications*, second ed. Princeton University Press, 1971.

[25] FIEBIG, H., AND MUSGROVE, D. Testing for detailed balance in a financial market. *Physica A: Statistical Mechanics and its Applications 427* (2015), 26–33.

[26] FISHER, D. S., AND HUSE, D. A. Wetting Transitions: A Functional Renormalization-Group Approach. *Physical Review B 32*, 1 (July 1985), 247.

[27] FISHER, M. E. Walks, Walls, Wetting, and Melting. *Journal of Statistical Physics 34*, 5 (1984), 667–729.

[28] FISHER, M. E. Renormalization Group Theory: Its Basis and Formulation in Statistical Physics. *Reviews of Modern Physics 70* (1998), 653.

[29] FLOOD, R., ROSE, A., AND MATHIESON, D. An empirical exploration of exchange-rate target-zones. *Carnegie-Rochester Conference Series on Public Policy 35* (1991), 7–65.

[30] FRANKEL, J. A. No Single Currency Regime is Right for all Countries or at all Times. *Nber Working Paper Series*, Working Paper 7338 (1999).

[31] FRIEDRICH, R., SIEGERT, S., PEINKE, J., LÜCK, S., SIEFERT, M., LINDEMANN, M., RAETHJEN, J., DEUSCHL, G., AND PFISTER, G. Extracting Model Equations from Experimental Data. *Physics Letters A 271*, 3 (2000), 217–222.

[32] GARDINER, C. W. *Handbook of stochastic methods*. Springer, 1985.

[33] GRIGORIU, M. *Stochastic Calculus - Applications in Science and Engineering*. Springer Science+Business Media, LLC, 2002.

[34] GROENEVELD, R. A., AND MEEDEN, G. Measuring Skewness and Kurtosis. *Journal of the Royal Statistical Society 33*, 4 (December 1984), 391–399.

[35] HILDEBRAND, P. M. Speech by Philipp M. Hildebrand, Member of the Governing Board of the Swiss National Bank. In *Swiss National Bank Sales - Lessons and Experiences* (May 2005).

[36] HUANG, K. *Statistical Mechanics*, second ed. Wiley, 1987, ch. 17, 18, p. 493.

[37] INTERNATIONAL MONETARY FUND. Annual Report on Exchange Arrangements and Exchange Restrictions. Tech. rep., International Monetary Fund, 2013.

[38] JEANBLANC, M., YOR, M., AND CHESNEY, M. *Mathematical Methods for Financial Markets*. Springer Finance Textbooks. Springer, 2009.

[39] KALLENBERG, O. *Foundations of Modern Probability*, second ed. Springer Berlin-Heidelberg, 2002.

[40] KALOS, M. H., AND WHITLOCK, P. A. *Monte Carlo Methods*, second ed. Wiley, 2008.

[41] KLEINERT, H. *Path Integrals in Quantum Mechanics, Statistics, Polymer Physics and Financial Markets*, fifth ed. World Scientific, 2009.

[42] KOPIETZ, P., BARTOSCH, L., AND SCHÜTZ, F. *Introduction to Functional Renormalization Group*. Springer Berlin-Heidelberg, 2010.

[43] KRUGMAN, P. R. Target Zones and Exchange Rate Dynamics. *The Quarterly Journal of Economics 106*, 3 (1991), 669–682.

[44] KRYLOV, N. Mean Value Theorems for Stochastic Integrals. *The Annals of Probability 29*, 1 (January 2001), 395–410.

[45] LAU, A., AND LUBENSKY, T. C. State-dependent diffusion: Thermodynamic consistency and its path integral formulation. *Physical Review E 76* (2007), 011123.

[46] LEIBLER, S. *Equilibrium Statistical Mechanics of Fluctuating Films and Membranes*. World Scientific Pub Co Inc, 2004, ch. 3, pp. 49–101.

[47] LEISINGER, C. Der Frankenschock Zieht Weitere Kreise. NZZ, January 2015.

[48] LEVINSON, M. *Guide to Financial Markets*, fourth ed. Bloomberg Press, 2000.

[49] LEVY, M., AND ROLL, R. The Market Portfolio may be Mean-Variance Efficient After All. *Review of Financial Studies 23* (2010), 2464–2461.

[50] LIPOWSKY, R. Critical Effects at Complete Wetting. *Physical Review B 32* (August 1985), 1731.

[51] LIPOWSKY, R. *Random Fluctuations and Pattern Growth: Experiments and Models*, vol. 157 of *NATO ASI Series*. Springer Netherlands, 1988, ch. Scaling Properties of Interfaces and Membranes, pp. 227–245.

[52] LIPOWSKY, R. Critical Behavior of Interacting Manifolds. *Physica A 177*, 1-3 (September 1991), 182–188.

[53] LIPOWSKY, R., AND LEIBLER, S. Unbinding Transitions of Interacting Membranes. *Physical Review Letters 56* (June 1986), 2541.

[54] LO, A. W., AND MACKINLAY, A. C. *A Non-Random Walk Down Wall Street*, fifth ed. Princeton University Press, 2002.

[55] LORENTZ, H. A. *Abhandlungen über theoretische Physik*. BG Teubner, 1907.

[56] MAXWELL, J. C. *A Treatise on Electricity and Magnetism*, vol. 1. Cambridge University Press, 1873.

[57] MIL'SHTEJN, G. Approximate Integration of Stochastic Differential Equations. *Theory of Probability & Its Applications 19*, 3 (September 1973), 557–562.

[58] MULDOWNEY, P. Understanding Stochastic Differential Equations. arXiv, 2014.

[59] Ni, X., Malevergne, Y., Sornette, D., and Woehrmann, P. Robust reverse engineering of cross sectional returns and improved portfolio allocation performance using the CAPM. *Journal of Portfolio Management 37*, 4 (2011), 76–85.

[60] NZZ. Starker Franken Sorgt Für Nervosität. Online, November 2014.

[61] NZZ. Verwirrung Über Verletzung des Mindestkurses. Online, December 2014.

[62] Ohr, R., Starbatty, J., and Bofinger, P. Zeitgespräch: Warum ist der Euro so Schwach? *Wirtschaftsdienst: Zeitschrift für Wirtschaftspolitik 81*, 7 (2001), 371–379.

[63] Øksendal, B. *Stochastic Differential Equations*, sixth ed. Springer-Verlag, 2003.

[64] Parkinson, M. The Extreme Value Method for Estimating the Variance of the Rate of Return. *Journal of Business 53*, 1 (January 1980), 61–65.

[65] Peskin, M. E., and Schröder, D. V. *An Introduction to Quantum Field Theory*. Westview Press, 1995, ch. 9. Functional Methods.

[66] Protter, P. E. *Stochastic Integration and Differential Equations*, second ed. Springer Berlin-Heidelberg, 2005.

[67] Record, N. *Currency Overlay*. Wiley, 2003.

[68] Risken, H. *The Fokker-Planck Equation*. Lecture Notes in Mathematics. Springer Berlin-Heidelberg, 1996.

[69] Roehner, B., and Sornette, D. The Sharp Peak-Flat Trough Pattern and Critical Speculation. *Europhysics Letters 4* (1998), 387–399.

[70] Roll, R. A Simple Implicit Measure of the Effective Bid-Ask Spread in an Efficient Market. *The Journal of Finance 39*, 4 (September 1984), 1127–1139.

[71] Ruseckas, J., and Kaulakys, B. 1/f noise from nonlinear stochastic differential equations. *Physical Review E 81*, 3 (2010), 1–7.

[72] Ryder, L. H. *Quantum Field Theory*. Cambridge University Press, 1996, ch. 5. Path Integrals in Quantum Mechanics.

[73] Samuelson, P. A. Proof that Properly Anticipated Prices Fluctuate Randomly. *Industrial Mangement Review 6.2* (1965), 41–49.

[74] Samuelson, P. A. Proof That Properly Discounted Present Values of Assets Vibrate Randomly. *The Bell Journal of Economics and Management Science 4*, 2 (1973), 369–374.

[75] Sarno, L., and Taylor, M. *The economics of exchange rates*. Cambridge, University Press, 2003.

[76] Schmidt, Anatoly, B. *Econophysics Approaches to Large-Scale Business Data and Financial Crisis*. Springer Japan, 2010, ch. Microstructure and Execution Strategies in the Global Spot, pp. 49–65.

[77] Schweizerische Eidgenossenschaft. Economic and Financial Data. Online.

[78] Schwenk, A., and Polonyi, J., Eds. *Renormalization Group and Effective Field Theory Approaches to Many-Body Systems*, vol. 852 of *Lecture Notes in Physics*. Springer Berlin-Heidelberg New York, June 2012.

[79] SHAMAH, S. *A Foreign Exchange Primer*. Wiley, 2008.

[80] SHARMA, P. Entropic Force Between Membranes Reexamined. *Proceedings of the National Academy of Sciences of the United States of America 110*, 6 (February 2013), 1976–1977.

[81] SHREVE, S. *Stochastic Calculus in Finance II*. Springer Finance. Springer Berlin-Heidelberg New York, 2004.

[82] SONDERMANN, D. *Introduction to Stochastic Calculus for Finance*, vol. 579 of *Lecture Notes in Economics and Mathematical Systems*. Springer Berlin-Heidelberg New York, 2006.

[83] SORNETTE, D. Steric Interaction Between Wandering Walls. Study of the Strong Deviation from Mean Field Theory. *Europhysics Letters 2* (1986), 715.

[84] SORNETTE, D. Fluctuations and Interactions Between Membranes. In *Physics of Amphiphilic Layers*, J. Meunier, D. Langevin, and N. Boccara, Eds., Springer Proceedings in Physics. Springer-Verlag, 1987, pp. 80–96.

[85] SORNETTE, D. *Critical Phenomena in Natural Sciences, Chaos, Fractals, Self-organization and Disorder: Concepts and Tools*, second ed. Springer-Verlag, 2000, ch. 2.3 and 11.

[86] SORNETTE, D. Physics and financial economics (1776-2014): puzzles, Ising and agent-based models. *Reports on Progress in Physics. Physical Society (Great Britain) 77*, 6 (2014), 062001.

[87] SORNETTE, D., AND OSTROWSKY, N. Lamellar Phases: Effect of Fluctuations (Theory). In *Micelles, Membranes, Microemulsions and Monolayers*, W. Gelbart, A. Ben-Shaul, and D. Roux, Eds. Springer New York, 1994, pp. 251–302.

[88] STOOF, H. T., DICKERSCHEID, D. B. M., AND GUBBELS, K. Renormalization Group Theory. In *Ultracold Quantum Fields*, Theoretical and Mathematical Physics. Springer Netherlands, 2009, pp. 329–355.

[89] STUDER-SUTER, R., AND JANSSEN, A. The Swiss franc's honeymoon. *SSRN*, Working Paper No. 170 (2014).

[90] SURA, P., AND BARSUGLI, J. A Note on Estimating Drift and Diffusion Parameters from Timeseries. *Physics Letters A 305* (2002), 304–411.

[91] SVENSSON, L. E. O. An interpretation of recent research on exchange rate target zones. *Journal of Economic Perspectives 6*, 4 (1992), 119–144.

[92] SWISS NATIONAL BANK. Swiss National Bank sets minimum exchange rate at CHF 1.20 per euro. Press Release, September 2011.

[93] SWISS NATIONAL BANK. Discussion on the Topic of the Eur/Swiss-Franc Minimum Exchange Rate. Press Release, April 2012.

[94] SWISS NATIONAL BANK. Gold Initiative. Online, 2014.

[95] SWISS NATIONAL BANK. Swiss National Bank Discontinues Minimum Exchange Rate and Lowers Interest Rate to -0.75%. Press Release, January 2015.

[96] THE ROYAL SWEEDISH ACADEMY OF SCIENCES. The Prize in Economic Sciences 2013 - Press Release. Nobelprize.org, October 2013.

[97] UHLENBECK, G., AND ORNSTEIN, L. On the Theory of the Brownian Motion. *Physical Review 36* (September 1930), 823.

[98] UNITED STATES DEPARTMENT OF STATE. PUBLICATION: Proceedings and Documents of the United Nations Monetary and Financial Conference, Bretton Woods, New Hampshire. United States Department of State.

[99] VILFAN, I. Lecture Notes in Statistical Mechanics. Abdus Salam ICTP, 2002.

[100] WILSON, K. G. The Renormalization Group: Critical Phenomena and the Kondo Problem. *Reviews of Modern Physics 47* (October 1975), 773.

[101] WILSON, K. G. Problems in Physics with many Scales of Length. *Scientific American 241*, 2 (1979).

[102] WOLFGANG, P., AND BASCHNAGEL, J. *Stochastic Processes - From Physics to Finance*, second ed. Springer Berlin-Heidelberg, 2013.

[103] YURA, Y., TAKAYASU, H., SORNETTE, D., AND TAKAYASU, M. Financial brownian particle in the layered order-book fluid and fluctuation-dissipation relations. *Physical Review Letters 112*, 9 (2014), 1–5.

[104] ZHANG, L., MYKLAND, P. A., AND AÏT-SAHALIA, Y. A Tale of Two Time Scales: Determining Integrated Volatility with Noisy High-Frequency Data. *Journal of American Statistical Association 100*, 472 (December 2005), 1394–1411.

[105] ZHOU, B. High-Frequency Data and Volatility in Foreign-Exchange Rates. *Journal of Business and Economic Statistics 14*, 1 (July 1996), 44–52.